12-17-2018

Properties of Mixing SAC Solder Alloys with Bismuth-containing Solder Alloys for a Low Reflow Temperature Process

Tayler John Swanson
tjs1634@rit.edu

R.I.T.

Properties of Mixing SAC Solder Alloys with Bismuth-containing Solder Alloys for a Low Reflow Temperature Process

A Thesis Presented

By

Tayler John Swanson

Submitted in Partial Fulfillment of the Requirements for a Master of Science degree in Manufacturing and Mechanical Systems Integration

Advisor

Dr. Martin K. Anselm

Department of Manufacturing and Mechanical Engineering Technology

College of Applied Science and Technology

Rochester Institute of Technology

Rochester, NY

December 17, 2018

Properties of Mixing SAC Solder Balls with Bismuth-containing Solder Pastes for a Low Reflow Temperature Process

College of Applied Science and Technology

Department of Manufacturing and Mechanical Engineering Technology

Rochester Institute of Technology

Rochester, New York

Certificate of Approval

M.S. Degree Thesis

The members of the committee approve the Thesis of

Tayler John Swanson

Presented on 27th April 2018

Date:

Tayler John Swanson
Student- R.I.T. Dept. of Manufacturing and Mechanical Engineering technology

Date:

Dr. Martin K. Anselm

Advisor- R.I.T. Dept. of Manufacturing and Mechanical Engineering technology

Date:

Dr. Christopher Lewis

Assistant Professor- R.I.T. College of Engineering Technology

Date:

Dr. Robert Garrick

Dept. Chair- R.I.T. Dept. of Manufacturing and Mechanical Engineering technology

DEDICATION

To my parents, family and friends thank you.

ACKNOWLEDGMENTS

A special Thank you to all of those that have taught me and gave me inspiration to pursue a career in electronics including, Dr. Manian Ramkumar, Dr. Martin Anselm, Dr. Bill Destler, Dr. Richard Coyle, Dr. Chen Xu, Ms. Charmaine Johnson, Mr. Richard Popowich, Dr. Ronald Pratt, Mr. Jeff Shake, Mr. Jeff Lonneville, Mr. Drew Ake, Ms. Sarah Frisicano, Mr. Andrew Daya, Mr. Abner Argueta, Dr. Reza Ghaffarian, Dr. Raiyo Aspandiar, Ms. Debbie Fleming, Dr. Serendra Gupta, Dr. Richard Hailstone, Mr. Michael Parthum, Mrs. Renee Michalkiewic, Mr. Carl Lundgren, Dr. Ti-Lin Lui, Dr. George Zion, Mr. Randolph Bogdan, Mr. Bill Bond, Mr. Mark Henry, Mr. Mark Hinman, Mom&Dad, Digital Instruments, Rochester Institute of Technology, Intel, IEC Electronics, Lockheed Martin, Harris Corp., ASM Assembly Systems, Heller Industries, KIC, IPC and The Surface Mount Technology Association.

ABSTRACT

The subject of extensive research has been the establishing of lower temperature soldering of electronic assemblies that are similar to the once common yet still preferred eutectic Tin-Lead (SnPb) soldering manufacturing processes that are below 217˚C. This research opportunity will contribute data on mixed solder alloy assemblies that can be formed at lower process temperatures. There are many environmental and economic benefits of avoiding the current reliability concerns of assembling electronics at the standard high temperatures which peak at 230˚C 260˚C. To reduce this temperature the use of Bismuth containing solder pastes are mixing with the standard high temperature SAC solders for electronic assemblies. The materials evaluated are the (in weight percentages) 96.5Tin/3Silver/.5Copper (Sn/Ag/Cu) solder ball mixed with each solder paste, the eutectic 58Bismuth/42Tin (58Bi/42Sn), 57Bi/42Sn /1Ag and a propriety alloy that has a lower Bismuth content along with various micro alloys, 40-58Bi/Sn/X (X representing proprietary micro alloys or doping). In the assembly portion of this research the solder alloys were exposed to three different peak temperatures 180˚C, 195˚C, 205˚C. Another reflow profile attribute of focus was times above 138˚C the melting point of the eutectic Sn58Bi alloy. The ball and paste assembly portion of this research used the times above melting of 120sec and 240sec to represent process extremes and verify their significance on improving mixing level results. These times above melting did not consistently improve the mixing levels and therefore are not recommended or required during mixed low temperature solder assemblies. The results in this study suggest the recommended and optimum reflow profile to have a time above the melting point to be less than or equal to 90 seconds for mixed solder alloy assemblies in "low" (<200˚C) peak temperature reflow oven profiles. This attribute ensures a reflow window similar to that of the eutectic SnPb processing. The second leg of this research was with a component assembly of a large ball grid array at the same various peak temperatures with a single time above 138˚C, 90sec. This "large" (>20mm a side) component is a SAC405 solder balled BGA with the dimensions of 42x28x0.8mm. With any large component the temperature gradient across the component is a risk factor and the results show that there are significantly differences of mixing from the center of the component to the edge due to an average 2.3 ˚C temperature difference during convection reflow. The average mixing % levels recorded for T_{peak}= 180˚C for the solder pastes with a 58Bi = 47%, 57Bi = 47% and 40-58Bi = 44%. The average mixing % levels recorded for T_{peak}= 195˚C for the solder pastes with a 58Bi = 69%, 57Bi = 77% and 40-58Bi = 57%. The conclusions found also match previous work identifying the reflow peak temperatures remain a significant factor on the mixing %. This work's goal was to add to the knowledge of the electronics industry to better understanding the microstructure and mixing mechanisms of Bi/Sn/X-SAC solder joints for low temperature reflow assembly processes.

TABLE OF CONTENTS

Page

LIST OF TABLES

Table Page

List of Equations

LIST OF FIGURES

Figure Page

INTRODUCTION

The subject of extensive research has been implementing Low Temperature soldering of electronic assemblies that are a near drop in alternatives to the eutectic SnPb manufacturing process.

The objective for nearly two decades has been replacing the hazardous SnPb solder alloy with a suitable alternative based off manufacturability, cost, reliability at high temperature and long life (Schroeder, et al. 2001). The widely adopted alloy at this point has been 96.5Sn-3.0Ag-0.5Cu (by weight percentage) and is a hypoeutectic alloy from the Sn-Ag-Cu (SAC) ternary system and has a melting point starting at 217˚C which is 34˚C above the tradition eutectic SnPb temperature of 183C (Bath et al., 2000) (NSMS, 2001).

The acceptance of SAC305 came after considerable research on the many other Pb-free alloy alternatives including Sn-Bi that better fits as a near drop in alternative alloy to fit the SnPb manufacturing process, though it lacked comparable mechanical properties. (Felton, et al. 1993) (Glazer, et al. 1994) (Vianco, et al. 1995) (Miao, et al. 2001)

SAC alloy adoption in the electronics industry has disrupted manufacturing processes along with component supply chain. This Pb-free solder alloy era came to be from a European Commission directive for the Removal of Hazardous Substances (RoHS) targeting electronics to no longer comprise of Lead (Pb) among other elements. (RoHS, 2007)

The RoHS directive was explicit for consumer electronics and while high reliability equipment producers for medical, military, and avionics were given exemption for time to enable development of high reliable Pb-free alternatives. The EMS providers and the component supply chain have had to adjust their materials while also managing the new higher temperatures of the

new manufacturing processes that accommodated the wide spread use of Pb-free solders particularly the SAC solder alloys. The initial stress on the component supply chain has since evolved and now Pb-free components are readily available. The new dilemma that exists for the RoHS exempt group is their ability to source compatible components for their electronic assemblies that still use SnPb solder alloys. (iNEMI, 2007) Considerable effort to address this dilemma has been driven by industry collaborations in consortia organizing massive data analysis projects to contribute more data on mixed solder alloy assemblies that can be formed at lower process temperatures. (Snugovsky, et. al., 2007) (Kinyanjui, et al., 2010) (Coyle, et. al., 2017) The rationale behind this paper is to data mixing data and optimal reflow profiles for industries efforts to implementing low temperature soldering processes.

BACKGROUND

1.1 Electronic Manufacturing Assembly Basics

The role of an electronics manufacturing services (EMS) provider is to accurately assemble all the components of a designed electronic product to enable functionality of the device. The modern electronic products require the EMS provider to use a Surface Mount Technology (SMT) assembly line to first apply the material solder paste through a stencil over metallic pad locations on a printed circuit board (PCB) of the electrical design. That first step in the SMT assembly process referred to a Printing. The next step is component placement on top of the solder paste and PCB. The last step in a typically SMT assembly line is the convection reflow oven that heats and melts the solder to the components and PCB, forming soldered joints. These solder joints have mechanical, electrical and thermal properties that will determine performance and reliability of the life of the assembly. The end of life of the millions of consumer electronic devices a year adds a burden on the environment and with regulation the solder that electronic manufactures preferred to use for decades, the eutectic composition of the alloy Tin-Lead has had to be replaced with much attention still today after a more than a decade.

1.2 Removing Lead-Free Solder

From the first computers to the raise of millions of other electronic devices the matter of their proper disposal and material regulations has significantly influenced and impacted the electronics industry.

The electronic waste (e-waste) that is disposed in landfills risks the hazardous materials of the assemblies to negatively impacting the environment. (MacKay, et al., 1985) (Vianco, et al. 1993)

The main hazardous element in electronics was the Lead (Pb) in the solders alloy composition, specifically the eutectic Sn63Pb37 (by weight percentage) solder alloy. The use of Sn63Pb37 solder is the most widely preferred solder choice of EMS providers globally and it was most likely to be found in every electronic assembly prior to 2006. (Loomans, 1994)

Lead (Pb) has been a hazardous material addressed in many industries from plumbing, paint and now in electronics posing global concerns of its negative impact on human health and the environment. There is a serious risk that the hazardous material could be released into the environment by for example, seeping into municipal water supplies if not properly disposed. Other liability risks on human health include workers exposure to elevated lead levels, and also of the poorest people who are beginning to collect and try and resell e-waste by scavenging any materials/parts that might be of value. (Seeling, 1995)

The years around 2001 are when escaladed discussions for regulations were backed up by data that estimated electronic waste was ~10 million tons in just the European Union and increasing ~5% annually, a shocking stat that initiated the directive the European Commission for the Removal of Hazards Substances (RoHS) in electronics assemblies. (Lau & Lui, 2004)

The European Commission created the Directive in 2002 and had the mission statement of the following, “Directive 2002/95/EC aims to restrict hazardous substances in electrical and electronic equipment so as to contribute to the protection of human health and the environmentally sound recovery and disposal of waste electrical and electronic equipment.” (RoHS, 2003)

The main 6 substances are shown in the figure below alongside electronic parts where they would be found.

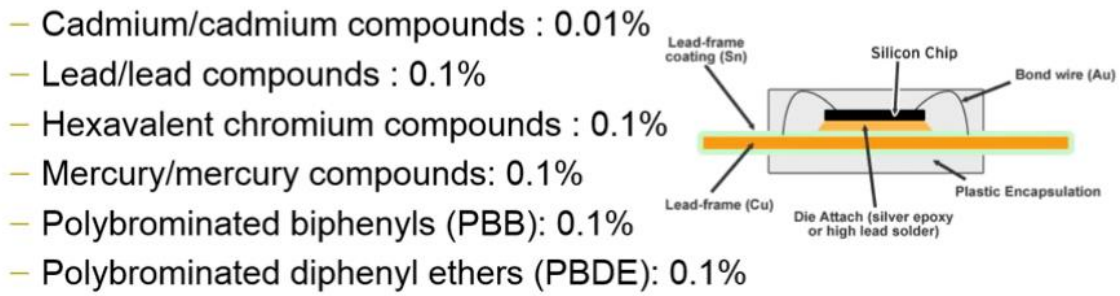

Figure 1 RoHS Substance restrictions inside an electronic component (RoHS, 2007)

Another directive around the same time was the Waste from Electrical and Electronic Equipment (WEEE) Directive, and its objective defined the responsibility of the e-waste, “A Producer Responsibility directive aimed at reducing waste from electrical and electronic products by increasing recovery and recycling and minimizing environmental impact.” (WEEE, 2003)

Together RoHS and WEEE added a new level of complexity to electronic designs/manufacturing, the most dramatic impact being finding an alternative Pb-free solder paste.

Alternative Pb-Free Solders

The push for a preferred replacement of a Pb-free solder alloy has created the new criteria for an alloy that has the acceptable electro/mechanical and thermal properties, nonhazardous, good wetting, low cost and possibly with a similar or lower melting and processing temperature compared to SnPb. (Surashi, et al., 2001) These new criteria raised the call for research to provide the industry with adequate amount of data on what are the suitable alloy compositions and their material properties, reliability models, cost-effectiveness and feasibility for implementation for the entire industry. (Vianco, et al., 1995)

The Pb-free solder will continue to be Tin-Based for its historic data on performance, available, and low cost. The alternative element/s considered with Sn as a binary or ternary system etc., included in this study are SnAgCu alloys, the eutectic SnBi, and the hypoeutectic SnBiAg and SnBiAgX.

Eutectic alloy compositions were the initial focus as suitable alternative due to the melting properties of a eutectic alloy, like Sn63Pb37 that has a specific melting temperature at 183C. There are fatigue life benefits for a solder joint with a lamellar microstructure as a result of the uniform times to solidification and diffusion of the solders intermetallic. (Glazer, 1994) (Dunford, et al., 2004)

The options of elements that create a eutectic system with Tin are limited in terms of feasibility that the elements are either toxic, not accessible or too expensive. (Kang, et al., 1994) (Loomans, et al., 1994) The eutectic Tin-Bismuth binary system was admissible at first especially with the fact that the element Bismuth lows the melting temperature of the system to 138C while maintaining the ability to wet to other metals. (Tomlinson, et al., 1987) (Felton et al., 1993) Overall the Sn-Bi solder alloy lost favor as results of research revealed its deficiencies including

the negative effects of various element impurities on wetting and also risks of all the deficiencies of using Bismuth that include, low ductility, poor thermal and mechanical reliability. (Mackay, et al., 1985) (Felton, et al. 1993) (Glazer, et al., 1995) (Miao, et al. 2001)

After extensive research for the optimal alternative to SnPb solder alloy the industry consortiums recommended the near-eutectic Sn-Ag-Cu (SAC) alloys. (NSMS, 2001) (SPVC, 2005) The specific SAC alloy highlighted is 96.5Sn-3.0Ag-0.5Cu (by weight percentage) also r(SAC305) for its lower cost and competitive performance. (Bath, et al. 2000) (Ngoh, et al., 2004) (Zhu, et. al., 2005)

Deficiencies of SAC Alloys

The composition of SAC solder alloys has some disadvantages, the largest obstacle EMA's have to account for is the higher solder melting temperature which increased from 183℃ for Leaded solder to 217℃ for SAC305 a 34℃ change. There have been numerous studies and white papers on PCBA challenges and failure modes that have been attributed to the higher process temperature requirements of SAC305 alloy use. (Wada, et al., 2017) The high temperature remains a hindrance of the mechanical strength of the SAC alloys surface. (Bukhari, et al., 2004) As the mechanical properties are affected by these high temperatures, it is also been found how a variety of components form solder joint defects from their warpage. Warpage studies have continued to be a concern for EMS providers as these solder joint defects impact yield with the formation of open defects, head and pillow and bridging. (Amir, et al., 2009) (Mokller, et al., 2016) (Kondrachova, et al., 2012) The increased concurrent costs associated with working at these high process temperatures are found to compounding as advanced material technology requirements force the use of PCBs with high Tg substrates to manage the heat. (Mei, et al., 1996) Another initial backlash

regarding cost is in the SAC alloy element composition containing silver (Ag) which alone is more expensive than other elements, but its effects on yield loss has been seen to lower drop test results and compromise thermal cycling performance. (Mei, et al., 1996) (Shnawah, et al., 2012) Another disadvantage of the higher Ag alloys is that they will form more intermetallic within the bulk solder. These intermetallic are Ag_3Sn platelets and risk the solder joints reliability since an interface like this will degrade its surrounding from thermal differences and mechanical stresses.

Another defect exposed through use of SAC alloys in electronic assemblies is the growth of tin whiskers on weak locations on the surface of the solder joint causing failures from electrical shorts to risking cracks propagating. (Oresjo, 2005)

From a sustainability point of view the use of SAC alloys require a larger power load that EMS providers facilities need to maintain the higher temperatures of their ovens. In terms of environmental impact, the power plants supporting the EMS's need to supply more power and a resulting in increased CO2 emissions levels. (Aspandiar et al., 2015) This increased power demand at the geolocations of EMA's can require additional power production on the electrical grid that could be running older power plants that are less efficient and more pollutant on a global scale

Lower Temperature Solder Projects

A method explored to enable lower process temperatures is mixing SnPb solder alloys with components designed for Pb-free/SAC solder alloys, and is referred as research of backwards compatibility. As mentioned, those selected in the RoHS exempt group face supply chain issues of availability and cost to get components for their SnPb soldered assemblies (2007). The mixed

assembly research consists of SAC alloyed components like ball grid arrays (BGAs) with SnPb solder paste. The key factors found are in getting acceptable mixing greater than 30% to the defect of hot tearing at the PCB land interface yet less than 80% to avoid the defect of brittle rupture at the package land-solder interface. (Fu, et al. 2017) Related mixing research has been tested at temperatures peaking as low as 208℃ yielding non-homogenous solder joints exhibiting uneven compositions and microstructures that do outperform traditional leaded assemblies in thermal fatigue testing. (Hua, et al., 2003) (Handwerker, et al., 2004) The literature also reveals information on partial mixed solder joints that show a measurable degradation in reliability compared to full mixing which enable self-alignment and fully collapsed joints that yield key characteristics of acceptable solder joint geometry and quality. (Coyle, et al., 2013) The limitation of the impact of these mixing studies is that they are not applicable to the entire industry only those currently still exempt from RoHS. These leads to the synthesis of another mixed alloy assembly approach revisiting the various of Pb-free solders like Sn-Bi or Sn-Bi compositions that could further reduce the manufacturing process temperatures required for SAC solder alloys.(Snugovsky, et al., 2007) (Snugovsky, et al., 2007) (Chen, et al., 2016)(Tang, et al. 2016) (Coyle, et al., 2017) The reducing the peak temperatures can lead to even greater yields demonstrated by the warpage of a common component in was found to be reduced by 30-50% when reflow peak temperatures were in the range of 160-180C (Mokler, et al., 2016)

Bismuth Based Solder Alloys

The use of Bi as a micro alloy with as little as less than 5 % of Bi to form Sn-Ag-Cu-Bi (SACBi) solder alternative showed promising results of interest as research done at organizations including the Department of Defense and NASA, presenting improvements in thermal cycling

reliability and reduce melting temperature by 10-11degrees compared to SAC Alloys while also increasing solder joint performance in thermal shock testing. (Sampathkumar, et al., 2005) (Mattila, et al., 2007) (Woodrow, 2008) (Woodrow, 2010) Another benefit Bradley and colleagues also demonstrated that the minor amounts of Bismuth with SAC alloys can reveal reduction in tin whisker growth at concentration levels of Bi between 2-4 the weight % to Sn. (Bradley, 2007) (Guene, 2013) (Maalekian, et al., 2015)

Bismuth was of great interest for a SnBi solder alloy alternative to SnPb in the years surrounding the RoHS directive mainly for its cost and availably. [1-46] Promising results of tensile strength and creep resistance of eutectic SnBi which melts at 138C compared to be better than that of SnPb same properties. (MacKay, et al., 1985) (Tomlinson, et al. 1987) (Felton et al., 1993) (Kang, et al., 1994) (Hwang, 2000) (Sandy et al., 2011) Still the eutectic SnBi was discredited as a viable solution from poor mechanical shock and fatigue resistance from the very nature of the element Bismuth is known to be more brittle than most. (Mei, et al., 1996) (Pandher & Healey, 2008) These properties of Bi lead to an understanding of poor drop performance compared to Sn-Ag3.0-Cu0.5 that has a drop shock performance 4x of the SnBi alloy. (Ribas, et al., 2014). Despite the decline in Sn-Bi the results of many micro alloying studies show the addition of Ag by 0.25wt% to 1.0wt% to SnBi improved the ductility and reduced brittleness an increase in tensile strength and elongation and young's modulus, a good indicator of drop shock performance of a SnBi solder joint. (McCormack, et al., 1997) (Schroeder, et al., 2001) Recent studies confirmed these improved mechanical and thermal properties of SnBi with small Ag additions and the preferred alloy being commercialized is Sn42/Bi57.6/Ag0.4. (Lee, 2015)

The struggle still exists of the high temperatures of SAC alloys and alternatives for use in microelectronic interconnections and for package-on-package assemblies still continues to be

researched to enable lower temperature processes. (Liang, et al., 2007) (Vijayaragavan, et al., 2008) (Garrou, 2014) Also the goal remains for EMS providers to once again utilize low Tg substrates and other component materials previously reliable for SnPb to further reduce costs. (Juarez, et al., 2013)

Review of Past Studies and Deficiencies

The large efforts of implement Low Temperature solder alloys drives the need to establishing the industries state of knowledge and understanding to focus and address research gaps. Areas of knowledge gaps regarding mixed alloy assemblies are associated with the challenges in manufacturing processes and reliability. Mixed alloy assembly studies are beginning to raise in numbers attempting to fully characterize the complex microstructure of mixed SnBi with SAC solder alloy and the influence on electrical, mechanical and thermal properties.

As the industry considered backwards compatible mixed SAC/SnPb alloy assembles there are cross references to be made including the complex solidification behavior of mixed alloy assemblies revealing that shrinkage voids in rework or crack propagations can occur through the low melt accumulation region of a mixed SAC Sn-Pb alloy assembly, therefore an indication of potentially similar challenge for mixed SAC-SnBi alloy assemblies. (Snugovsky, et al., 2007) (Snugovsky, et al., 2008) (Henshall, et al., 2008) (Ribas, et al., 2013)

Research must address manufacturing process influences on mixing with the concern of proper solder joint collapse related to correct volumes of pastes and optimal profiles of various size components or risk further reduction of mechanical properties compared to SAC alloy solder joints. (Yoon, et al., 2004) (Fu, et al., 2010) (Sandy, et al., 2011) (Liu, et al., 2014)

Optimal reflow profiles are a key factor for mixing and solder joint collapse height as a function of peak temperature. (Fu, et al., 2010) (Chen, et al., 2016) (Mokler, et. al., 2016) (Chen, et al., 2016) (Mutuku, et al., 2018)

Anselm et al. has presented extensive work of the relationship of mixed SAC/SnBi alloy assemblies including results showing the Bismuth mixing with various peak temperatures and the associated shear strength associated with the microstructures of these mixed solder joints. Palaniappan et al., assembled the mixed SAC/SnBi and SAC/SnBiX alloys at the reflow process temperatures of typical of SnPb and SAC, then observed the locations of the cracks that propagated through the Bi phases consist for both reflow profiles, while also observing the significant differences of mixing levels between the profiles. Valooran et al., built upon the previous study by corelating shear strengths to the mixing percentages of a SAC/SnBi system at peak temperatures 175C and 185C, both well in the accepted "low" temperature zone. Gomez et al. recently published work that advanced LTS process development by characterizing the mixing relationship of three SnBiX solders mixed with SAC305 assembled at peak temperatures 175C-215C increment every 5C degrees to begin to build a modeling database for EMS providers. It was found that there existing mixing mechanisms that are more dominant in some solder alloys than others. (Aspandiar, et al., 2017) One mixing mechanism came the center of the solder joint heating similarly to the outside of the solder joints diffusion more of the Bismuth uniformly across the solder joint. The other mechanism showed the wetting of the solder going higher on the outside of the solder joint then compared to the center which remained significantly lower, this was determined to be a function of flux as well as melting temperature.

In 2017, Gomez et. al., and industry partners at Intel determined two mixing mechanisms for mixed solder alloys. (Aspandiar, et. al., 2017) (Gomez, et. al., 2017) Mechanism #1 Center diffusion is when the BiSn solder paste diffuses into the solder ball via the center of the solder

joint shown in Figure 5 Significant factors to increase lattice or grain boundary diffusion of Bi would dependent on the Bismuth concentration gradient and from the SAC Ball alloy composition and just identifying there is a difference between solder paste can be another low temperature attribute for implementors to recognize. (Aspandiar, et. al., 2017)

In Figure 6 represents mechanism #2 Wetting for which a lower temperature solder paste will be able to mix more with a solder ball by wetting around the undiffused high melting solder ball. This wetting/wicking of solder paste over the solder ball limits the ability for the solder ball to get higher center diffusing levels driven by the paste flux covering the ball reducing its energy. (Aspandiar, et. al., 2017)

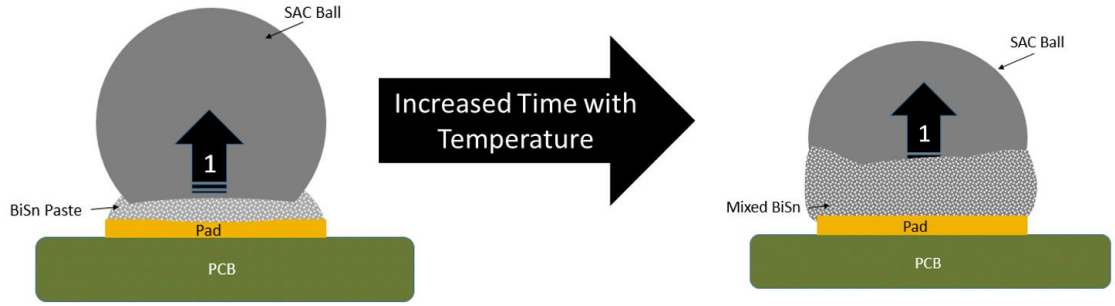

Figure 2 Mixing Mechanism #1

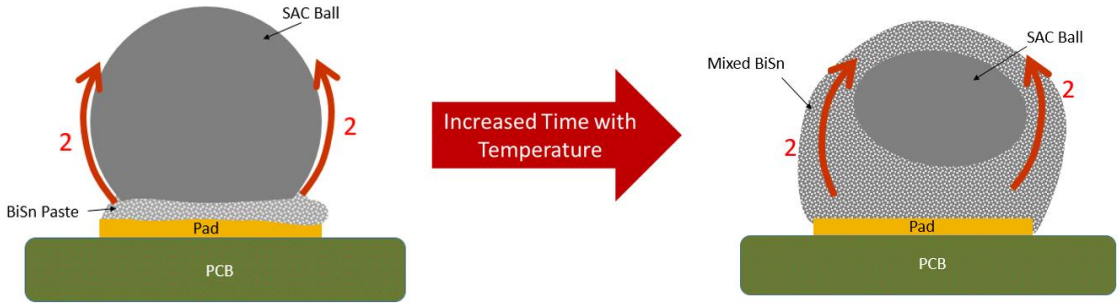

Figure 3 Mixing Mechanism #2

The limitation of the previous three studies merely remain in the assembly method of the mix solder joints being of isolated solder balls manually placed on low temperature solder paste. This practice of ball and paste assembly is efficient for metallurgical comparisons though full system testing of actual components could alter the results significantly.

This study addresses the research opportunity is to add more data for characterizing the mixing relationship of multiple SnBiX solders mixed with SAC alloys specific to component size while also gaining insight on the influence that the time above the melting point of the SnBiX solders will impact mixing.

EXPERIMENT #1 BALL AND PASTE ASSEMBLY

Objective and Motivation

The objective of this study was to observe the mixing of SnBiX-SAC Solder Ball Joints at extended reflow times above melting ≥ 138ºC at various peak temperatures.

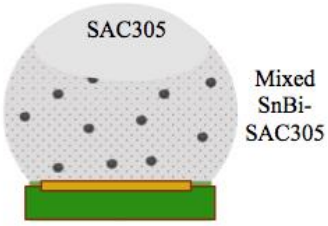

Figure 4 Ball and Paste Illustration

The results of this experiment will enable manufactures to understand that non-realistic times above melting will produce larger mixing results. Part of the goal of alternative low temperature Pb-free solders is that they are adopted by the industry, a factor that would hinder this adoption would that more time is added to produce a single device negatively effecting through put. Consider the costs that a major electronics manufacturer would have if they needed to add more than 30-150 seconds on to there through-put time; that is why this study will aim to eliminate speculation that only more time can achieve optimal results when mixing SnBi solder pastes with SAC Solder balls.

Test Matrix

DOE Test Matrix	Level-1	Level-2	Level-3
Reflow Profile Max. Temperature, °C	180°C	195°C	205°C
Lead Free Paste	Indalloy #281 (58%Bi 42%Sn)	OM550 (40%-58% of Bi)	Indalloy #282 (57%Bi 42%Sn 1% Ag)
Time Above Melting (TAM) ≥ 138ºC	120 sec	240 sec	
Solder Ball Details	Sn3.0Ag0.5Cu (SAC305) Diameter = 18 mils		

Table 1 Experiment #1 Test Matrix

This study will be quantitative and yield Bismuth mixing percentages to explore the correlational to time above melting. The significance of the direct correlation between higher peak convection reflow temperatures with longer times above melting and higher mixing percentages of SnBi-SnAgCu Solder Ball Joints will be analyzed.

The independent variables include; Reflow Profile Maximum Temperature, Low Temperature Solder Pastes, Time Above Melting (TAM). The dependent variables; Mixing Percentage of Solder Pastes and Solder Ball. The control factor in this experiment is the Solder Ball Composition of Sn96.5%Ag3.0Cu0.5%, SAC305.

Materials

Three Tin-Bismuth solder alloy pastes have been selected to validate and further accumulate data similar to another low temperature solder project. (Gomez, et al., 2017) These solder pastes

mixed with widely accepted default Pb-Free solder alloy SAC305. The alloy names, constituent elements, minimum melting temperatures are shown below.

Table 2. Experiment #1 Material Properties

#	RIT Solder Alloy Name	Known Alloy Constituents and Composition	Melting Temp. (˚C)	Sphere Diam.
1	Indalloy #281	58%Bi/Sn42%	138ºC	Type 4
2	Indalloy #282	57%Bi/42%Sn/1%Ag	~140ºC	Type 4
3	OM550	Bi% between 40% and 58% plus additional micro-alloy additives	Around ~151 ˚C	Type 4
4	SAC305 Solder Ball	96.5%Sn3%Ag0.5%Cu	~217ºC	18 mils

Indalloy #281 is the Eutectic Tin-Bismuth solder alloy and represents the largest percentage of Bismuth for a Pb-Free solder paste alternative. Indalloy #282 has a slightly lower Bi content and includes Ag while also having an increased melting temperature. The OM550 is characterized to be a more reliable LTS in harsher environments all for an affordable cost compared to SAC305. (Alpha, 2018)

Test Vehicle

This study utilizes a PCB with the following attributes defined in Table 3 and can be seen in Figure 1. The assembly location is outlined in red, reflow direction indicated by the arrow, and reflow profiling thermocouple locations marked in yellow.

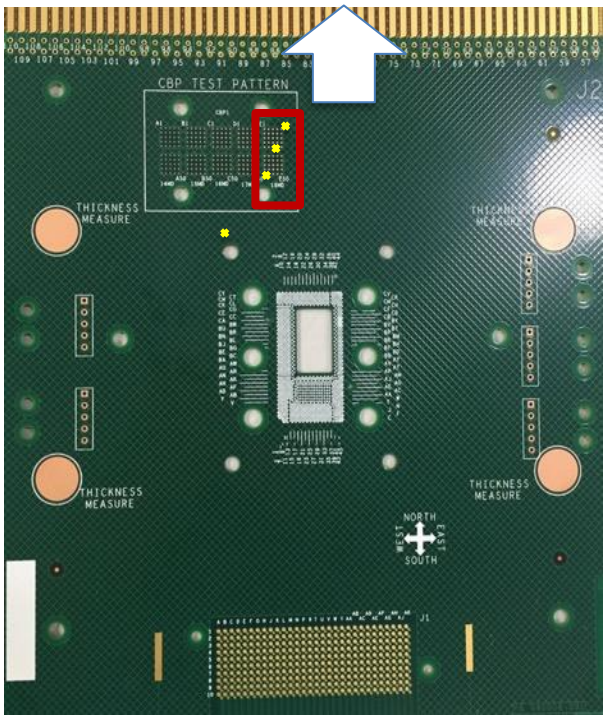

Figure 5. Experiment #1 Test Vehicle

Table 3. Experiment #1 Test Vehicle Details

PCB Attributes	
Dimensions	140.8 x 153mm
Thickness	0.0355 mm
Surface Finish	Cu OSP
No. Cu Layers	8
Pad Diameter	0.4572 mm (18mils)
No. Pads	10

Assembly Details

The assembly technique used is categorized as a Ball and Paste (BP) method, this is describing that a solder ball will be placed on the solder pad locations that have solder paste. The procedure of this assembly technique follows the following modified surface mount assembly steps:

1.) Application of Solder by Stencil and Squeegee

2.) Placement of Solder balls by operator using tweezers and microscope

3.) Convection Reflow Oven to melt and join solder

There is risk of errors associated with the manually placement of the solder balls with this assembly method. The cost and academic nature of the expected results justified manually

placement despite the risk of misalignment and or placement pressure variability. The overall effects on results have been anticipated and have been qualitatively not deemed a significant error on the mixing of the solder ball to solder joint. This is still acknowledged as a deficiency within this method of assembly. This method of assembly is not realistic for production and the results to provide metallurgical evidence of the broad influence of Time Above Melting on practical manufacturing process parameters.

SMT Assembly Equipment Parameters

Stencil Printing

In the Printing process of the solder pastes on the board the DEK Horizons 01ix Proactive Stencil Printer was programmed with a speed of 50 mm/s and a pressure of 5.0 kg force. All solder paste printed locations were analyzed with an inline Koh Young Solder Paste inspection machine along with manual visual inspection to determine paste transfer efficiency of each print. Each board was analyzed with a pass/fail criterion that accounted for volume, area, shape and height of each solder paste deposits. The volume of solder Paste to volume of the solder sphere is a 0.21:1 ratio.

Stencil Details	
Thickness	5 mils
Aperture	18 mils
Finish	Laser Cut
Size	VG260 (23” Vector Guard)
Stencil Printer Machine Setting	
Speed	50 mm/s
Pressure	5.0 kg
Squeegee	Metal, 60˚
Supports	Magnetic

Table 4 Experiment #1 Stencil Printing Details

Solder Mixture Composition Calculations

The aperture design of the stencil and the weight percentage of the elements in the solder paste and solder ball enable an approximation for determining the mixed solder joints element composition to compare. Finding the theoretical volume of the paste uses the volume of a cylinder

formula V= πr2h. Assuming that the radius of the stencil is 9 mils and that the thickness of the stencil is 5 mils, we can obtain the following:

Vol. paste deposit = π x $(0.009 \text{ mils})^2$x 0.005

= 1.2717×10^{-6} inch^3

= $2.084 \times 10^{-5} \text{cm}^3$ ($1 \text{ inch}^3 = 16.387 \text{ cm}^3$)

Since all the solder pastes that were used are a Type 4 Solder Paste, they are 50% metal content and 50% flux, requiring the necessity to divide the Vol. paste deposit in two which will estimate the volume of the metal of the solder deposited.

Vol. paste deposit = $1.042 \times 10^{-5} \text{cm}^3$

Taking the volume of the metal content and knowing that the density of 58Bi/Sn42 is 8.56 g/cm^3, we can calculate the Mass of the metal content:

Mass = Density x Volume

= 8.56 g/cm^3 x ($1.042 \times 10^{-5} \text{cm}^3$) = 0.0892 mg

Mass of the metal content for 58Bi/42Sn = 0.0892 mg

Next, we can calculate the metal content of the 96.5Sn/3.0Ag/0.5Cu (SAC305) solder ball, V = 4/3 πr^3. Assuming that the radius of the stencil is 9 mils, we can obtain the following:

Vol. SAC305 = 4/3 * π * $(0.009)^3$

= 3.05×10^{-6} inch^3

= $5.0 \times 10^{-5} \text{cm}^3$ ($1 \text{ inch}^3 = 16.387 \text{ cm}^3$)

Taking the volume of the metal content and knowing that the density of SAC305 is 7.40 g/cm^3, we can calculate the Mass of the metal content:

$= 7.40\ g/cm^3 \times 5.0 \times 10^{-5} cm^3 = 0.00037g$

Mass SAC305 = 0.37 mg

The total mass would be Mass 58Bi/Sn42 + Mass SAC305 = 0.4592 mg

The composition of the 58Bi/Sn42 Paste is: Bi - 58 wt% /Sn - 42 wt% , and that the composition for SAC305 is: Sn - 96.5 wt% / Ag - 3.0 wt% / Cu - 0.5 wt%. We can then multiply the composition of the 58Bi/Sn42 paste with the mass of the 58Bi/Sn42 paste in order to obtain the mass of each element in the 58Bi/Sn42 paste deposit:

Bi - 0.05174 mg/ Sn - 0. 03746 mg (6)

Repeat for SAC305:

Sn – 0.3571 mg / Ag - 0.0111 mg / Cu - 0.00185 mg

Add the masses of all the elements

Sn - 0. 3946 mg / Bi – 0.05174 mg/ Ag - 0. 0111 mg / Cu - 0. 00185 mg (8)

Finally, to obtain the wt% the mass of each element in the alloy divided by the total mass 0.4592mg

Sn% – 85.91 wt%
Bi% – 11.27 wt%
Ag% – 2.42 wt%
Cu% - 0.40 wt%

This was done for the 57Bi/Sn42/1Ag in the table below, missing due to proprietary restrictions is the OM550.

Mixed Solder Alloy	Composition in Wt% of Solder Mixture
58Bi/42Sn + 96.5Sn/3.0Ag/0.5Cu	Sn% – 85.91 wt% Bi% – 11.27 wt% Ag% – 2.42 wt% Cu% - 0.40 wt%
57Bi/42Sn/1Ag + 96.5Sn/3.0Ag/0.5Cu	Sn% – 85.91 wt% Bi% – 11.08 wt% Ag% – 2.61 wt% Cu% - 0.40 wt%

Table 5 Composition in wt.% for 58Bi/Sn42 +SAC305 Alloy Mixtures

Reflow Oven Profile Details

The convection reflow oven used was the 8-heating zone Heller 1808 MK III and profile developments utilizing the KIC RPI Reflow Software and SPS wireless reflow profiler hardware. This profile development software enabled accurate process parameters to be met according to our research design of peak temperatures and times above melting. K-type thermocouples were epoxied to the locations marked in yellow in Figure 1 to get temperature distribution data across the assembly location. This temperature data also enabled the KIC RPI Reflow Software to utilize its prediction algorithms to enhance profile development. The reflow profile process specifications for this study are shown in the table below and were defined in collaboration with our industry partner.

Table 6. Experiment #1 Reflow Profile Parameters

Process Parameter	#1	#2	#3	#4	#5	#6
Peak Reflow Temperature (ºC)	180ºC	180ºC	195ºC	195ºC	205ºC	205ºC
Time Above Melting (TAM) ≥ 138ºC	120 sec	240 sec	120 sec	240 sec	120 sec	240 sec
Cooling Rate (ºC/sec)	1-3 ºC/sec					
Initial Ramp Rate (ºC/sec)	1-3 ºC/sec					
Soak Time (100 – 120 ºC) sec	60 – 90 sec					

To develop the reflow profile on of the PCBs was required to be scrapped for the attachment of thermocouples with an epoxy and resin. The locations of these thermocouples enabled temperature data at various points of where the solder joints will be formed including at pads and board temperature. An example of one such profile developed is below as a screenshot within the profiling software that collects your temperature data and analyzes it as a Process Window Index (PWI) % across all specifications.

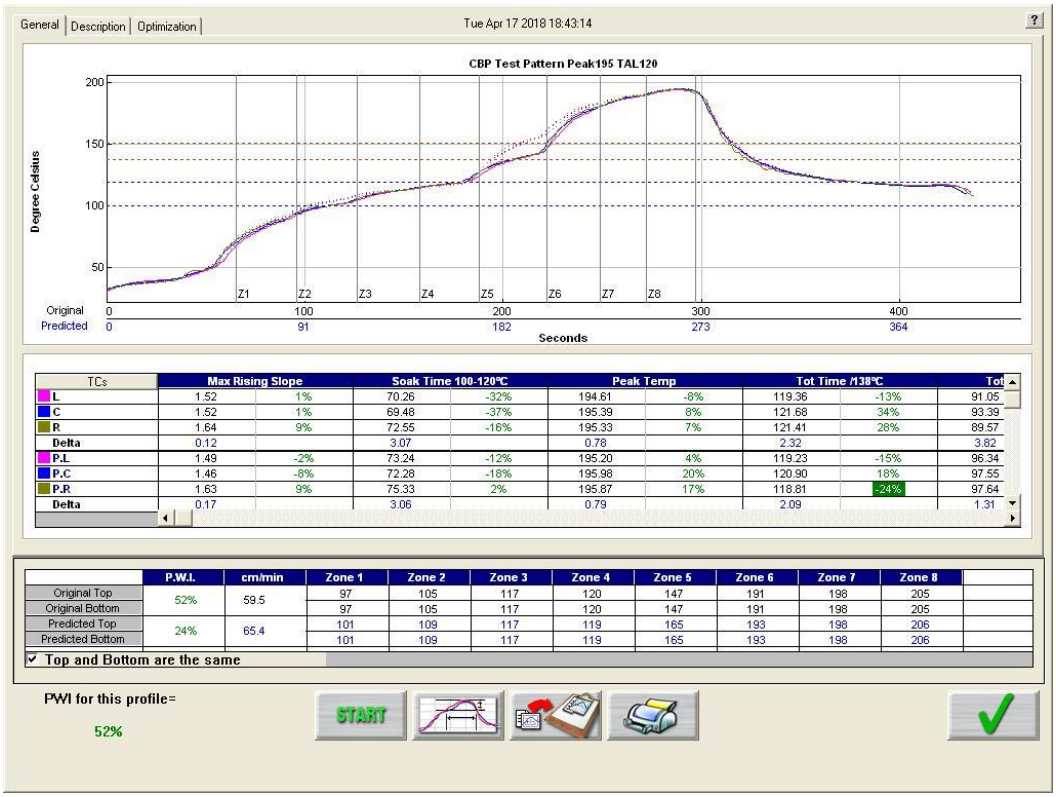

Figure 6 Reflow Oven Profiling Sample, Peak Temp. 195˚C and TAM: 120 sec

When a PWI% is determined acceptable typically PWI%<75% then the profile development is complete. Figure 2 is the completed profile showing the conveyer belt speed and all the reflow oven zone temperatures of Profile #3 that has a Peak Temperature 195ºC and a TAM = 120 sec., ready for production use as the final step in the assembly process before enabling the next step of cross-sectional analysis. Reflow oven profiles used in each leg of the experiment can be found in Appendix A along with the details of each temperature of the zones of the oven for any given profile used.

Build Matrix

Table 7. Experiment #1 Build Matrix

Board #	Reflow Condition	Reflow Condition	Solder Paste
1	180C Peak	120 sec TAM	Indalloy #281 (58%Bi 42%Sn)
2	195C Peak	120 sec TAM	
3	205C Peak	120 sec TAM	
4	180C Peak	240 sec TAM	
5	195C Peak	240 sec TAM	
6	205C Peak	240 sec TAM	
Board #	Reflow Condition	Reflow Condition	Solder Paste
7	180C Peak	120 sec TAM	ALPHA Paste (40%- 58% Bi)
8	195C Peak	120 sec TAM	
9	205C Peak	120 sec TAM	
10	180C Peak	240 sec TAM	
11	195C Peak	240 sec TAM	
12	205C Peak	240 sec TAM	
Board #	Reflow Condition	Reflow Condition	Solder Paste
13	180C Peak	120 sec TAM	Indalloy #282 (57%Bi 42%Sn 1% Ag)
14	195C Peak	120 sec TAM	
15	205C Peak	120 sec TAM	

16	180C Peak	240 sec TAM	
17	195C Peak	240 sec TAM	
18	205C Peak	240 sec TAM	

Test Method

Measurement Methods

The assembled test boards went through the process of being potted completely in an epoxy resin to enable grinding and polishing of the cross-sectional view of half the mixed alloy solder joint. The diamond particles used polishing of the cross-section will rid the surface of any scratched that might otherwise be hindering our ability to measure the mixing levels of the solder joint.

The method of measuring the mixed SAC305 + SnBi solder joints is determined by the heights of the diffusion of the Bi region into the solder joint on the left, right and center of the solder joint along with the overall height of the solder joint. (Kinyanjui, et. al., 2010)

The equation below shows a method to use the heights for the average mixing percentage of a solder joint. The Figure 3 shows what each suffix in the equation represents. (Aspandiar, et. al., 2017) (Gomez, et. al., 2017)

Equation 1 Average Mixing %

$$Average\ Mixing\% = \frac{((HL + HC + HR)}{3 * HSOH} * 100$$

H_L= Height Left H_C = Height Center
H_R= Height Right H_{SOH}= Solder Overall Height

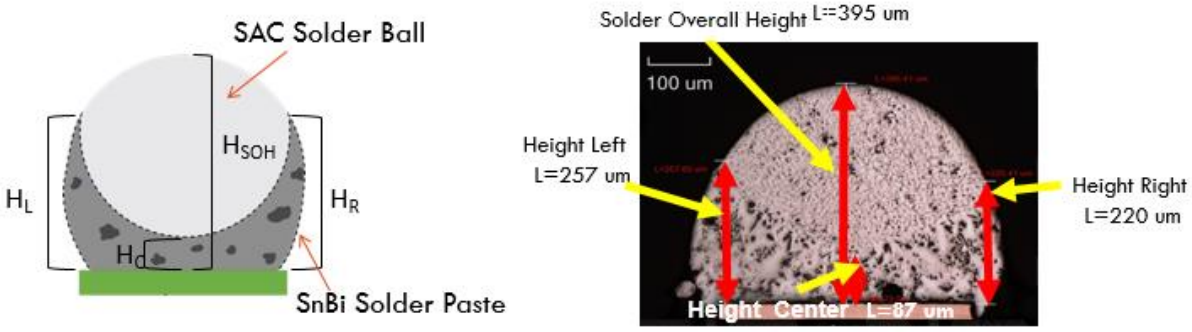

Figure 7 Average Mixing % Measurement Example

Previous mixed alloys studies have been able to use these linear measurement methods and calculations though this study brought upon a new need for measuring surface area to calculate mixing. Shown in Figure 4 is the method used to measure mixing % with the surface areas of a cross-section. Utilizing a polygon selection tool in the NIH Image-J software, measurements were possible to calculate mixing percentages of solder joints that had solder paste wet over top of the SAC305 Solder ball without first fully diffusing the two solder alloys in the center.

$$Average\ Mixing\% = \frac{(Solder\ Joint\ Surface\ Area - \ SAC305\ Surface\ Area)}{Solder\ Joint\ Surface\ Area} * 100$$

Equation 2 Alternate Mixing % Calculation from Solder Joint Surface Area

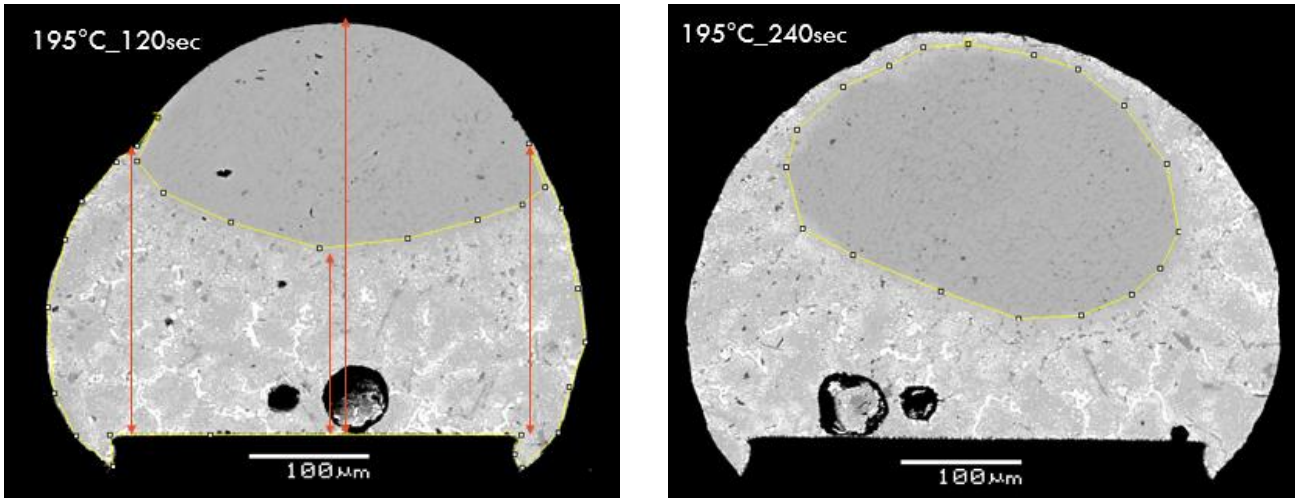

Figure 8 Mixing Measurement Alternative Method

Experimental Results

Bismuth Mixing Results at TAM=120sec

Summary of Mixing% Results, TAM = 120 sec			
Peak Temp.	SnBi40-58%	SnBi57%	SnBi58%
180˚C	**33%**	**41%**	**33%**
195˚C	**58%**	**54%**	**57%**
205˚C	**81%**	**87%**	**73%**

Table 8 Summary of Mixing % Results TAM=120 sec

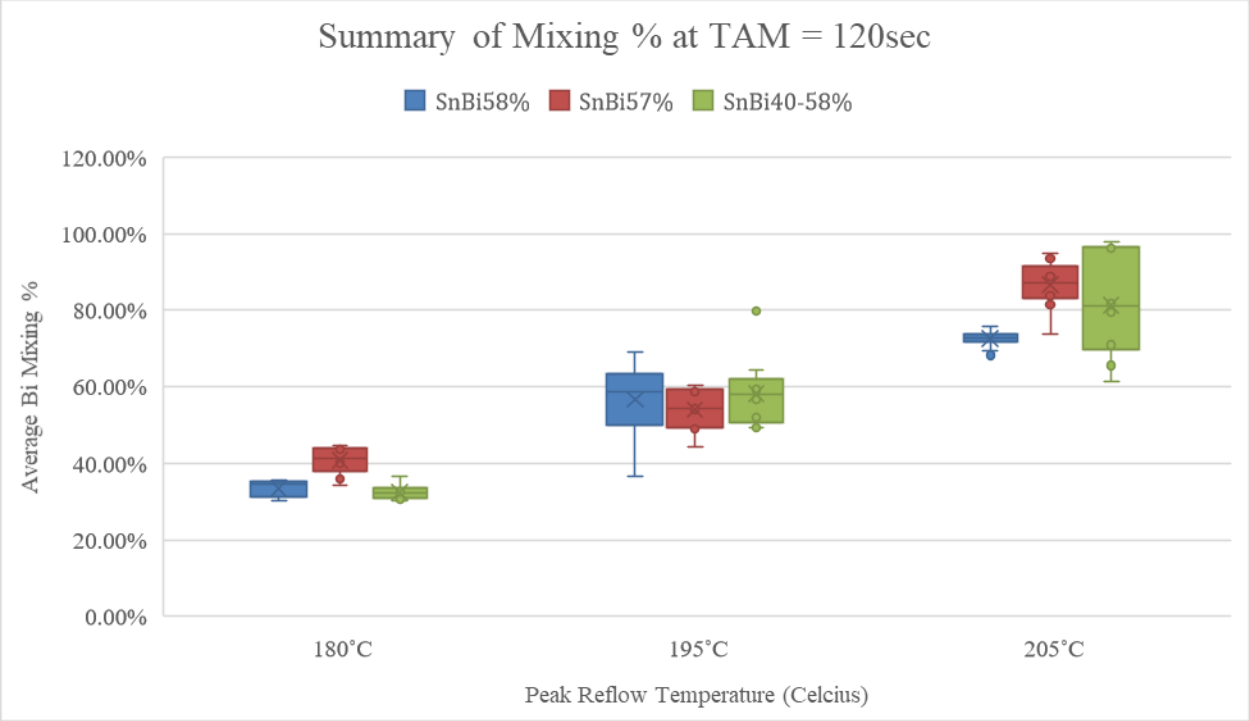

Figure 9. Plot Summary of Mixing % at TAM=120sec

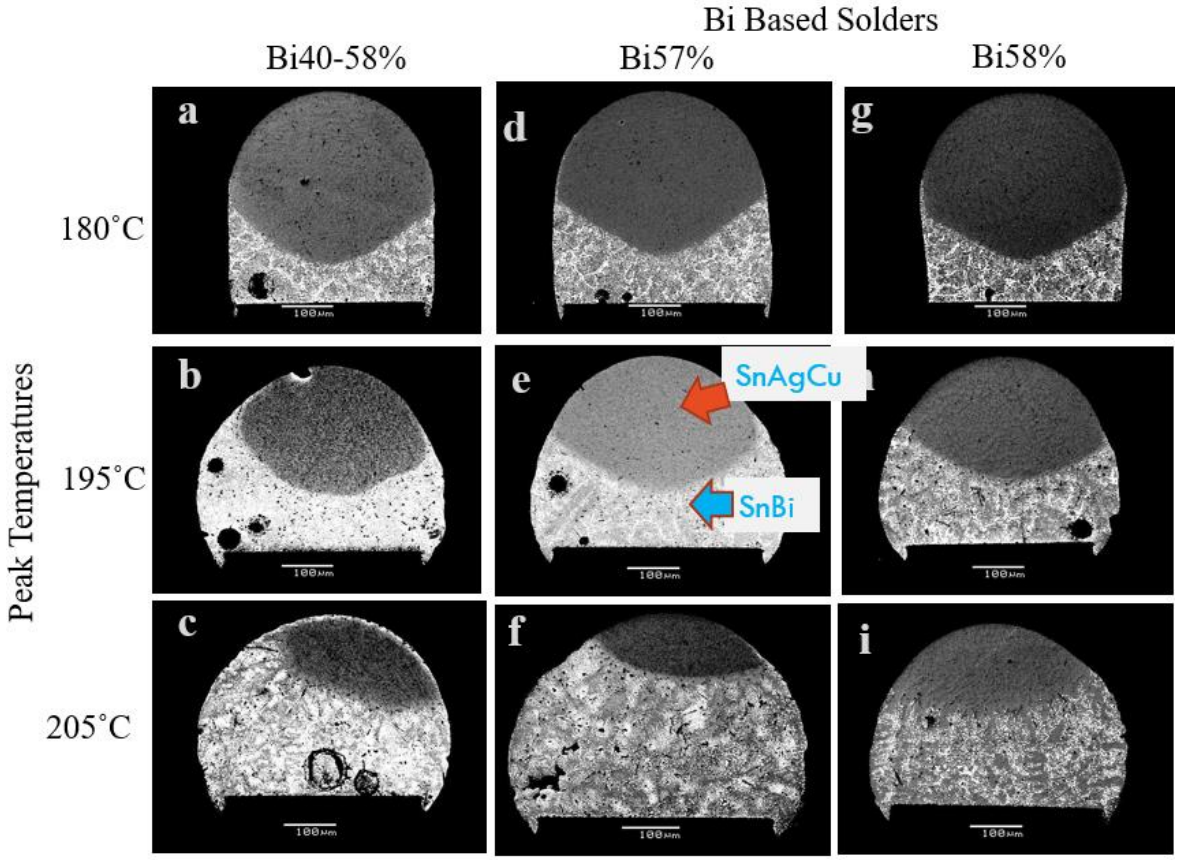

Figure 10 Crossectional SEM Images, Average Mixing Sample TAM:120

The raw data reveals that there are no significantly different mixing levels at 195˚C between all three solder pastes. The solder pastes OM550(40-58%Bi) and Indalloy#281(58%Bi) had no significantly differences between them. A summary of the statistically significant differences between the three solders pastes at each peak temperature for the 120 seconds above melting can be seen in the table below. Table 11 and Table 12 indicate that there is not a significant difference with “No” and with a “Yes” followed by

Solder	TAM:120sec		
	Tpeak	40-58%Bi	58%Bi
57%Bi	180C	Yes More	Yes More
	195C	No	No
	205C	No	Yes More
58%Bi		40-58%Bi	57%Bi
	180C	No	Yes Less
	195C	No	No
	205C	No	Yes Less
40-58%Bi		58%Bi	57%Bi
	180C	No	Yes Less
	195C	No	No
	205C	No	No

Table 9 Summary of Statistical Differences of Mixing Levels between the solder pastes at TAM: 120sec

The example of the two-sample t-tests that was used to calculate significant differences between mixing levels throughout both experiments in this report is shown below in Figure 11 and in Appendix B.

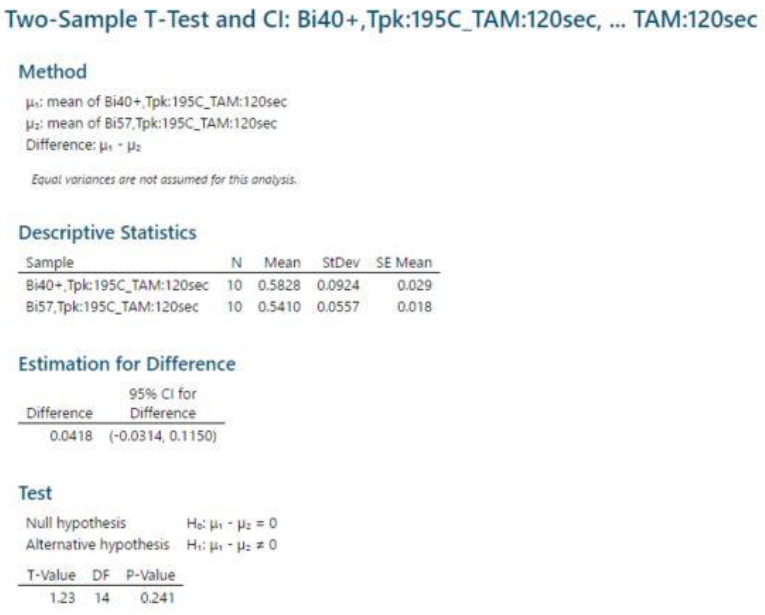

Two-Sample T-Test and CI: Bi40+,Tpk:195C_TAM:120sec, ... TAM:120sec

Method

μ_1: mean of Bi40+,Tpk:195C_TAM:120sec
μ_2: mean of Bi57,Tpk:195C_TAM:120sec
Difference: $\mu_1 - \mu_2$

Equal variances are not assumed for this analysis.

Descriptive Statistics

Sample	N	Mean	StDev	SE Mean
Bi40+,Tpk:195C_TAM:120sec	10	0.5828	0.0924	0.029
Bi57,Tpk:195C_TAM:120sec	10	0.5410	0.0557	0.018

Estimation for Difference

Difference	95% CI for Difference
0.0418	(-0.0314, 0.1150)

Test

Null hypothesis $H_0: \mu_1 - \mu_2 = 0$
Alternative hypothesis $H_1: \mu_1 - \mu_2 \neq 0$

T-Value	DF	P-Value
1.23	14	0.241

Figure 11 Two Sample T-Test Example Calculation

Scanning Electron Microcopy and EDX Analysis

The longer times above melting revealed that at the solder pastes were more susceptible to begin to start wetting up and around the solder ball. The cross-sectional images of the solder joints in Figure 10 are in a greyscale though the bright areas that contrast are the Bismuth rich areas along the unmixed SAC305 regions. The element analysis feature on the SEM identifies elements present on the surface in view and on the next page the EDX capture the presence of Bi, Sn, Ag along separating them by color. The locations of the red area on the EDX map would overlay right on top of the lighter regions of the bright regions of the Bismuths presence. In Figure 10 location “c” the Bismuth paste has wetted up over the top of the solder ball, a feature that is not desired. Figure 11 below separates the elements of the mixed solder joint and the top left image is the presence of the Bismuth that wetted over top of the solder ball and could pose as a reliability threat if this was an electronics assembly that would now have two brittle interfaces at the top and bottom of the solder joint.

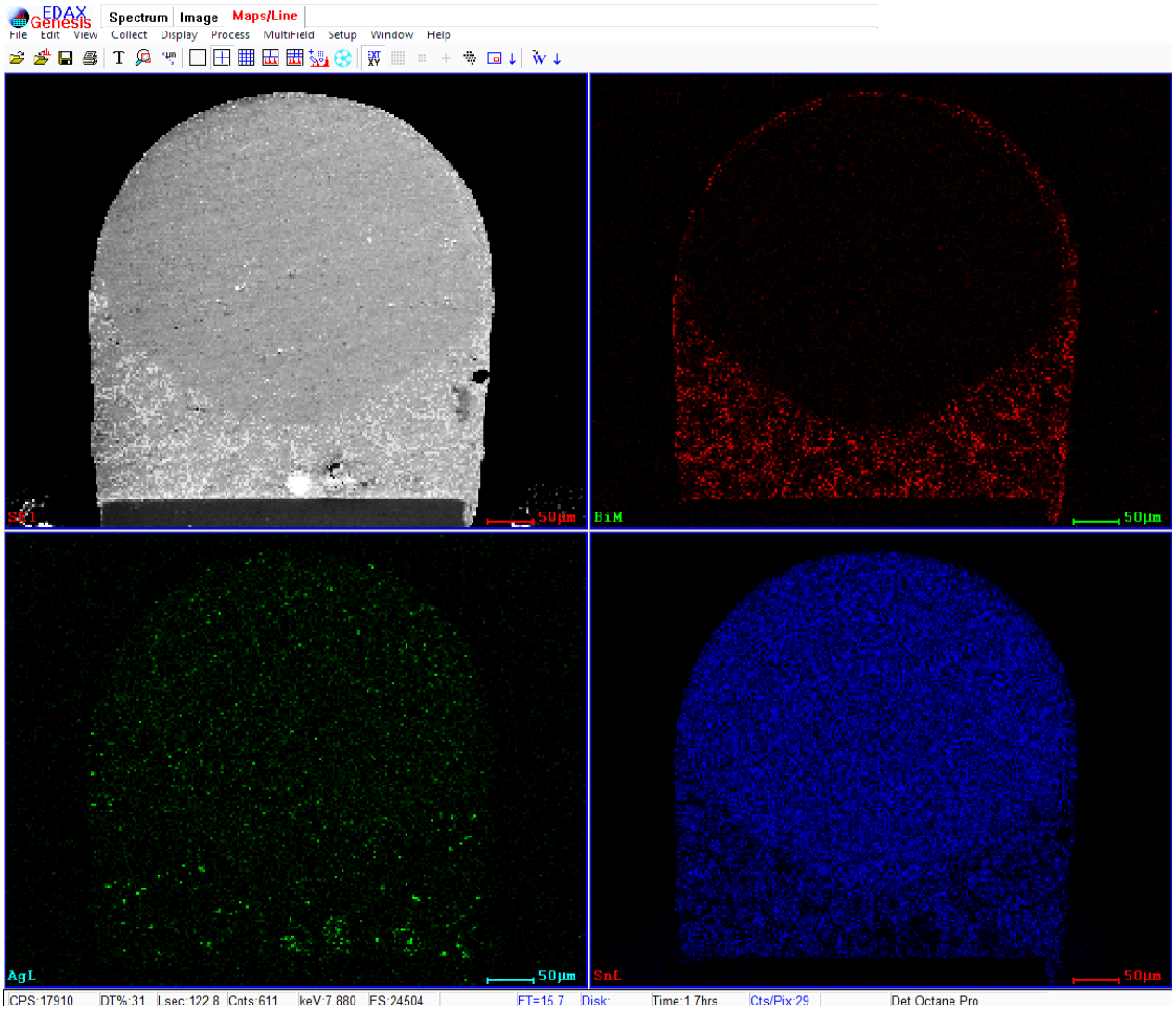

Figure 12 SEM EDX Map of Mixed SnBi-SAC Solder Joint

To confirm the presence of Bismuth the EDX spectrum analysis is seen in Figure 13 and quantifies the Bismuth located at the top center of a solder joint.

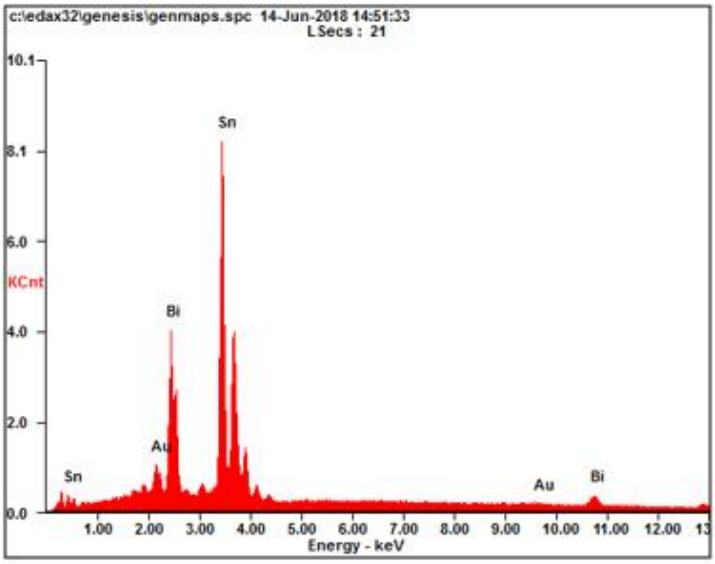

Element	Wt%	At%
BiM	27.32	17.97
SnL	67.97	78.74
AuL	04.71	03.29
Matrix	Correction	ZAF

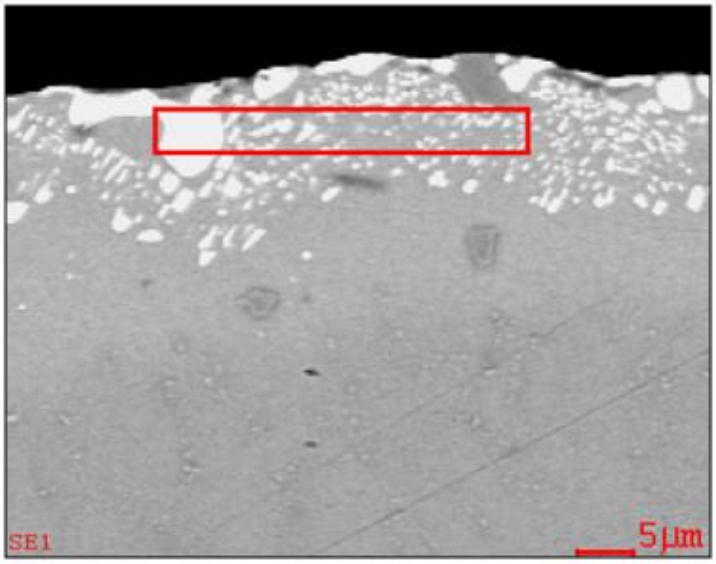

Figure 13 EDX Analysis of Top Surface of Mixed Solder Joint

This spectrum analysis covers an area at the top of a solder joint and illustrates the presence of Bismuth mixed with the major element Sn. The Au presence was due to the sample being sputter coated to be used in the SEM.

Bismuth Mixing Results at TAM=240sec

Summary of Mixing% Results, TAM = 240 sec			
Peak Temp.	SnBi40-58%	SnBi57%	SnBi58%
180˚C	**43%**	**40%**	**45%**
195˚C	**51%**	**61%**	**60%**
205˚C	**89%**	**94%**	**95%**

Table 10 Summary of Mixing % Results at TAM=240sec

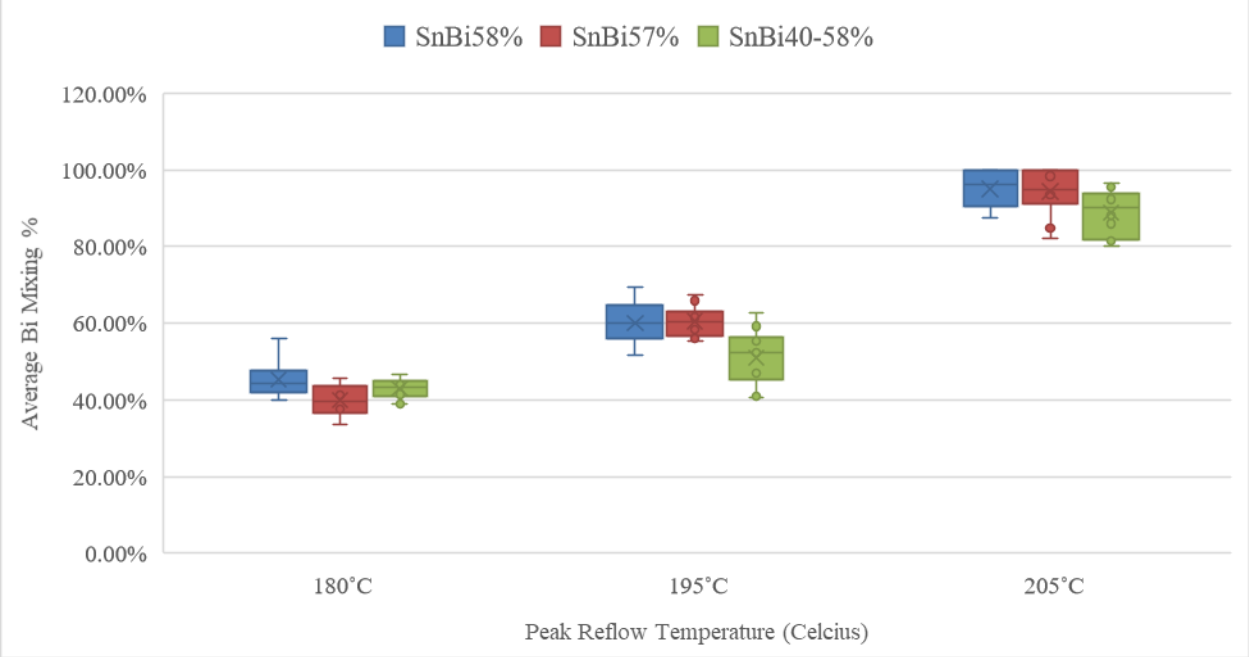

The mixing results for SnBi40-58 are significantly different at the peak temperature of 195C.

Figure 14 Plot Summary of Mixing% Results, TAM=240sec

The complete summary of signigcant differences between the solder paste can be seen in Table 11 below.

Solder	TAM:240sec		
	Tpeak	40-58%Bi	58%Bi
57%Bi	180C	No	Yes Less
	195C	Yes More	No
	205C	No	No
58%Bi		40-58%Bi	57%Bi
	180C	No	Yes More
	195C	Yes More	No
	205C	No	No
40-58%Bi		58%Bi	57%Bi
	180C	No	No
	195C	Yes Less	Yes Less
	205C	No	No

Table 11 Summarized Statistical Differences at TAM: 240 sec

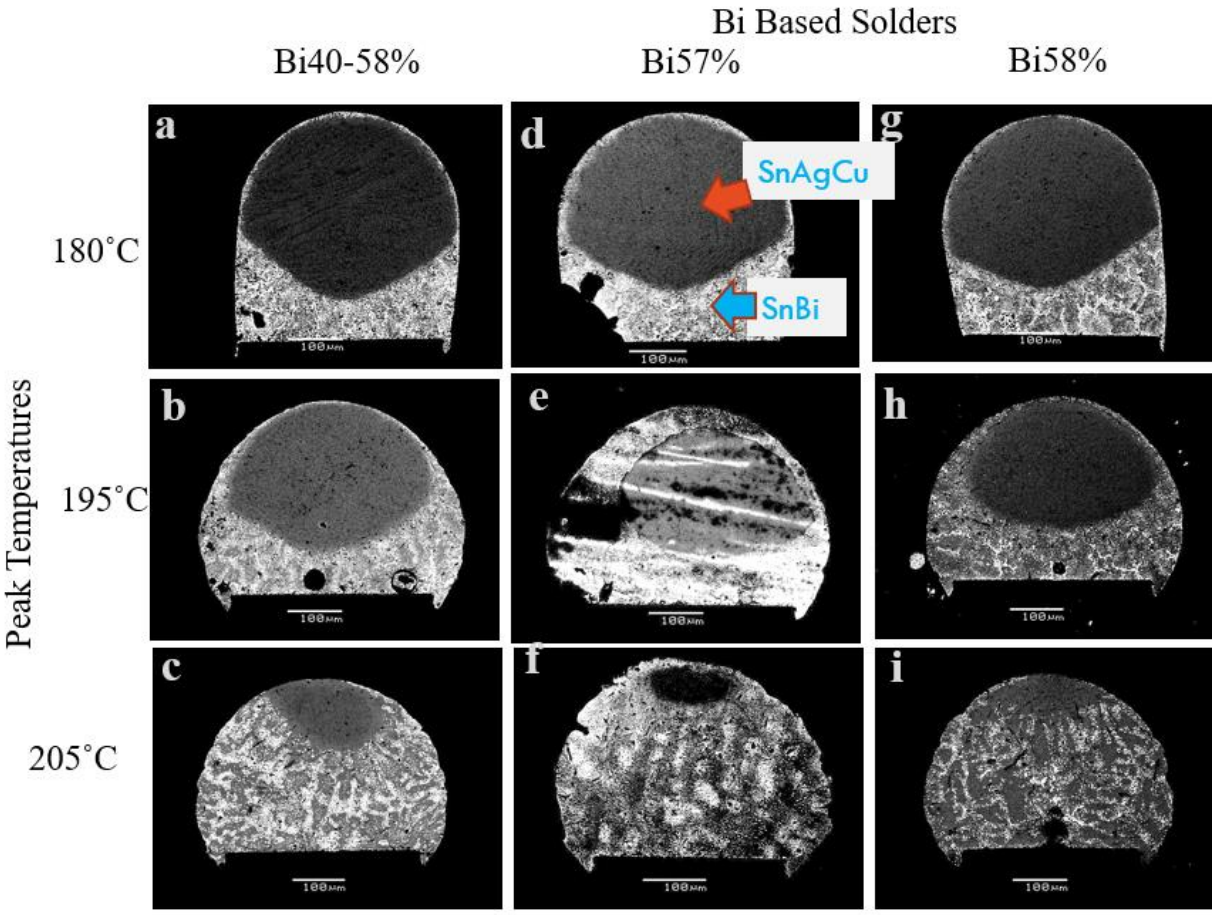

Figure 15 Crossectional SEM Images Avg. Mixing for TAM:240sec

These cross-sectional SEM images of TAM:240sec expose the explicit mixing mechanism that the solder joints create with an extremely long time above their melting point. At each peak temperature the solder joint has the Bi-based solder paste wet to the top of the solder joint risking the strength of the solder joint.

Comparison of Times Above Melting

Mixing % Results of SnBi58%

SnBi58% Mixing% Results			
Peak Temp.	Time Above Melting		
	85sec	120sec	240sec
180˚C	**31%**	**33%**	**45%**
195˚C	**53%**	**57%**	**60%**
205˚C	**97%**	**73%**	**95%**

Table 12 Summary of SnBi58% Mixing% Results

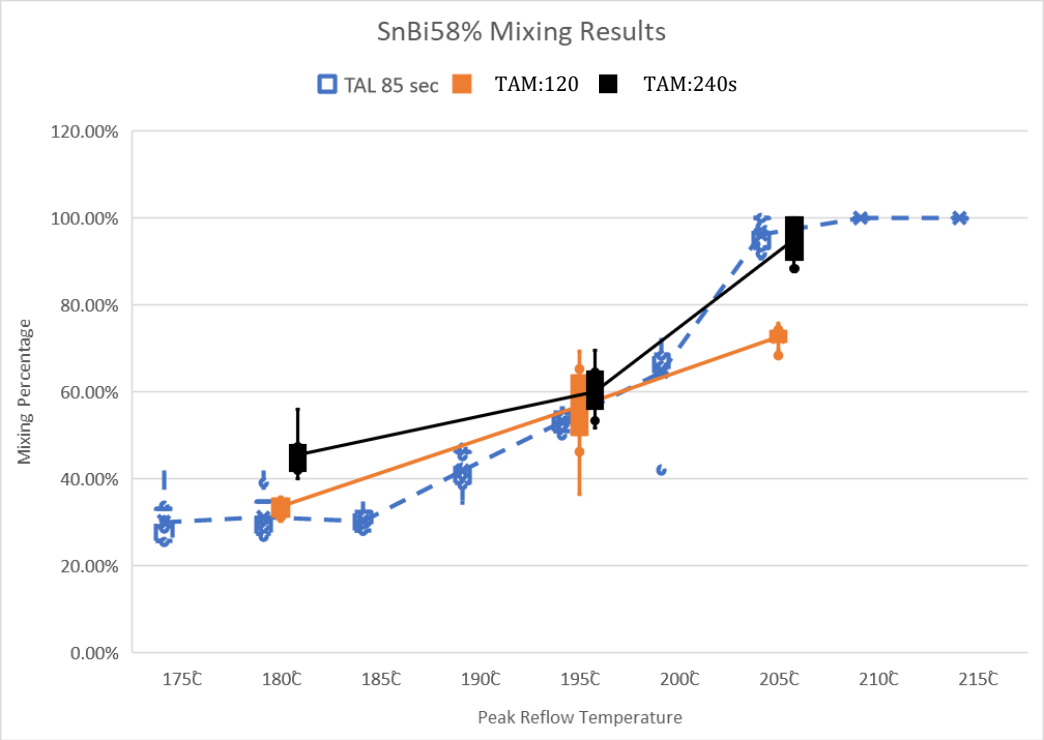

Figure 16 SnBi58 Mixing % at TAM: 85s, 120s, 240s

This combined results plot displays three different TAMs: 85sec, 120sec, 240sec from which their overlapping data can be observed. The dashed data is from a previous study and was a trendline of mixed solder joints at various peak temperatures for a TAM: 85sec. (Gomez, et al. 2017) The mixing results at TAM: 120sec are very similar to those at TAM: 85sec for both 180˚C and 195˚C.

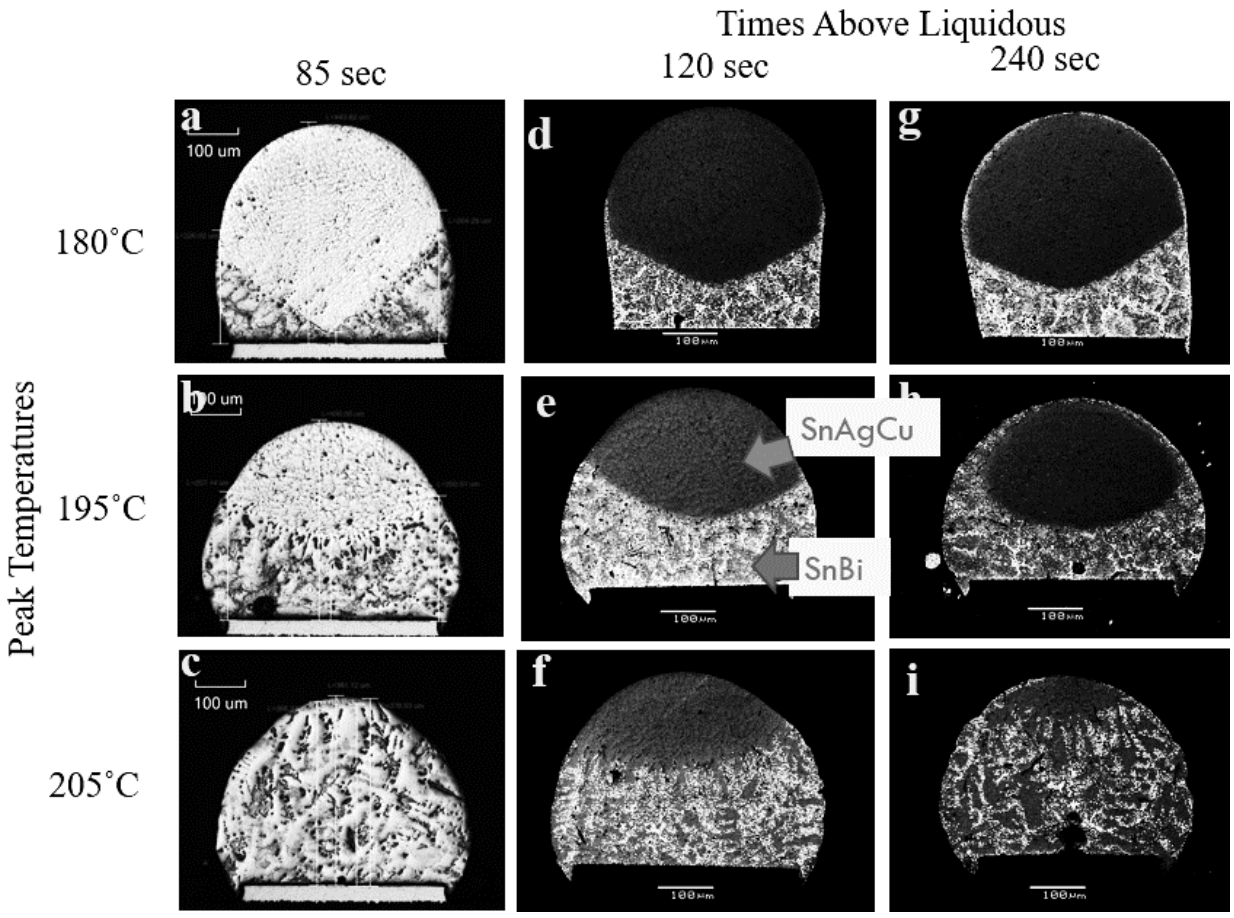

Figure 17 Crossectional Images of SnBi58-SAC305 Samples

The outside mixing heights of SnBi58 at 180C location “a” have a steep angle to the outside edges from the center of the solder joint as the time above melting increases from “a” to “d” this outside mixing edge develops into a thinner morphology until it can eventually wet its way fully around the solder ball seen in the image at “g”. The increased temperatures for this particular solder paste enable it to have the center diffusion to catch up to the hotter more exposed edges.

Mixing % Results of SnBi57%

SnBi57% Mixing% Results			
Peak Temp.	Time Above Melting		
		120sec	240sec
180˚C		**41%**	**40%**
195˚C		**54%**	**61%**
205˚C		**87%**	**94%**

Table 13. Summary of SnBi57% Mixing% Results

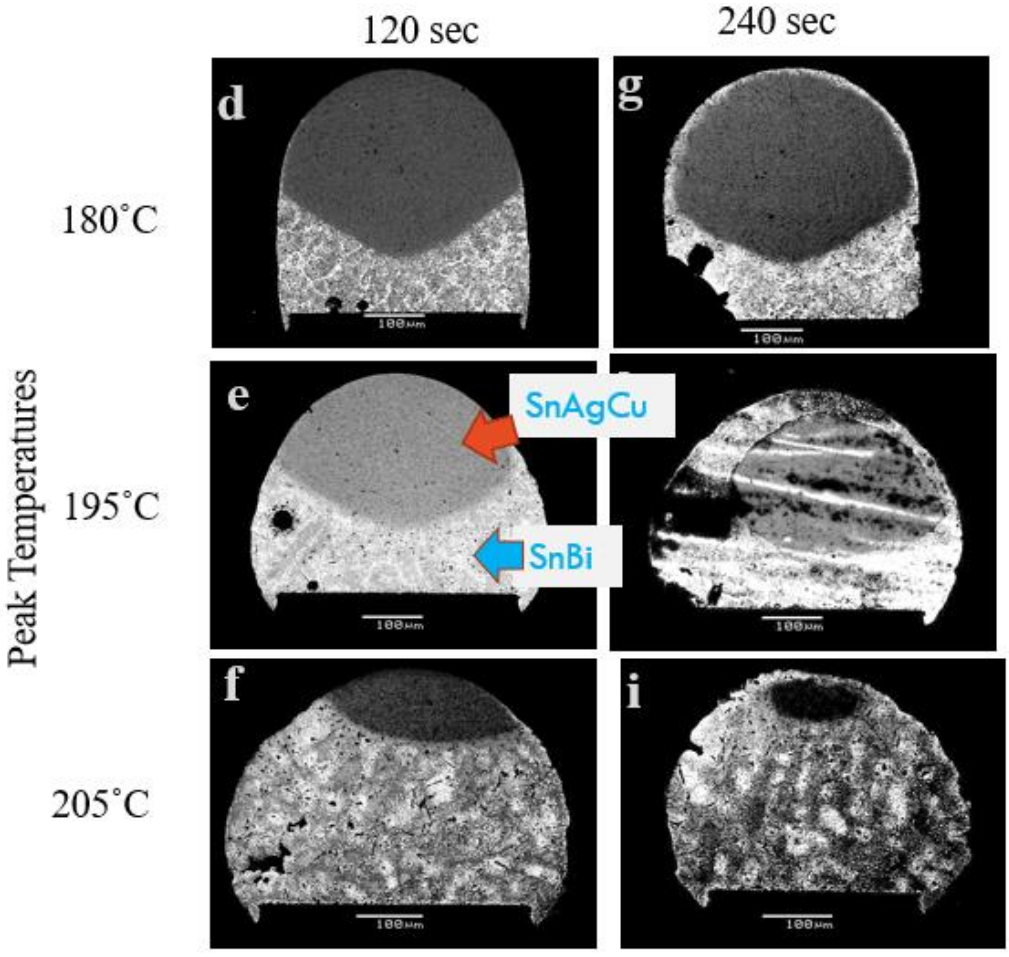

Figure 18 Crossectional Images of SnBi57 for TAM; 120s, 240s

Mixing % Results of SnBi40-58%

SnBi40-58% Mixing% Results			
Peak Temp.	Time Above Melting		
	85sec	120sec	240sec
180˚C	**27%**	**33%**	**43%**
195˚C	**41%**	**58%**	**51%**
205˚C	**87%**	**81%**	**89%**

Table 14. Summary of SnBi40-58% Mixing % Results

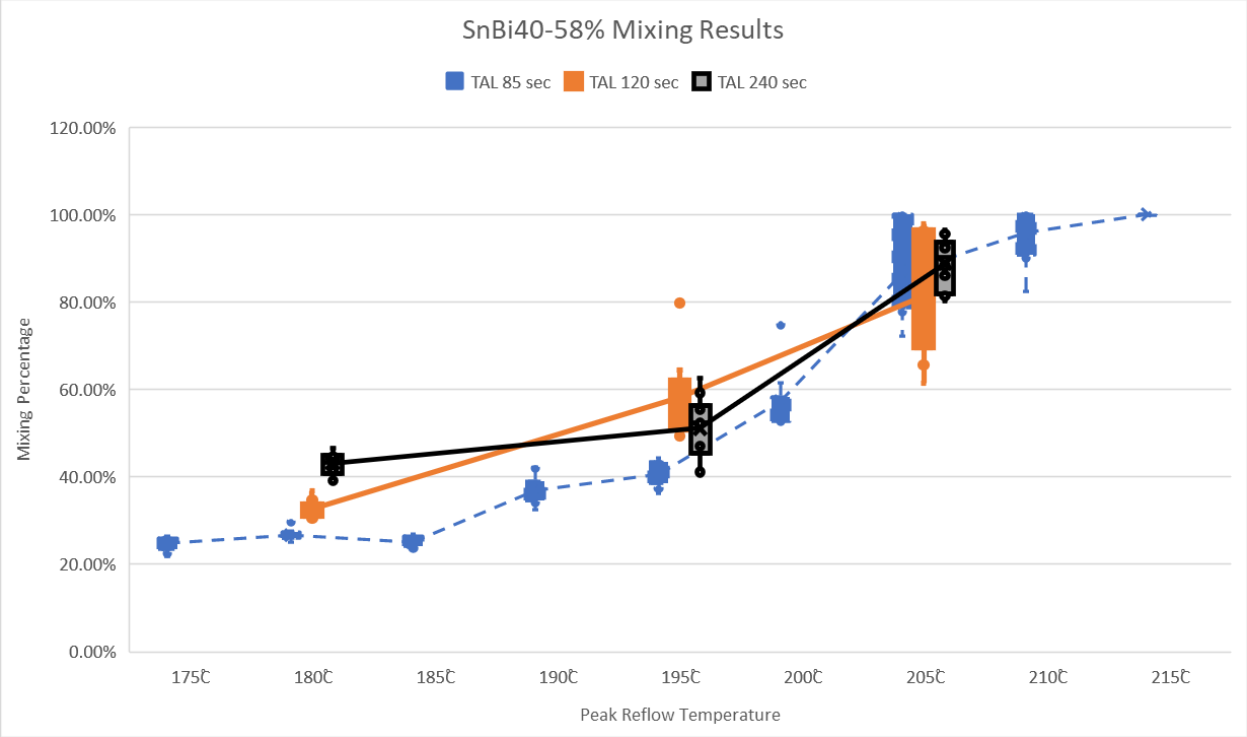

Figure 19 SnBi40-58 Mixing Results for TAM: 85s, 120s, 240s

Summary of Findings and Conclusions

The wetting of the solder paste around the SAC305 solder balls was a mixing mechanism that is not acceptable and makes the longer times above melting of 120sec and 240sec not suitable for an EMS provider utilizing low temperature solders. The lack of consistent statistically significant differences in the mixing levels between shorter times of melting of 85 secs and the longer 120sec and 240sec further prove this point from two-sample t-tests specifically at 180˚C in Figure 20 and at 195˚C in Figure 21.

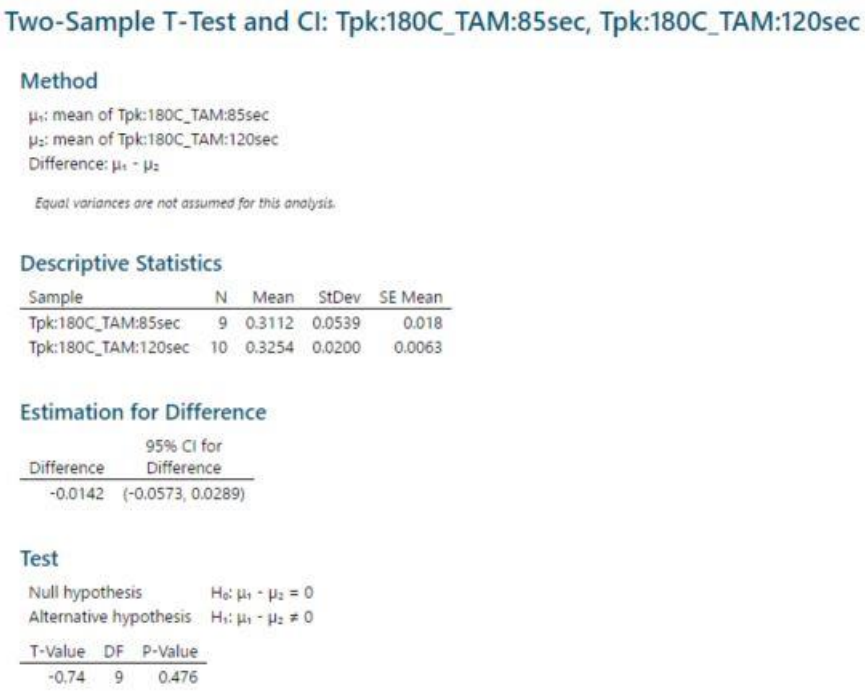

Two-Sample T-Test and CI: Tpk:180C_TAM:85sec, Tpk:180C_TAM:120sec

Method

μ_1: mean of Tpk:180C_TAM:85sec
μ_2: mean of Tpk:180C_TAM:120sec
Difference: $\mu_1 - \mu_2$

Equal variances are not assumed for this analysis.

Descriptive Statistics

Sample	N	Mean	StDev	SE Mean
Tpk:180C_TAM:85sec	9	0.3112	0.0539	0.018
Tpk:180C_TAM:120sec	10	0.3254	0.0200	0.0063

Estimation for Difference

Difference	95% CI for Difference
-0.0142	(-0.0573, 0.0289)

Test

Null hypothesis H_0: $\mu_1 - \mu_2 = 0$
Alternative hypothesis H_1: $\mu_1 - \mu_2 \neq 0$

T-Value	DF	P-Value
-0.74	9	0.476

Figure 20 T-test results of No Significant Differences in Mixing Levels between TAM:85sec and TAM:120sec at 180˚C

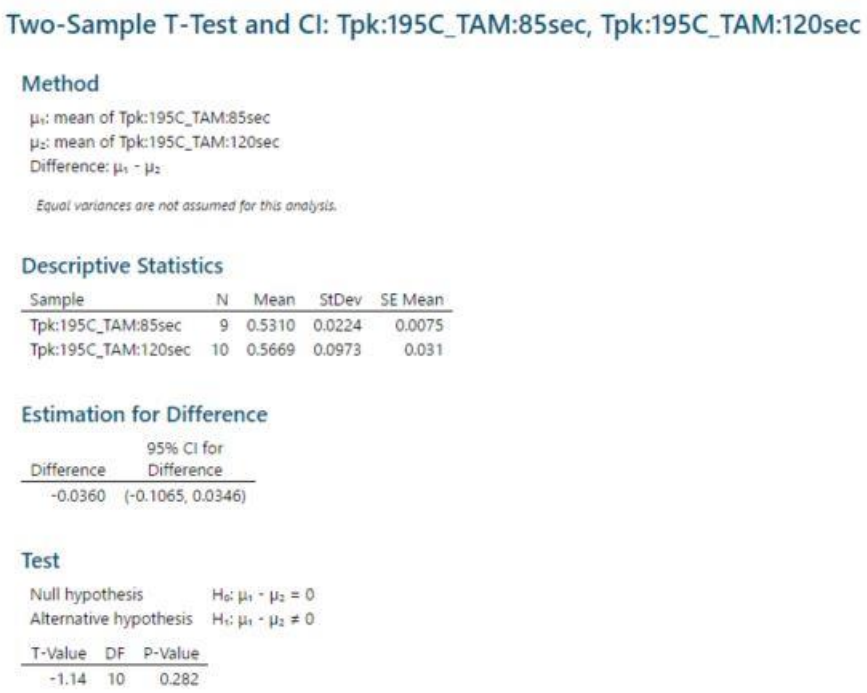

Two-Sample T-Test and CI: Tpk:195C_TAM:85sec, Tpk:195C_TAM:120sec

Method

μ_1: mean of Tpk:195C_TAM:85sec
μ_2: mean of Tpk:195C_TAM:120sec
Difference: $\mu_1 - \mu_2$

Equal variances are not assumed for this analysis.

Descriptive Statistics

Sample	N	Mean	StDev	SE Mean
Tpk:195C_TAM:85sec	9	0.5310	0.0224	0.0075
Tpk:195C_TAM:120sec	10	0.5669	0.0973	0.031

Estimation for Difference

Difference	95% CI for Difference
-0.0360	(-0.1065, 0.0346)

Test

Null hypothesis H_0: $\mu_1 - \mu_2 = 0$
Alternative hypothesis H_1: $\mu_1 - \mu_2 \neq 0$

T-Value	DF	P-Value
-1.14	10	0.282

Figure 21 T-test results of No Significant Differences in Mixing Levels between TAM:85sec and TAM:120sec at 195˚C

The key finding in this experiment have been understanding how the time above melting minimally effects the mixing dynamics of the low temperature solder paste/high temperature solder ball alloy joints. The observation concludes that the impractical extended times above liquidous (120sec-240sec) will not yield acceptable mixing levels. Along with the little benefits to the mixing levels are the through-put loses that form the longer reflow temperature profiles. Shown below in Figure 22 is a plot that has all the mixing levels of all the pastes at the peak temperatures, along with the results of the averaged mixing results for each leg of the experiment in Table 15. The results of this experiment verify that a time above melting ~90seconds should be sufficient to yield desired mixing results while implementing a practical manufacture process.

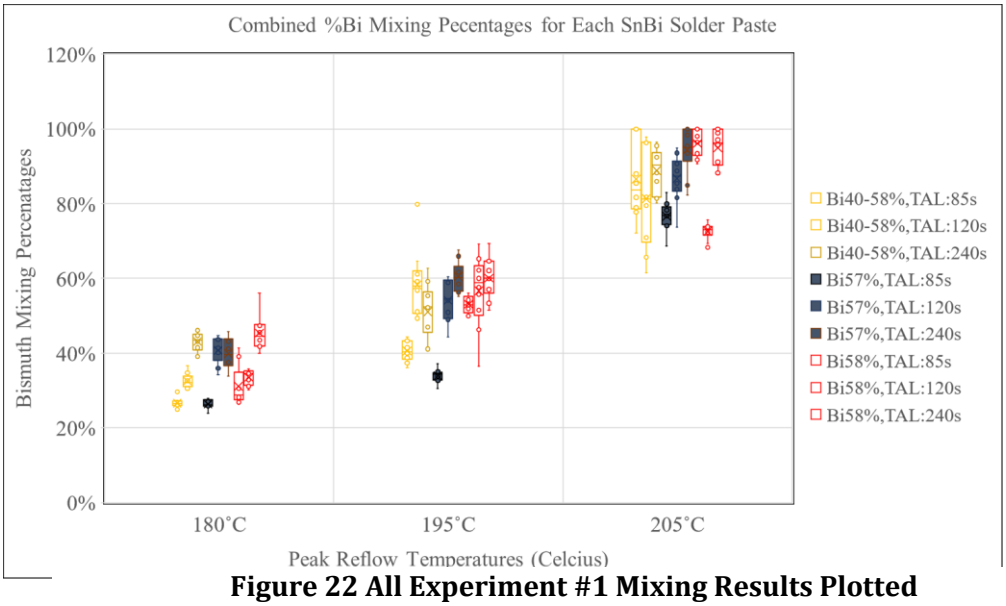

Figure 22 All Experiment #1 Mixing Results Plotted

Summary of Mixing% Results, TAL = 120 sec			
Peak Temp.	SnBi40-58%	SnBi57%	SnBi58%
180˚C	**33%**	**41%**	**33%**
195˚C	**58%**	**54%**	**57%**
205˚C	**81%**	**87%**	**73%**

Summary of Mixing% Results, TAL = 240 sec			
Peak Temp.	SnBi40-58%	SnBi57%	SnBi58%
180˚C	**43%**	**40%**	**45%**
195˚C	**51%**	**61%**	**60%**
205˚C	**89%**	**94%**	**95%**

Table 15 All Experiment #1 Mixing Results

EXPERIMENT #2

Objective and Motivation

The mixing of solder alloys of a component assembly particularly, large ball grid array components, will give insight to variance within the microstructure the mixed solder alloys. Subjecting test vehicles under various reflow soldering profiles will also add to the knowledge base for the industry to utilize for further implementation of low temperature solders. The results of the mixing levels found at each leg of this experiment will be the starting point for further research regarding failures due to fatigue testing. The objective is to also have the results of this experiment enable a prediction model to be formulated for estimating the mixing dynamics any of the three Bismuth based solder pastes with a practical and complex large ball grid array component.

Test Matrix

The matrix below describes each of the factors and the levels that will be tested with in this experiment.

DOE Test Matrix	Level-1	Level-2	Level-3
Reflow Profile Max. Temperature, °C	180°C	195°C	205°C
Lead Free Paste	Indalloy[1] #281 (58%Bi 42%Sn)	OM550 (40%-58% of Bi)	Indalloy[1] #282 (57%Bi 42%Sn 1% Ag)
Time Above Melting (TAM) (TAM) ≥ 138ºC	90 sec		

Table 16 Test Matrix for Experiment #2

Materials

This experiment will utilize the same three Bismuth based solders from Experiment #1 the difference is in the metallurgy of the solder ball in shown in Line #4 of the table below. This solder ball that is attached to the component prior to assembly has slightly different properties including a smaller sphere diameter of 16 mils and 1% more Silver. This alloy is 95.5%Sn4%Ag0.5%Cu (SAC405) and is commonly used for the BGA solder balled components of the telecommunications industry.

#	RIT Solder Alloy Name	Known Alloy Constituents and Composition	Melting Temp. (˚C)	Sphere Diam.
1	Indalloy #281	58%Bi/Sn42%	138ºC	Type 4
2	Indalloy #282	57%Bi/42%Sn/1%Ag	~140ºC	Type 4
3	OM550	Bi% between 40% and 58%	Around ~151 ˚C	Type 4
4	SAC405 Solder Ball	95.5%Sn4%Ag0.5%Cu	~217ºC	16 mils

Table 17 Solder Alloys for Experiment #2

Test Vehicle

More details of the component and board details are described in the table below.

Description	
BGA	Size: 42x28x0.8 mm Pitch: 0.65 mm
PCB	Size: 165x127x1.6 mm Surface Finish: OSP Layers: 8-Layer HF

Table 18 Stencil Details

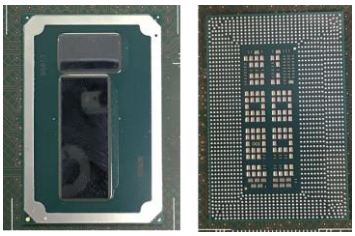

Figure 24 Actual BGA for Component Placement

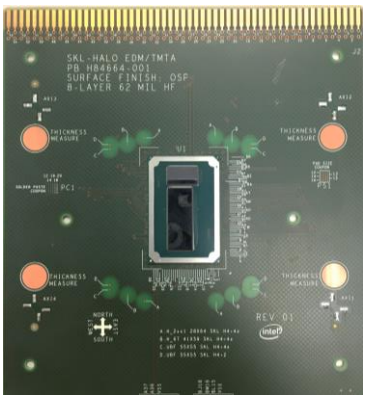

Figure 23 Test Vehicle

Test Method

Measurement Methods

The measurement method to be used is the same as the previous experiment utilizing Equation #1.

$$Average\ Mixing\% = \frac{((HL + HC + HR)}{3 * HSOH} * 100$$

Assembly Details

SMT Assembly Equipment Parameters

Stencil Printing

As in the previous experiment the Printing process of the solder pastes was performed on the board the DEK Horizons 01ix Proactive Stencil Printer was programmed with a speed of 50 mm/s and a pressure of 7.0 kg force. All solder paste printed locations were analyzed with an inline Koh Young Solder Paste inspection machine along with manual visual inspection to determine paste transfer efficiency of each print. Each board was analyzed with a pass/fail criterion that accounted for volume, area, shape and height of each solder paste deposits.

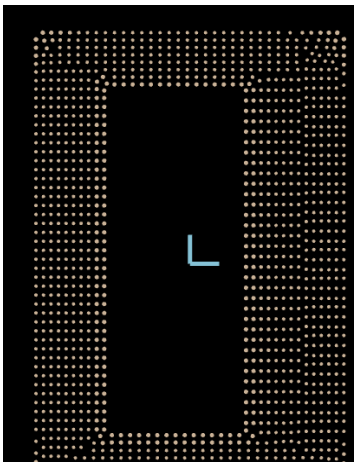

Figure 25 Stencil Design

Stencil Details	
Thickness	4 mils
Aperture Dimension	16 mils
Aperture Shape	Rounded Square
Rounded Edges	0.2 mm
Finish	Laser Cut
Size	VG260 (23" Vector Guard)
Stencil Printer Machine Setting	
Speed	50 mm/s
Pressure	5.0 kg
Squeegee	Metal, 60˚
Supports	Magnetic

Table 19 Printing Process Details Experiment #2

Solder Mixture Composition Calculations

The weight percentage of Bismuth is calculated in this next section due to the fact that the element Bismuth is brittle and will affect the mechanical strength of the mixed solder joint.

The theoretical volume of the paste uses the volume of a cylinder formula $V= \pi r^2 h$.

Vol. paste deposit = π x $(0.02032cm)^2$x 0.01016cm

Vol. paste deposit = 1.318×10^{-5} cm^3

This paste was a Type 4 Solder Paste, so we divide the Vol. paste deposit in two which will estimate the volume of the metal of the solder deposited.

Vol. metal content of paste deposit = $0.65 \times 10^{-5} cm^3$

The density of 58Bi/Sn42 is 8.62 g/cm^3, calculate the Mass of the metal content:

Mass = Density x Volume
= 8.56 g/cm^3 x ($0.65 \times 10^{-5} cm^3$) = 0.0556 mg
Mass of the metal content for 58Bi/42Sn = 0.0556 mg (1)

Next, we can calculate the metal content of the 95.5Sn/4.0Ag/0.5Cu (SAC405) solder ball,

Volume of sphere = $4/3\ \pi r^3$
Vol. SAC405 = $4/3 * \pi * (0.02032cm)^3$
= $3.5 \times 10^{-5} cm^3$

Taking the volume of the metal content and knowing that the density of SAC405 is 7.40 g/cm^3, we can calculate the Mass of the metal content:

= 7.40 g/cm^3 x $3.5 \times 10^{-5} cm^3$ = 0.259 mg

Mass SAC405 = 0.259 mg

The total mass would be Mass 58Bi/Sn42 + Mass SAC405 = 0.3146 mg

The composition of the 58Bi/Sn42 Paste is: Bi - 58 wt% /Sn - 42 wt% , and that the composition for SAC405 is: Sn - 95.5 wt% / Ag - 4.0 wt% / Cu - 0.5 wt% . We can then multiply the composition of the 58Bi/Sn42 paste with the mass of the 58Bi/Sn42 paste in order to obtain the mass of each element in the 58Bi/Sn42 paste deposit:

Bi mass = (Mass of Paste deposit) *(Bi wt%) = (0.0556 mg) *(58%)

Bi mass = 0.03225 mg

Sn mass = (Mass of Paste deposit) *(Sn wt%) = (0.0556 mg) *(42%)

Sn mass = 0. 02335 mg

Repeat for SAC405

Sn = 0.2473 mg / Ag = 0.01036 mg / Cu - 0.001295 mg

Add the masses of all elements:

Sn - 0.2707 mg/ Bi - 0.03225 mg/ Ag - 0. 01036 mg / Cu - 0. 001295 mg

Obtain the wt% of the elements by dividing mass by the total mass of the mixed solder (0.3146mg)

Sn% – 86.05 wt%
Bi% – 10.25 wt%
Ag% – 3.29 wt%
Cu% - 0.41 wt%

57Bi/Sn42/1Ag_ Composition Calculations

Vol. metal content of paste deposit = $0.65 \times 10^{-5} cm^3$

The density of 57Bi/Sn42/Ag1 is 8.57 g/cm^3, calculate the Mass of the metal content:

Mass = Density x Volume

= 8.57 g/cm^3 x ($0.65 \times 10^{-5} cm^3$) = 0.0557 mg

Mass of the metal content for 57Bi/Sn42/Ag1 = 0.0557 mg

Taking the volume of the metal content and knowing that the density of SAC405 is 7.40 g/cm^3, we can calculate the Mass of the metal content:

= 7.40 g/cm^3 x $3.5 \times 10^{-5} cm^3$ = 0.259 mg

Mass SAC405 = 0.259 mg

The total mass would be Mass 57Bi/Sn42/Ag1 + Mass SAC405 = 0.3147 mg

The composition of the 57Bi/Sn42/Ag1 Paste is: Bi - 57 wt% /Sn - 42 wt% /Ag – 1.0 wt%, and that the composition for SAC405 is: Sn - 95.5 wt% / Ag - 4.0 wt% / Cu - 0.5 wt% .

Bi mass = (Mass of Paste deposit) *(Bi wt%) = (0.0557 mg) *(57%)

Bi mass = 0.03175 mg

Sn mass = (Mass of Paste deposit) *(Sn wt%) = (0.0557 mg) *(42%)

Sn mass = 0. 02339 mg

Ag mass = (Mass of Paste deposit) *(Ag wt%) = (0.0557 mg) *(1.0%)

Ag mass = 0. 000557 mg

This is done for SAC405 elements and mg values are:

Sn = 0.2473 mg / Ag = 0.01036 mg / Cu - 0.001295 mg

Add the masses of all elements:

Sn - 0.2707 mg/ Bi - 0.03175 mg/ Ag - 0. 01092 mg / Cu - 0. 001295 mg

Obtain the wt% of the elements by dividing mass by the total mass (0.3147 mg)

Sn% – 86.02 wt%
Bi% – 10.09 wt%
Ag% – 3.47 wt%
Cu% - 0.41 wt%

The complete results can be found in the Table 18 below, missing due to proprietary restrictions is the OM550 solder paste results.

Mixed Solder Alloy	**Composition in Wt% of Solder Mixture**
58Bi/42Sn + 95.5Sn/4.0Ag/0.5Cu	Sn% – 86.05 wt% Bi% – 10.25 wt% Ag% – 3.29 wt% Cu% - 0.41 wt%
57Bi/42Sn/1Ag + 95.5Sn/4.0Ag/0.5Cu	Sn% – 86.02 wt% Bi% – 10.09 wt% Ag% – 3.47 wt% Cu% - 0.41 wt%

Table 20 Mixed BGA Solder Joint Compositions

The mixing element composition results reveal the expected outcome that Bismuth content will decrease and Silver content will increase from the eutectic 58Bi/42Sn to 57Bi/42Sn/1Ag.

It is to be noted that the ratio of the volume of solder paste (~1.318 x 10^{-5} cm^3) to the volume of the solder ball (3.5 x 10^{-5} cm^3) for this experiment is 0.37:1 paste to ball.

Reflow Oven Profile Details

The success criteria details of the reflow oven profiles are shown in the table below. The profiles were developed for the 8-Zone convection oven in the previous experiment.

Attributes	Value
Initial Ramp Rate (ºC/sec)	1 - 3
Soak Time (100 – 120 ºC) seconds	60 - 90
Peak Reflow Temperature (ºC)	180,195,205
Time Above Melting (TAM) ≥ 138ºC	85-95
Cooling Rate (ºC/sec)	1 - 3

Table 21 Reflow Profile Criteria Experiment #2

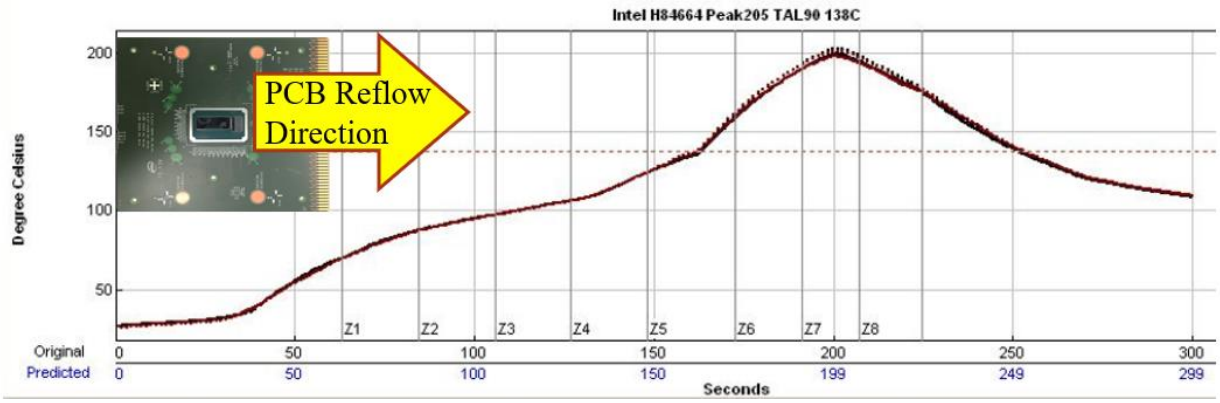

Figure 26 Reflow Profile Sample, Tpk: 195C

The reflow profile development process required the use of the KIC SPS Thermal Profile and KIC RPI Software. Below the image identifies the locations of the thermal couples. The key finding during profiling at each peak temperature is that there is an average difference in

temperature from the outer row of solder balls to the inner row, those location designations are #6 (outer), and #3(inner). The graph below also shows the difference in temperatures during each profile with the average to be 2.3 ˚C.

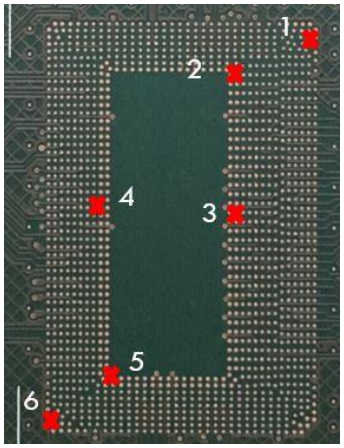

Figure 28 Thermocouple Locations

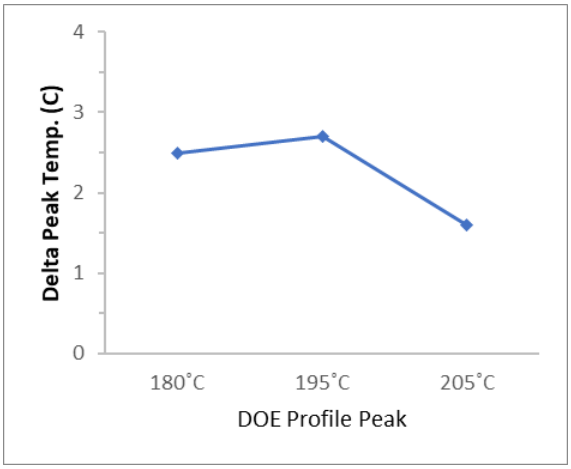

Figure 27 Delta T Across the BGA

Figure 26 shows the locations on the assembly where there will be micro-sections cut out of the board at the outer and inner row locations, a total of two for each leg of the experiment. These cross-sections enabled a better understanding of how the temperature gradient of "large" BGAs will mix and what mechanisms will be present at the mixing levels and solder joint height across the variations to peak temperature.

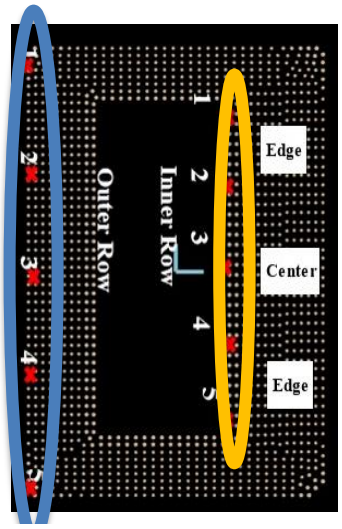

Figure 29 BGA Cross-Section Locations

Build Matrix

Board #	Peak Temp.	Reflow Condition	Solder Paste
1-5	180C	90 sec TAM≥ 138ºC	Indalloy[1] #281 (58%Bi 42%Sn)
6-10	195C		
11-15	205C		
16-20	180C		OM550 (40%-58% Bi)
21-25	195C		
26-30	205C		
31-35	180C		Indalloy[1] #282 (57%Bi 42%Sn 1% Ag)
36-40	195C		
41-45	205C		

Table 22 Experiment #2 Build Matrix

A total of five boards are completed at each leg of the experiment. It was determined that the flow of the build would be more efficient if for each solder paste every reflow profile should be run first before switching the solder paste from the stencil printer.

Experimental Results

Summary of Mixing Results for each Solder

SnBi40-58%			SnBi57%			SnBi58%		
Peak Temp.	Avg % Mixing		Peak Temp.	Avg % Mixing		Peak Temp.	Avg % Mixing	
180˚C	44%		180˚C	47%		180˚C	47%	
195˚C	58%		195˚C	77%		195˚C	70%	
205˚C	100%		205˚C	100%		205˚C	100%	
	Inner Perimeter	Outer Perimeter		Inner Perimeter	Outer Perimeter		Inner Perimeter	Outer Perimeter
180˚C	40%	48%	180˚C	43%	50%	180˚C	52%	44%
195˚C	54%	61%	195˚C	72%	82%	195˚C	62%	73%
205˚C	100%	100%	205˚C	100%	100%	205˚C	100%	100%

Table 23 Experiment #2 Results

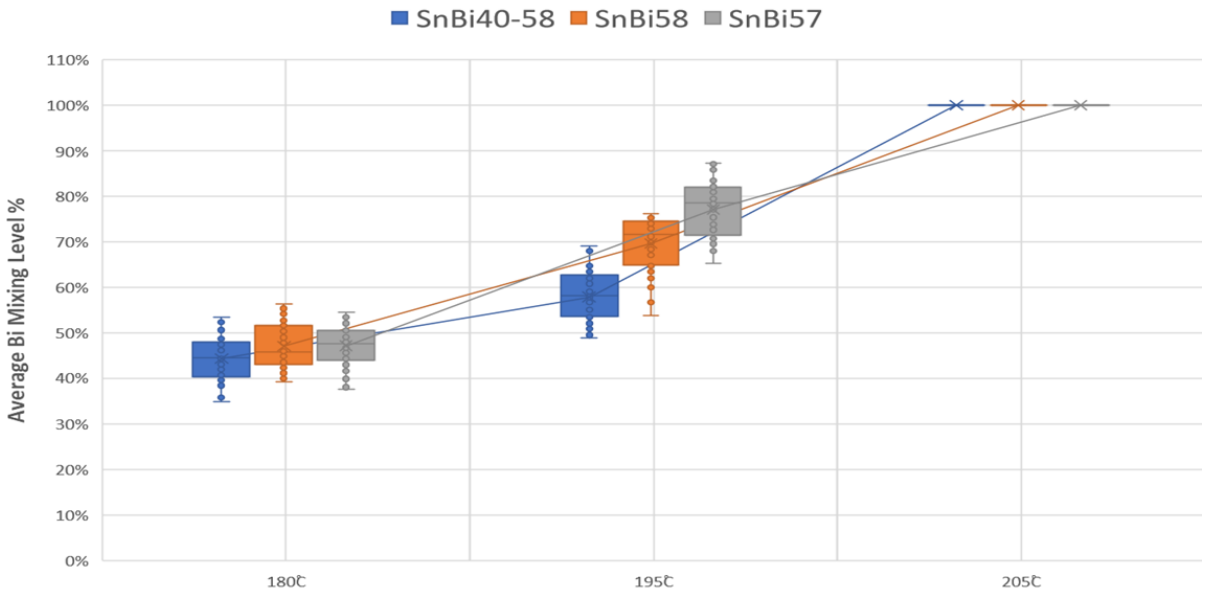

Figure 30 All Experiment #2 Mixing Results Plotted for each Solder Pastes

The results reveal the mixing levels for each solder paste at each peak temperature. Statistical analysis determined that SnBi40-48% was significantly lower than the other two pastes at peaks 180C and 195C. SnBi58 was only significantly lower than SnBi57 at temperature 195C. All three pastes were not significantly different at 205C. T-Test results can be found in Appendix B.

To achieve the desired mixing results of >30% and <80%, (~55%) the peak temperature of 190C with any of the three paste.

Microstructural Evaluation

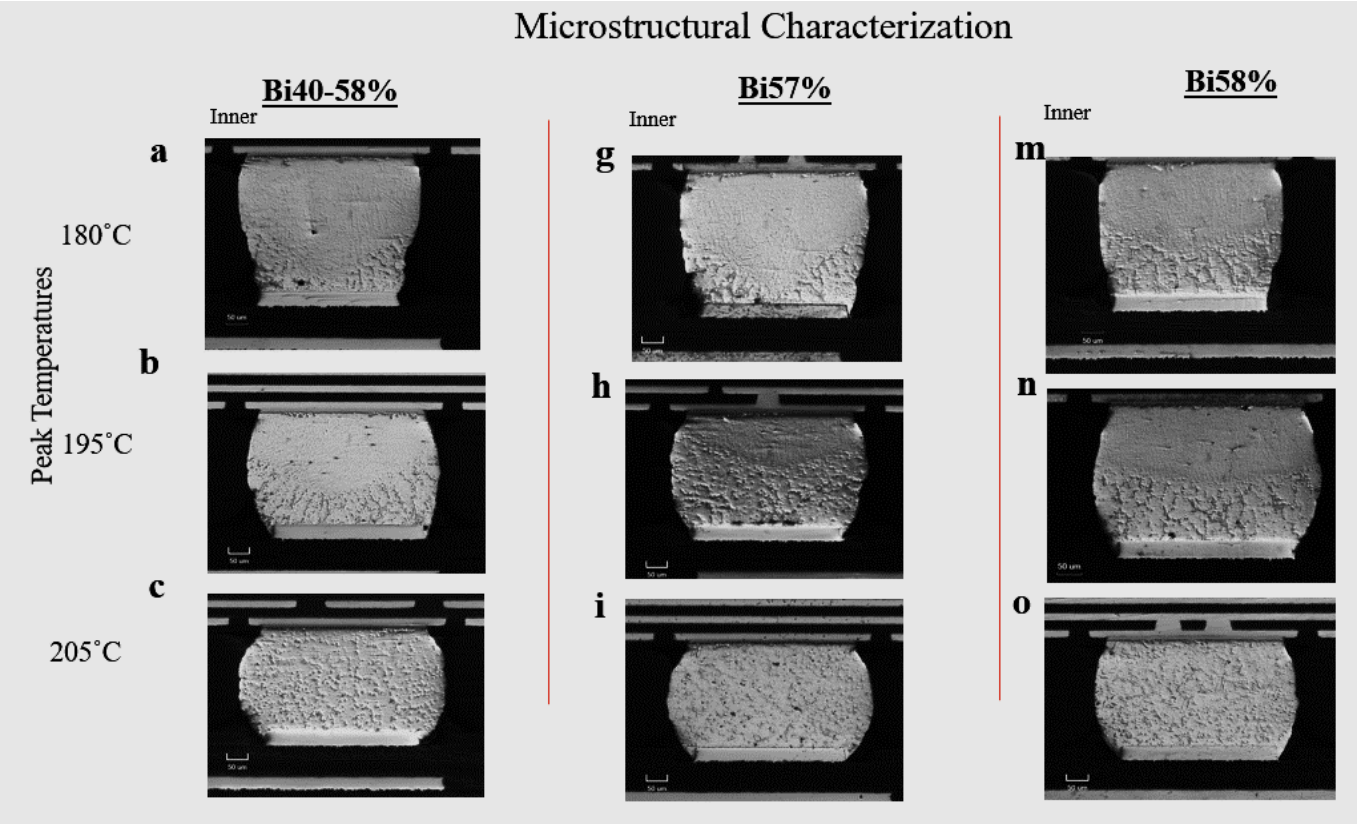

Figure 31 Microstructure Overview of All Results

This comparison of microstructure of each solder joint reveals the Mixing levels and the mixing mechanisms that these pastes going through in relation to peak temperature. At location “a” and “g” the Bi-solder paste appears to be wetting up the sides of the solder ball more so than diffusion through the center similar to “m”. As peak temperature hits 195C then the mixing uniformity is more dominant than outside wetting heights for “h” and “n” compared to “b” which is still having a large mean difference in max – min mixing levels. Consistent with the previous study on mixing mechanisms OM550 wetted up the side of the ball, 57%Bi exhibited more

wetting up the sides then more center diffusion at higher temperatures, and 58%Bi revealed steady mixing levels across the solder joint. A detailed view of each of the mixed solder joints is on the following pages, along with the complete set of images in the Appendix.

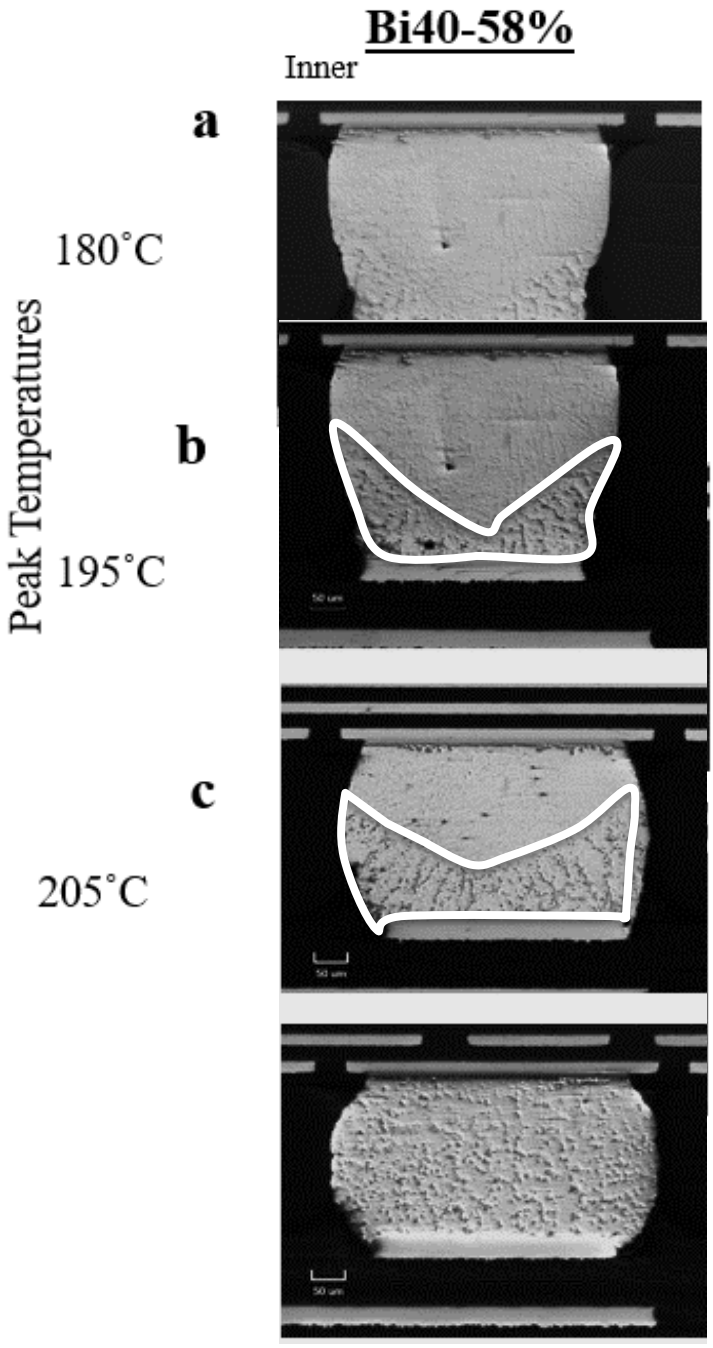

Figure 32 Average SnBi40-58 Cross-Sectional Images

In image “A” of Figure 29 the solder paste with Bismuth is outlined to show how this peak temperature of 180˚C does not get the center of the SAC405 hot enough to begin mixing. Image

"B" has a significantly higher amount of center solder ball and paste mixing at 195˚C and complete mixing at 200˚C. The Bismuth dendrites change morphology from long to small as peak temperature increases.

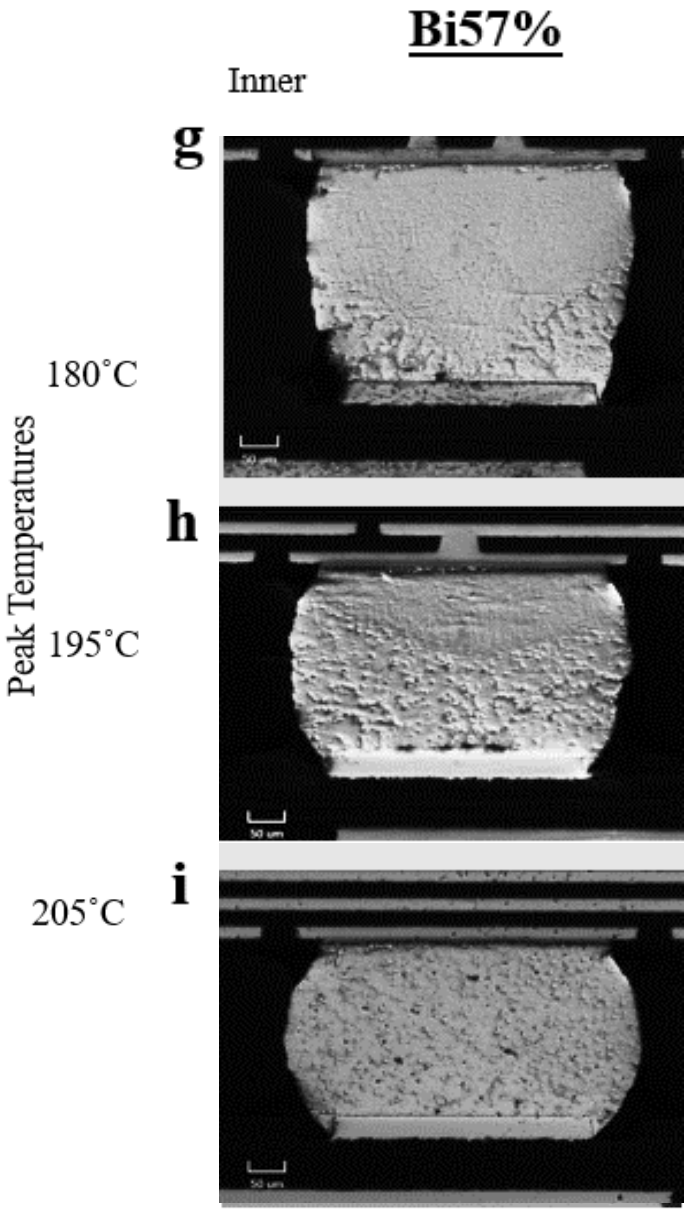

Figure 33 Average SnBi57 Cross-Sectional Images

The Bi57% solder paste exhibits a more extreme mixing mechanism transfer from wetting on the outside of the ball to more diffusion through center mixing, seen in Figure 30. The

microstructure reveals the bismuth dendrites as coarser at 195˚C as compared to Bi40-58% solder paste.

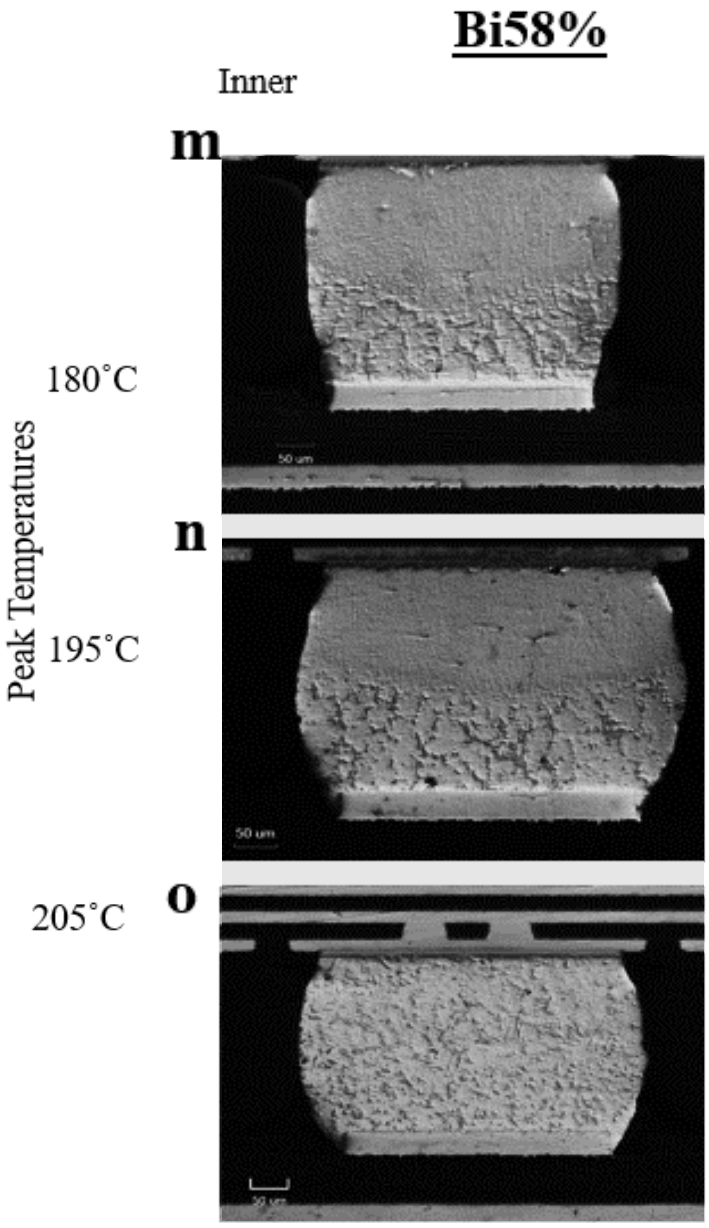

Figure 34 Average Bi58% Cross-Sectional Images

Figure 31 is the eutectic Sn58%Bi solder paste which shows consistent center mixing levels at both 180˚C and 195˚C (Images M and N). The Bismuth dendrites appear to stay larger and longer compared to the other solder pastes as peak temperature is applied.

Mixing Results for Each Solder Pastes

The large package size of this BGA had an average temperature gradient of 2.3˚C across it that unexpectedly was determined by sample t-tests to yield significantly different mixing level percentages from outer rows to inner rows. This significance was an interesting result in this experiment given that the 2.3˚C Temperature difference perceived to be minimal. All t-test results are in Appendix B. The mixing measurements from the edge, center and edge were plotted for both inner and outer rows at the various peak temperatures shown below.

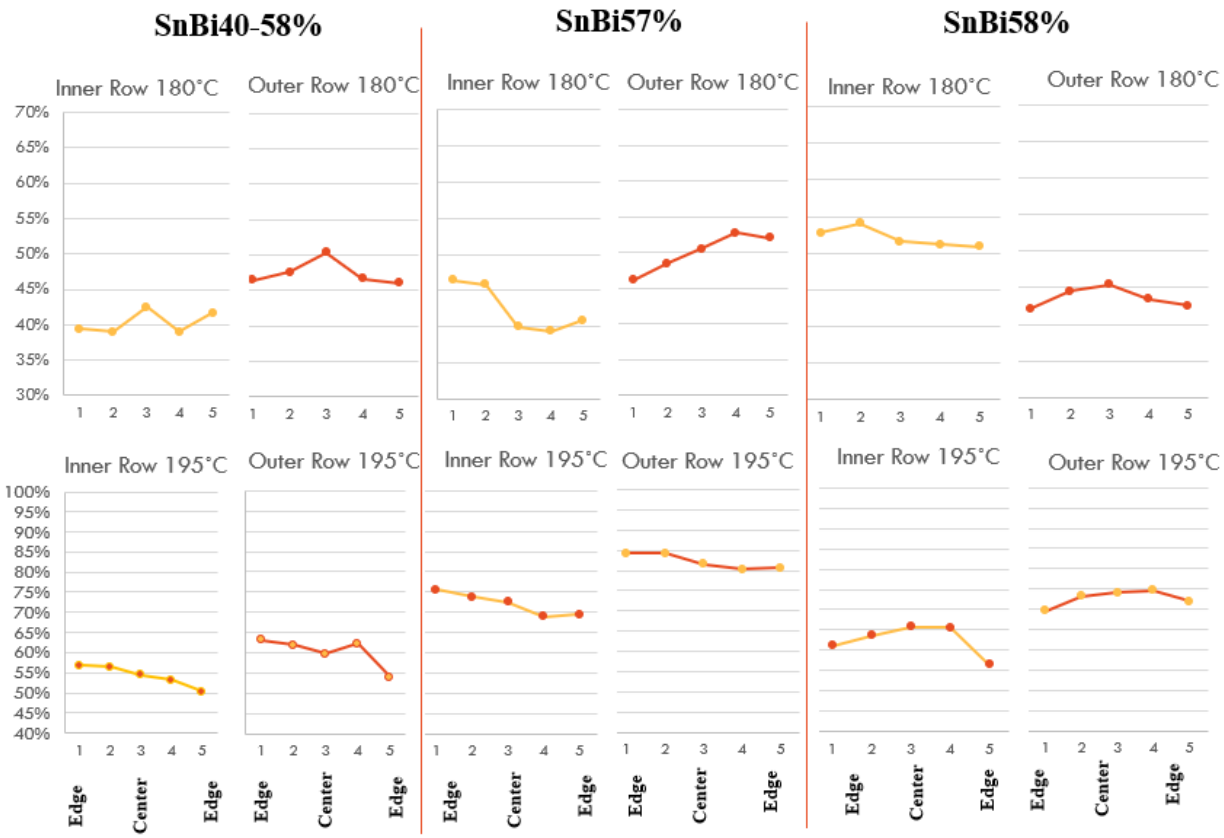

Figure 35 Mixing % Inner Row vs Outer Row

Summary of SnBi40-58% Mixing Results

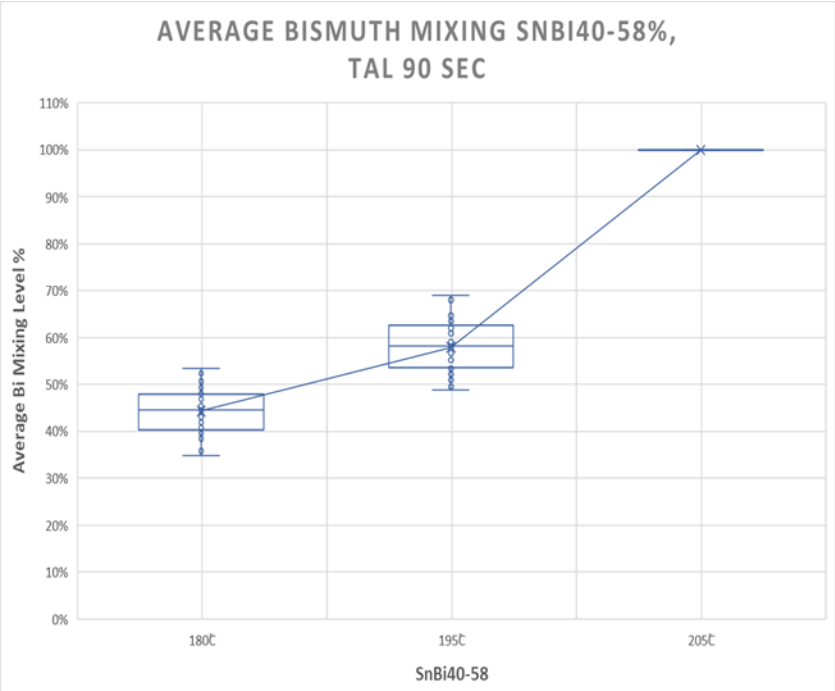

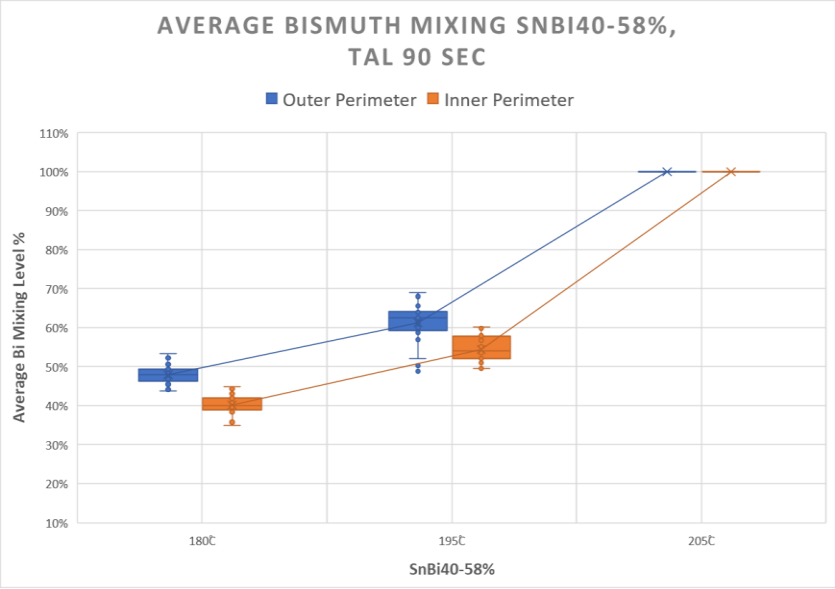

Figure 36 SnBi40-58 Mixing Results Plot, Inner vs Outer Row

SnBi40-58%		
Peak Temp.	Avg % Mixing	
180˚C	44%	
195˚C	58%	
205˚C	100%	
	Inner Perimeter	Outer Perimeter
180˚C	40%	48%
195˚C	54%	61%
205˚C	100%	100%

Table 24 SnBi40-58 Results Summary

Summary of SnBi57% Mixing Results

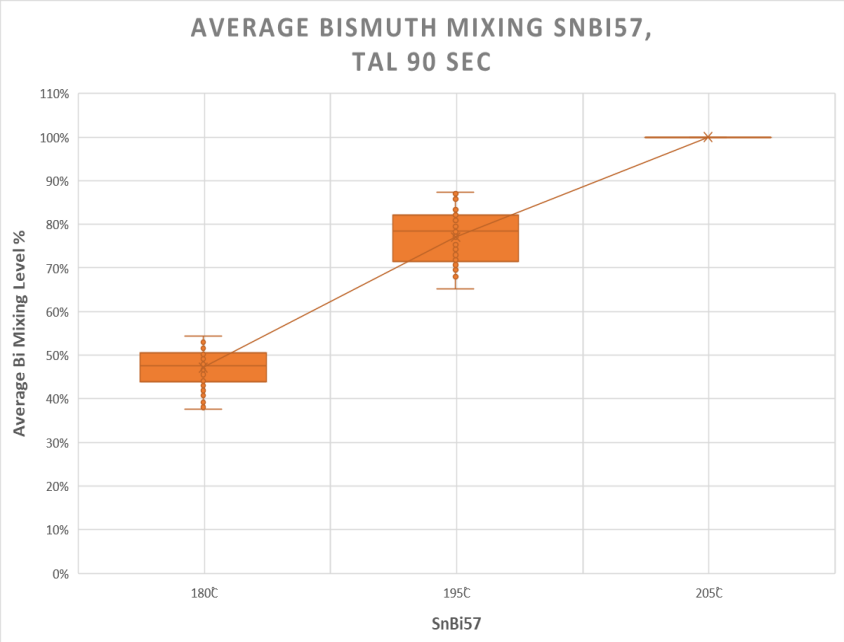

SnBi57%		
Peak Temp.	Avg % Mixing	
180°C	47%	
195°C	77%	
205°C	100%	
	Inner Perimeter	Outer Perimeter
180°C	43%	50%
195°C	72%	82%
205°C	100%	100%

Table 25 SnBi57 Mixing Results Summary

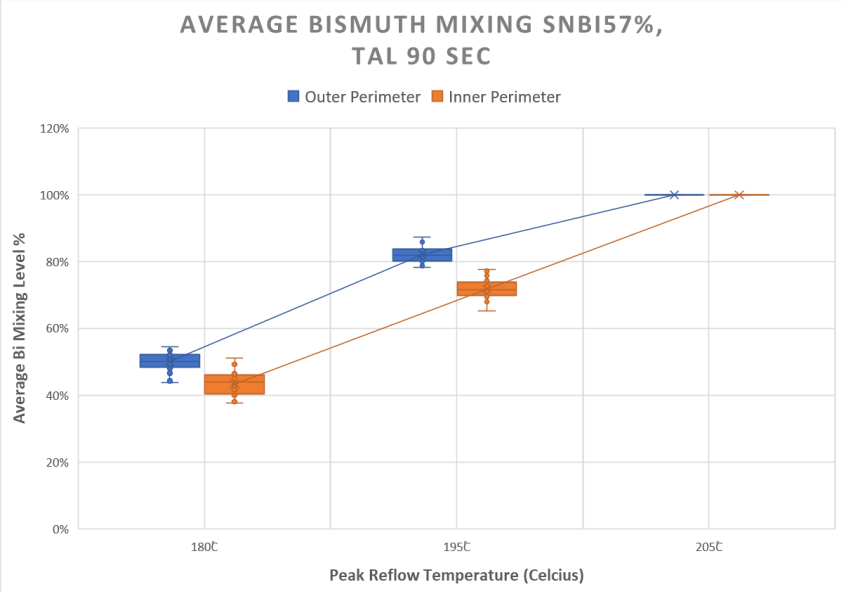

Figure 37 SnBi57 Mixing Results Summary Plot, Inner vs Outer Row

Summary of SnBi58% Mixing Results

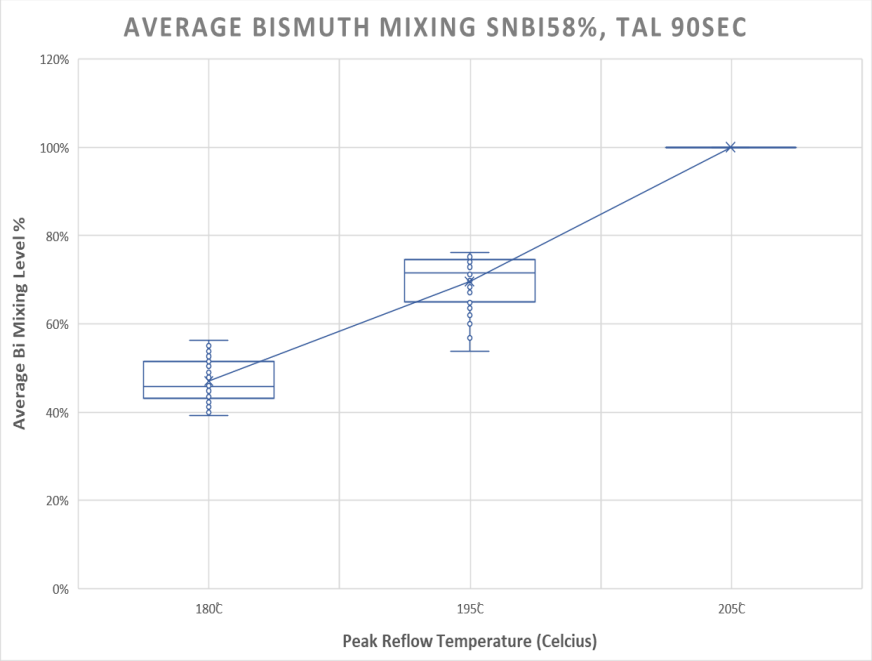

SnBi58%		
Peak Temp.	Avg % Mixing	
180°C	47%	
195°C	70%	
205°C	100%	
	Inner Perimeter	Outer Perimeter
180°C	52%	44%
195°C	62%	73%
205°C	100%	100%

Table 26 SnBi58 Mixing Results Summary

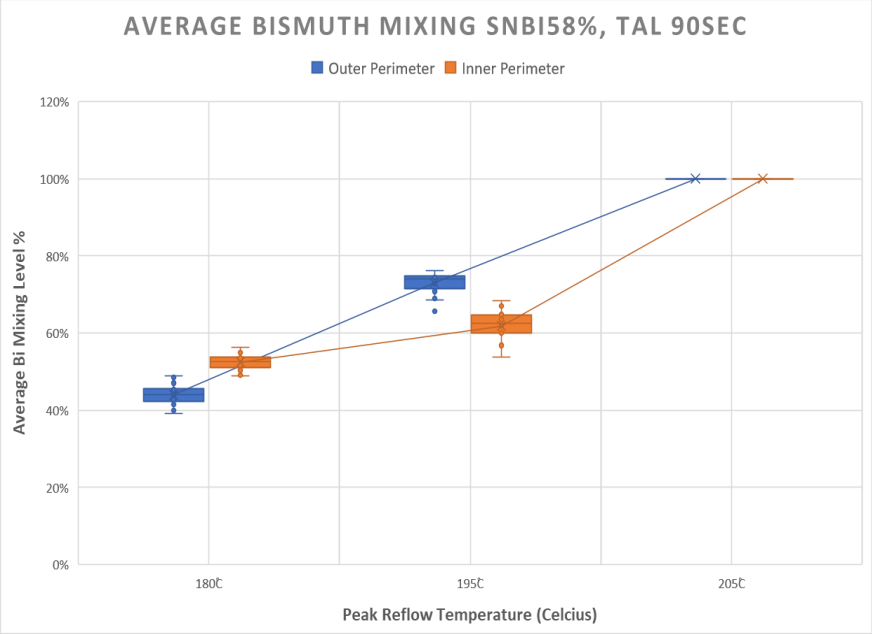

Table 27 SnBi58 Mixing Results Summary Inner Row vs Outer Row

Prediction Model Example

Prior to starting this experiment, the method of estimating mixing percentages was deemed not applicable for BGA component assemblies. The results of this BGA component assembly have enabled a regression model to be formulated to estimate mixing percentages with a 95% confidence for any of the three-solder paste used.

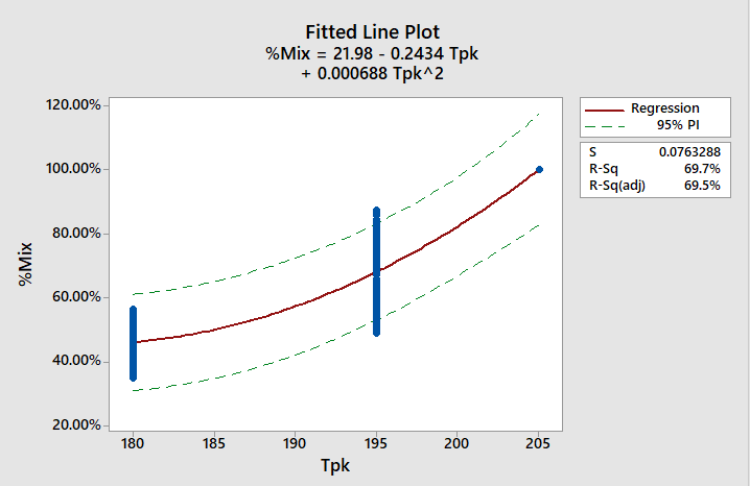

Figure 38 Prediction Model for both % Bismuth Mixing (left) and Solder Joint Height

Example of Prediction Model: An EMS wants to assemble the same assembly with a Bi-Based solder paste. The desired peak reflow temperature is 190˚C, what is an accurate estimation of the mixing % level?

Equation 3 Bi% Mixing Prediction Model

$$\%Mix = 21.98 - 0.2434*Peak_{Temp} + 0.000688* (Peak_{Temp})^2$$

$$\%Mix = 21.98 - 0.2434*(190C) + 0.000688* (190C)^2$$

$$\%Mix = 0.5708 (\sim 57\%)$$

Cumulative Conclusion

The data of both these studies can be utilized to better predict mixing results for three Bismuth-based solder pastes with SAC solder ball alloys. The significant findings are; no consistent benefit for extremely long times above melting, and that there was a significant difference in outer to inner rows mixing levels for “large” BGAs at a distance between the rows equal to or greater than 17mm apart.

FUTURE PLANS

Both these experiments have provided results to be stepping stones of expanding the industries knowledge base on mixed low temperature and high temperature solder assemblies. The ratio of paste volume to solder ball volume would be of interest to expand the knowledge base of previous work demonstrating the importance of this ratio. (Sandy et al. 2011) The ratio used for the BGA study, 0.185:1 paste to ball ratio and the first study used a 0.21:1 paste to ball volume ratio. These mixing results from the ratios of both studies could be the start of another experiment examining the effects of the ratio along with an optimization study on mixing levels.

There is an opportunity for a continuation study with the extra assemblies of Experiment #2 an accelerated life testing study along with potential rework research with low temperature solders. The reliability data of future mixed low temperature solder pastes with high temperature solder balls will drive the process optimization of achieving targeted mixing levels correlated accelerated life testing. An objective would be to expand the sample size of each leg of experiment #2 that way to enable greater understanding on the statistical difference of mixing levels between the outer and inner rows of the BGA, along with adding more data to improve the model developed for each of the three solder pastes.

BIBLIOGRAPHY

Amir, D., Aspandiar, R., Buttars, S., Chin, W., Gill, P., (2009). Head-on-Pillow SMT failure Modes. SMTA International Conference

Aspandiar, R., Byrd, K., Kok Kwan, T., Campbell, L., & Mokler, S. (2015). Investigation of Low Temperature Solders to Reduce Reflow Temperature, Improve SMT Yields and Realize Energy Savings. *IPC APEX EXPO* .

Aspandiar, R., Caputo, T., K. Bryd, and Mokler, S., 2017. Microstructural Analysis (Bi Mixing Percent) of The Ball Joint of Different BiSn Low Temperature Solder Pastes. Intel

Banerji, K., & Darveaux, R. F. (1993). Effect of aging on the strength and ductility of controlled collapse solder joints. Microstructures and Mechanical Properties of Aging Materials conference, pp 431- 442.

Bath, J., Handwerker, C., & Bradley, E. (2000). Research update: Lead free solder alternatives. *Circuits Assembly* , 31-40.

Bradley, E. (2003). Lead-free Solder Assembly: Impact and Opportunity. *Advanced Packaging* .

Bradley, E., Handwerker, C. A., Bath, J., Parker, R.D., Gedney, R.W., (2007). Lead-Free Electronics: iNEMI Projects Lead to Successful Manufacturing, Wiley-IEEE Press. October 2007.

Bukhari, S., Satos, D., Lehman, L., & Cotts, E. (2004). Evaluation of the Effects of Processing Conditions on Shear Strength and Microstructure on Pb free Surface Mount Assembly. *Pan Pacific Symposium Conference*.

Chen, O. H., Molina, A., Aspandiar, R., Byrd, K., Mokler, S., & Tang, K. K. (2015). Mechanical Shock and Drop Evaluation of the BGA Solder Joints Stack Up Formed by reflow Soldering SAC Solder Ball BGAs with BiSnAg and resin reinforced BiSn-Based Solder Pastes. *SMTA International, Rosemont, IL*, Pg 215 to 222.

Cheng Lee, D. (2015). Low Temperature Solders, New Developments and their Applications. *Indium corporation Journal*.

Coyle, R., Aspandiar, R., Vasudevan, V., Tisdale, S., Muntele, I., Popowich, R., Fleming D., Read, P.,(2013). The Effects of Pb Mixing Levels on Solder Joint Reliability and Failure Mode of Backward Compatible, High Density Ball Grid Array Assemblies. SMTA International. 2013

Coyle, R., Aspandiar, R., Osterman, M., Johnson, C., Popowich, R., Parker, R., Hillman, D.,(2017). Thermal Cycle Reliability Of A Low Silver Ball Grid Array Assembled With Tin Bismuth Solder Paste. SMTA International 2017. p.p.73-83.

Delhaise, A., Snugovsky, L., Perovic, D., Snugovsky, P., Kosiba, E., (2014). Microstructure and Hardness of Bi-containing Solder Alloys After Solidification and Ageing. SMTA, 2014.

Dunford, S., Canumalla, S., Viswanadham, P., (2004). Intermetallic Morphology and Damage Evolution Under Thermomechanical Fatigue of Lead (Pb)-Free Solder Interconnections. Electronic Components Technology Conference. 726-736. June 1-4, 2004.

Felton, L.E., Raeder, C.H. & Knorr, D.B. (1993). The properties of tin-bismuth alloy solders. JOM (1993) 45: 28. https://doi.org/10.1007/BF03222377

Fu, H., Aspandiar, R., Chen, J., Cheng, S., Chen, Q., Coyle, R., Feng, S., Feng, S., Krmpotich, Tang, K.K., Wu, G., Zhang, A., Zhen, W., (2017). SMTA International Conference 2017. 207-220

(2005). Understanding Lead-free Electronics Packaging, Material Selection, Process, Defects, Reliability and Implementation. Rochester Institute of Technology Center for Electronics Manufacturing and Assembly.

Garrou, P. (2014). Warpage in Microelectronic Packaging: a closer look. Chip Scale Review. pp. 5, Volume 18, No 4, July 2014

Glazer, J. (1994). Microstructure and mechanical properties of Pb-free solder alloys for low-cost electronic assembly: A review. Journal of Electronic Materials. August 1994, Volume 23, Issue 8, pp 693–700

Glazer, J. (1995). MeTAMlury of low temperature Pb-free solders for electronic assembly. *Internatial Material Review , 40* (2), 65-93.

Gomez, P., Anselm, M., (2017). A study on the minimum and maximum temperatures of the reflow process in SMT assembly on paste containing Bismuth alloys combined with lead-free solder spheres. Rochester Institute of Technology.

Guéné, E. (2013). Development of a Suitable Flux Medium for Cleanable and No-Clean Solder Pastes Based on Tin-Bismuth-Silver Alloy. International Conference on Soldering & Reliability 2013 Proceedings P.32

Handwerker, C., Bath, J., Benedetto, E., Bradley, E., Gedney, R., Snugosvsky, P., & Sohn, J. (2004). NEMI Lead Free Assembly Project: Comparison between PbSn and SnAgCu Reliability and Microstructure.

Henshall, G., Healy, R., Pandher, R., Sweatman, K., Howell, K., Coyle, R., Sack, T., Snugovsky, P., Tisdale, S., Hua, F. (2008). iNEMI Pb-Free Alloy Alternatives Project Report: State of the Industry. Proceedings SMTAI.

Hirose, A., Ide, H., Yanagawa, E., & Kobayashi, K. F. (2004). Joint strength and interfacial microstructure between Sn–Ag–Cu and Sn–Zn–Bi solders and Cu substrate. *Science and Technology of Advanced Materials 5, www.elsevier.com/locate/stam,* 267–276.

Hua, F., Aspandiar, R., Anderson, C., Clemons, G., Chung, C., Faizul, M. (2003). Solder Joint Reliability Assessment of Sn-Ag-Cu BGA Components Attached with Eutectic Pb-Sn Solder. *SMTAI 2003.*

Hwang, J. S. (2000, Aug). A Strong Lead-free Candidate: the Sn/Ag/Cu/Bi System. *Surface Mount Technology* .

(2007). iNEMI Availability of SnPb-Compatible BGA Workshop. March 1, 2007

Jin, S., McCormack, M., (1994) Dispersion additions to a Pb-free solder for suppression of microstructural coarsening. Journal of Electronic Materials, Vol. 23, no. 8, pp. 735–739. https://doi.org/10.1007/BF02651367

Juarez, J.M., Robinson, M., Heebink, J., Snugovsky, P., Kosiba, E., Kennedy, J., Bagheri, Z., Suthakaran, S., Romansky. M., (2013). Reliability Screening of Lower Melting Point Pb-Free Alloys Containing Bi. IPC APEX 2013

Kang, S.K. & Sarkhel, A.K., (1994). Lead (Pb)-free solders for electronic packaging. JEM (1994) 23: 701. https://doi.org/10.1007/BF02651362

Kinyanjui, R., Aspandiar, R., Coyle, R., Vasudevan, V., Tisdale, S., Arellano, j., & Parupalli, S. (2010). Challenges in reflow Profiling Large and high Density Ball Grid Array Packages suing Backward Compatible Assembly Processes. *IPC Apex 2010, S35-03*.

Kondrachova, L., Aravamudhan, S., Sidhu, R., & AMIR, D. (2012). Fundamentals' of the Non-Wet Open BGA Solder Joint Defect Formation. International Conference on Soldering and Reliability (ICSR).

Kotadia, H., Howes,P., Mannan, S., (2014). A review: On the development of low melting temperature Pb-free solders. Microelectronics Reliability. Volume 54. Issues 6–7.

Lau, J., & Lui, K. (2004). Global trends in Lead-free Soldering.

Liang, J., Dariavach, D., Subir, E., Lee, Y. C., & Wong, C. P. (2007). Metallurgy, processing and reliability of lead free solder joint interconnections in micro electronic materials, Physics, mechanics, design and reliability packaging. *Springer*.

Liu, V., Keck, J., Page, E., Lee, N.C., (2014). Voiding and Reliability of BGA Assemblies with SAC and 57Bi42Sn1Ag Alloys. in SMTA China East - NEPCON Shanghai, 2014.

Loomans, M.E., Vaynman, S., Ghosh, G. et al. .,(1994). Investigation of multi-component lead-free solders. JEM (1994) 23: 741. https://doi.org/10.1007/BF02651368

Maalekian, M., Xu, Y., & Seelig, K. (2015). Effect Of Bi Content on Properties Low Silver SAV Solder. *SMTA International, Rosemont, IL*, Pg 191 to 198.

MacKay, C. A., Voss von, W. D. (1985) Effect of compositional changes and impurities on wetting properties of eutectic Sn–Bi alloy used as solder, Materials Science and Technology, 1:3, 240-248 https://doi.org/10.1179/mst.1985.1.3.240" 10.1179/mst.1985.1.3.240

Mattila, T.T., Kaloinen, E., Syed, A., Kivilahti, J.K., (2007). Helsinki University of Technology. Reliability of SnAgCu Interconnections with Minor Additions of Ni or Bi under Mechanical Shock Loading at Different Temperatures. 2007 Proceedings 57th Electronic Components and Technology Conference

McCormack, M., Chen, H., Kammlott, G., Jin, S., (1997). Significantly Improved Mechanical Properties of Bi-Sn Solder Alloys by Ag-Doping. Journal of Electronic Materials, Vol. 26, no. 8, pp. 954 - 958, August 1997.

Mei, Z. & Morris, J.W. (1992) Characterization of eutectic Sn-Bi solder joints. JEM. 21: 599. https://doi.org/10.1007/BF02655427

Mei, Z., Holder, H. A., & Vander Plas, H. A. (1996). Low-Temperature Solders. *Article 10, Hewlett-Packard Journal*.

Miao, H.W., Duh, J.G., (2001). Microstructure evolution in Sn–Bi and Sn–Bi–Cu solder joints under thermal aging. Materials Chemistry and Physics. Volume 71. Issue 3.

Mokler, S., Aspandiar, R., Byrd, K., Chen, O., Walwadkar, S., Tang, K.K., Renavikar, M., Sane, S., (2016). The application of Bi-Based solders for Low Temperature Reflow to reduce Cost While Improving SMT Yields in Client Computing Systems. SMTA International.

Mutuku, F., Geng, J., Zhang, H., Lee, N. (2018). Low Temperature Solder Alloy with High Reliability. *IPC APEX 2018 S23_01.*

NSMS, Lead-Free, High-Temperature, Fatigue-Resistant Solder: Final Report, Ann Arbor, MI: National Center for
Manufacturing Science, 2001.

Ngoh, S., Zhou, W., Pang, H. L., & Shi, X. (2004). Growth of IntermeTAMlic Compounds during Isothermal Annealing of a Sn-Ag-Cu Lead-free Solder. *Soldering & Surface Mount Technology* .

Oresjo, S. (2005). Test and Inspection as a Part of the Lead Free Manufacturing Process. *ECWC 10 Conference at IPC Printed Circuits Expo Apex and Designer Summit.*

Palaniappan, S. K., & Anselm, M. (2016). A Study on Process, Strength and Microstructure Analysis of Low Temperature Bi Containing Solder Pastes with Lead Free Solder Balls. *RIT Scholar Works, RIT Department of Manufacturing and Mechanical Engineering Technology*

Pandher, R., & Healey, R. (2008). Reliability of Pb-Free Solder Alloys in Demanding BGA and CSP Applications. *Electronic Components and Technology Conference*.

Ribas, M., Chegudi, S., Kumar, A., Pandher, R., Raut, R., Mukherjee, S., et al. (2014). Thermal and Mechanical Reliability of Low-Temperaturer Solder Alloys for Handheld Devices. *IEEE 16th Electronics Packaging Technology Conference (EPTC)* .

RoHS. (2003, Feb). Directive 2002/95/EC Restriction of Hazardous Substances.

Sampathkumar, M., Rajesnayagham, S., Ramkumar, S. M., Anson, S., (2005). Investigation of the Performance of SAC and SAC-Bi Lead-Free Solder Alloys with OSP and Immersion Silver PCB Finishes. SMTA International.

Sandy, B., Briggs, E., & Lasky, R. (2011). Advantages of Bismuth-based Alloys for Low Temperature Pb-Free Soldering and Rework. *Indium Corporation Tech Paper*.

Schroeder, V., Hua, F., Gleason, J., (2001) Strength and Fatigue Behavior of Joints Made with Bi-42sn-1ag Solder Paste: An Alternative to Sn-3.5ag-0.7cu For Low Cost Consumer Products. SMTA International 2001.
Seeling, K. (1995, Sept). A Study of Lead-Free Solder Alloys.

Shnawah, D.A., Said, S.B.M., Sabri, M.F.M., Badruddin, I.A., Che, F.X. (2012). *Journal of Electronic Materials 41(9), pp. 2631-2658*

Snugovsky, P., Bagheri, S., Bagheri, Z., Romansky, M., (2007). The New Lead-Free Assembly Rework Solution Using Low Melting Alloys. IPC APEX, 2007.S24-01

Snugovsky, P., et al., (2008). Microstructure, Defects, and Reliability of Mixed Pb Free / SnPb Assemblies. TMS. vol 1. Material Processing and Properties. p.p. 631-642.

SPVC, I. S. (2005). Round Robin Testing and Analysis of Lead Free Solder Paste with Alloys of Tin, Silver, Copper - Final Report.

Surashi, D., & Seelig, K. (2001). The Current Status of Lead-Free Solder Alloys. *IEEE transactions on Electronics Packaging Manufacturing, Vol 24, No 4*.

Takao, H., Yamada, A., & Hasegawa, H. (2004). Mechanical Properties and Solder joint Reliability of Low Melting SnBiCu Lead Free Solder. *R&D Review of Toyota CRDL, Vol 39, No. 2*, Pg 49 to 56.

Tang, K.K., Wong, C., Chang K., Aspandiar, R., Mokler, S., Chen, O., Chang, W. J., Xin, W., Tsai, J., WoonBin, J., Chou, B., (2016). System Level Thermal Cycling and Shock Reliability Performance of Low Temperature Soldering. 2016 SMTA China East - NEPCON Shanghai Conference.

Tomlinson, W.J. & Collier, I. (1987). The mechanical properties and microstructures of copper and brass joints soldered with eutectic tin-bismuth solder. J Mater Sci (1987) 22: 1835. https://doi.org/10.1007/BF01132413

Valooran, R., Anselm, M., (2017). Investigation of the Factors Influencing the Performance of Low Temperature Solder. Rochester Institute of Technology.

Vianco, P T, Hosking, F M, & Rejent, J A., (1992). Wettability analysis of tin-based, lead free solders. United States.

Vianco, P.T. & Frear, D.R. (1993). Issues in the replacement of lead-bearing solders JOM (1993) 45: 14. https://doi.org/10.1007/BF03222374

Vianco, P.T., Kilgo, A.C., Grant, R., (1995). IntermeTAMlic Compound Layer Growth Kinetics in Non-Lead Bearing Solders. Sandia National Laboratories.

Vianco, P., Properties of Ternary Sn-Ag-Bi Solder Alloys: Part 2- Wettability and Mechanical properties Analysis. Journal of Electronics Materials, Vol.28, No.10, pp. 1138-1143, 1999.

Vijayaragavan, N., Carson, F. P., Mistry, A., (2008). Package-on-Package Warpage–Impact of Surface Mount Yields and Board Reliability. ECTC

WEEE. (2003, Feb). Directive 2002/96/EC on the eco-design of Energy-related Products (ErP).

Witkin, D., et al., (2012). Creep Behavior of Bi-Containing Lead-Free Solder. Journal of Electronics Materials, Vol.41, No.2, pp. 190-203, 2012

Woodrow, T., (2010) Modeling of the JCAA/JG-PP Lead-Free Solder Project Vibration Test Data. IPC/JEDEC Global Conference. Boston, 2010

Woodrow, T., (2008). JCAA/JG-PP Lead-Free Solder Project: -20°C to +80°C Thermal Cycle Test. Boeing Electronics Materials and Processes Report

Yoon, J.-W., Kim, S.-W., Jung, S.-B., (2004). IMC Growth and Shear Strength of Sn-Ag-Bi-In/Au/Ni/Cu BGA Joints During Aging. Materials Transactions, The Japan Institute of Metals and Materials, Vol. 45, no. 3, p. 727 to 733, 2004.

Zhu, F., Wang, Z., Guan, R., & Zhang, H. (2005). Mechanical Properties of a Lead-Free Solder Alloys. *International Conference on Asian Green Electronics* .

APPENDIX A

Ball and Paste Study

Mixing Images for SnBi40-58%

TAM:120_Peak Temp180C

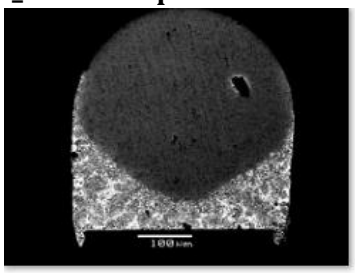
1

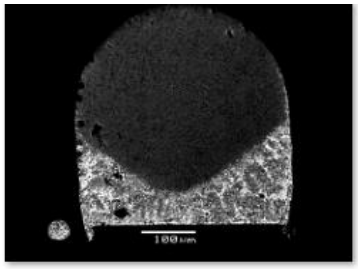
2

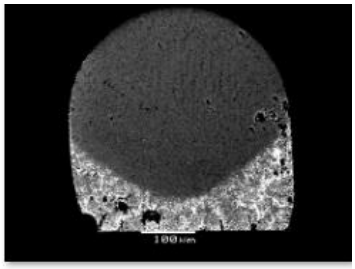
3

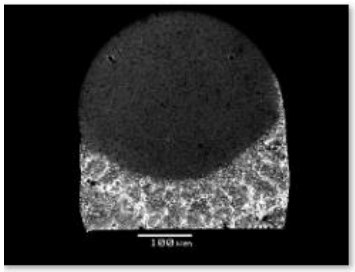
4

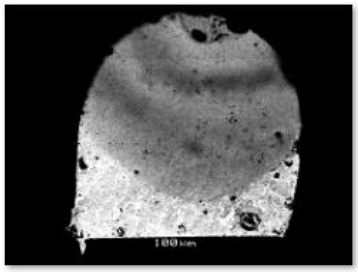
5

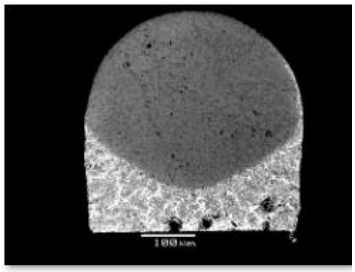
6

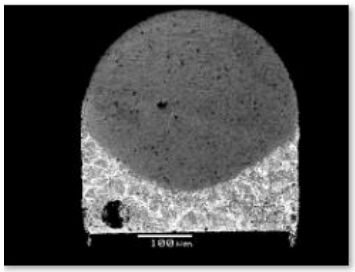
7

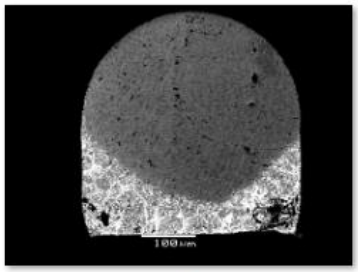
8

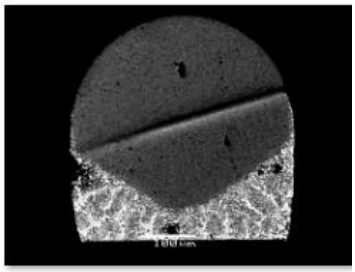
9

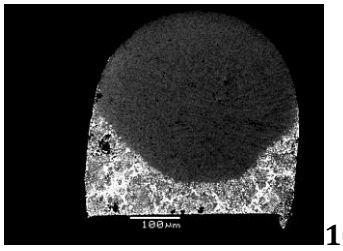
10

TAM:120_Peak Temp195C

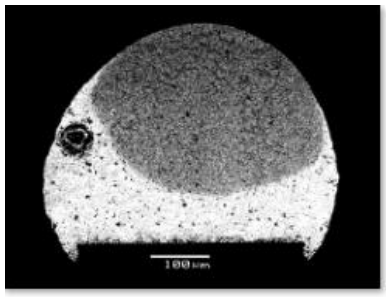

1

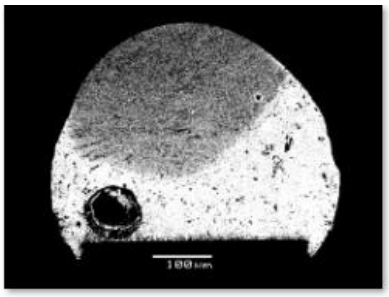

2

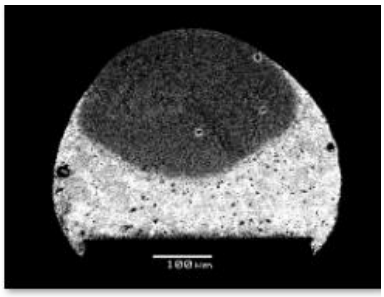

3

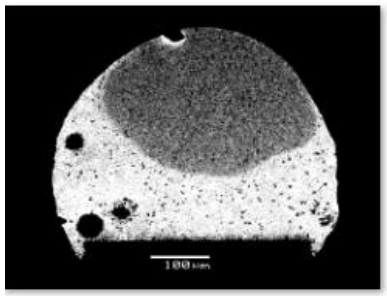

4

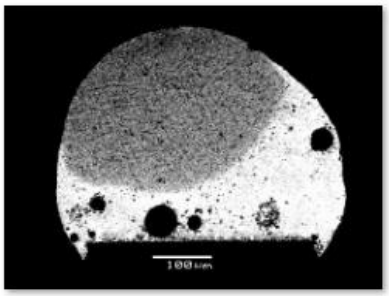

5

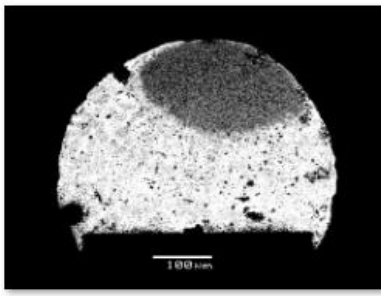

6

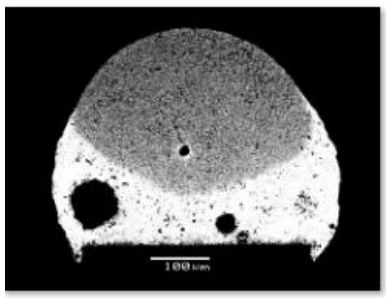

7

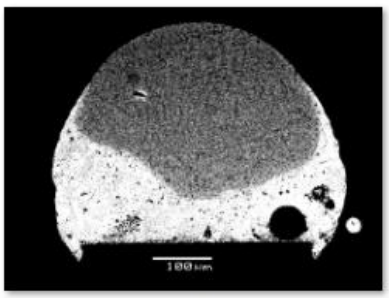

8

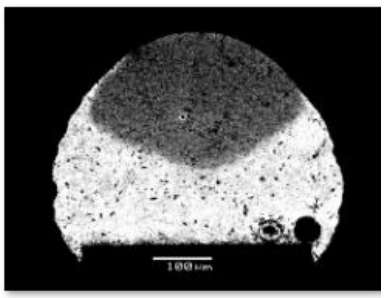

9

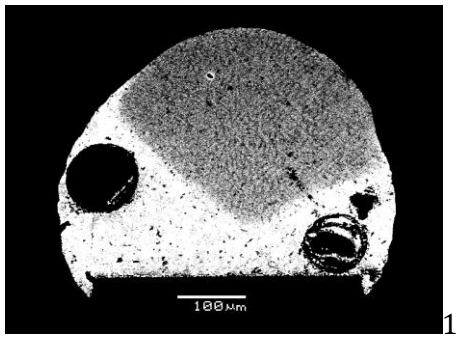

10

TAM:120_Peak Temp205C

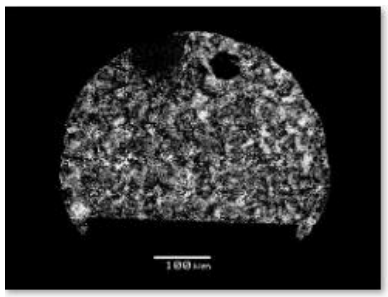

1

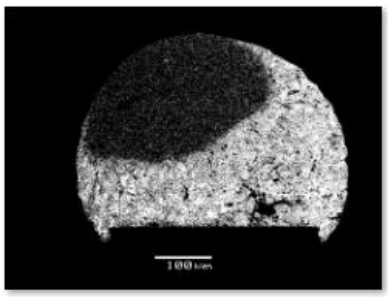

2

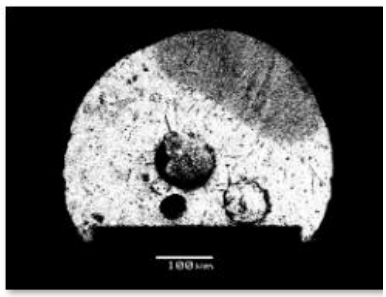

3

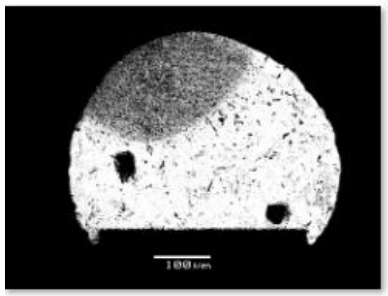

4

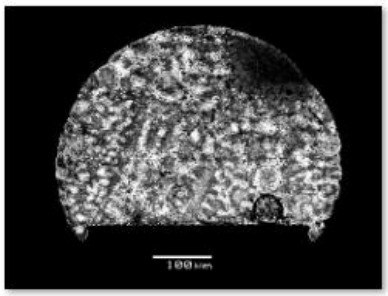

5

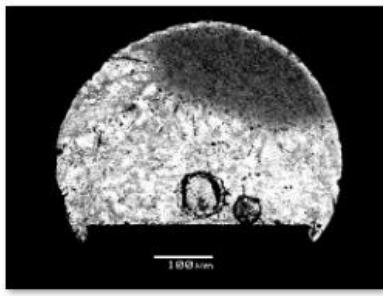

6

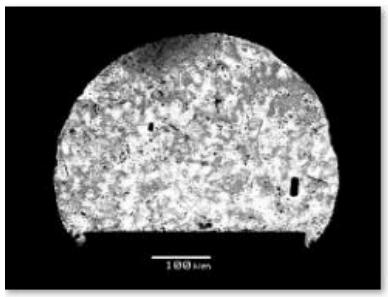

7

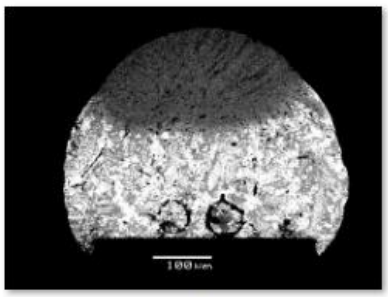

8

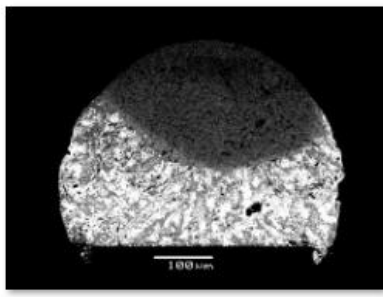

9

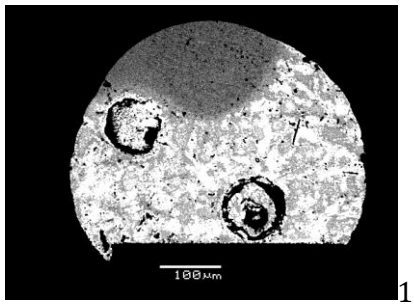

10

TAM:240_Peak Temp180C

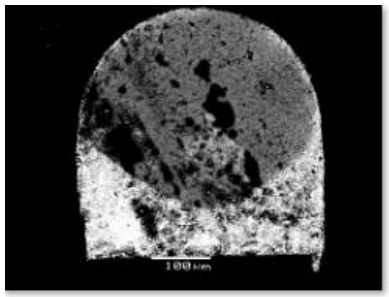

1

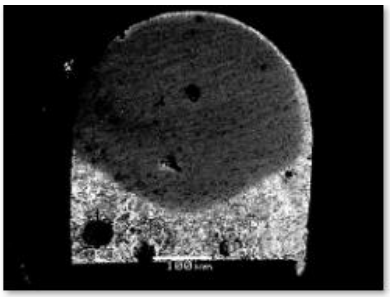

2

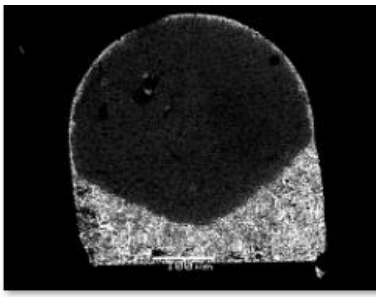

3

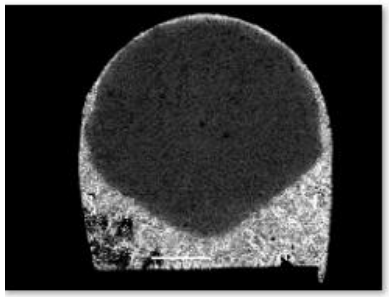

4

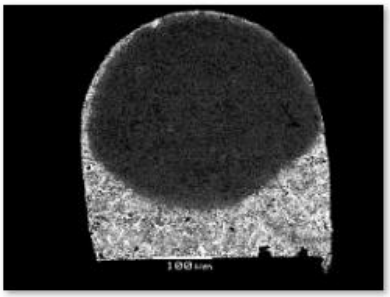

5

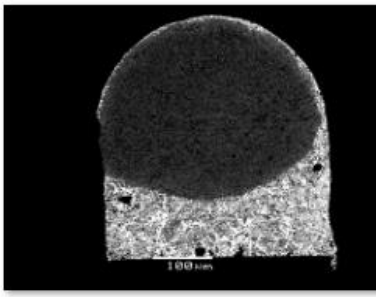

6

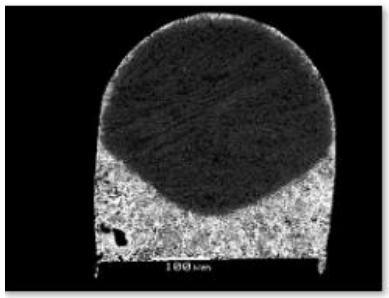

7

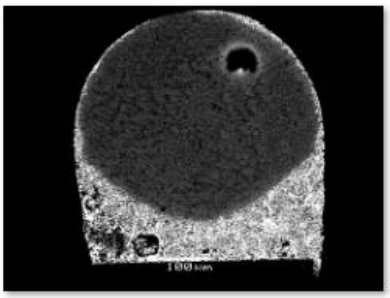

8

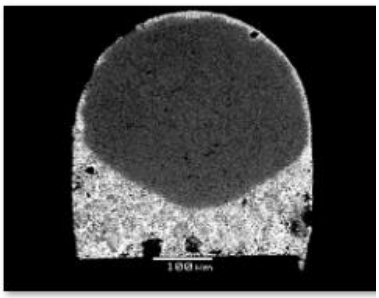

9

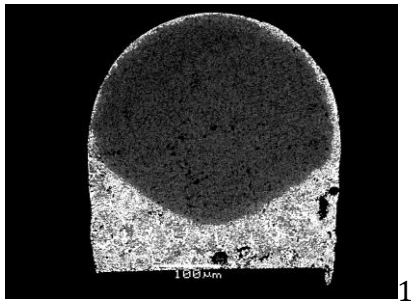

10

TAM:240_Peak Temp195C

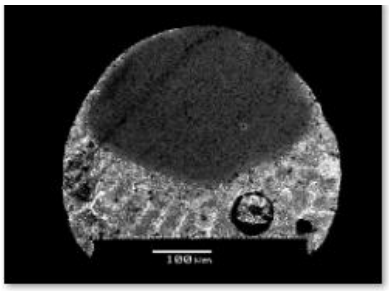

1

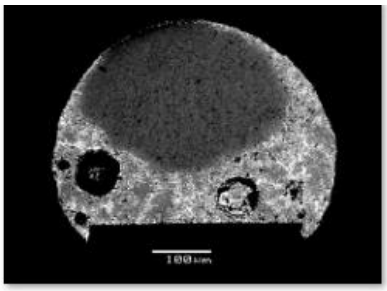

2

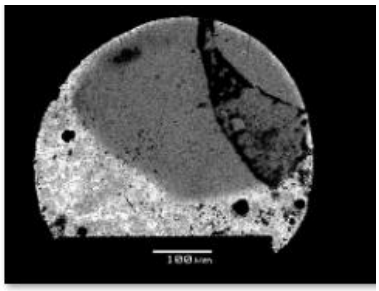

3

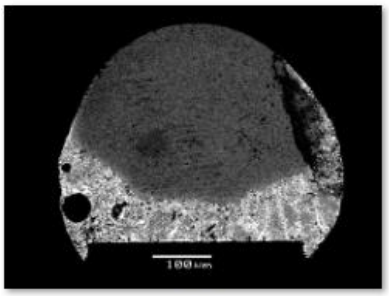

4

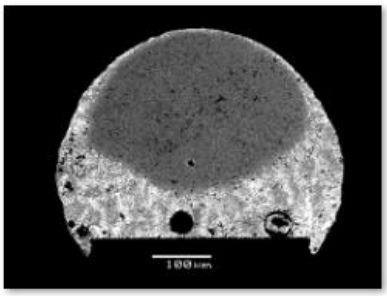

5

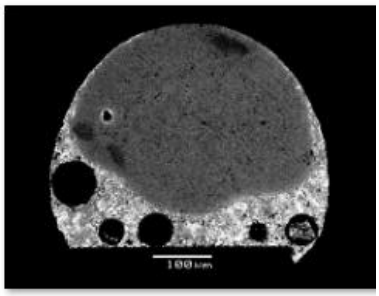

6

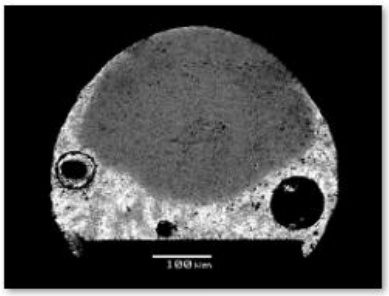

7

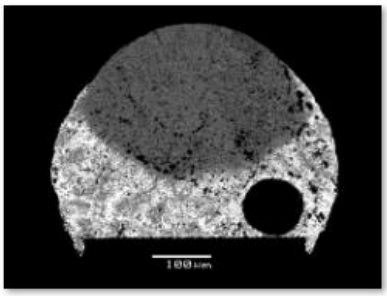

8

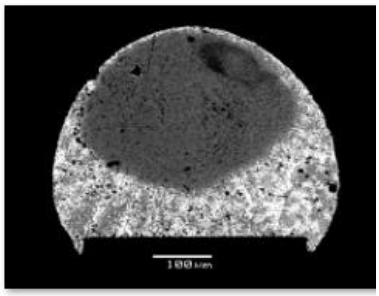

9

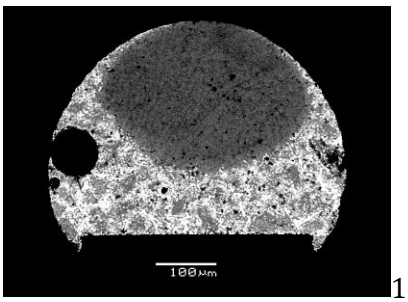

10

TAM:240_Peak Temp205C

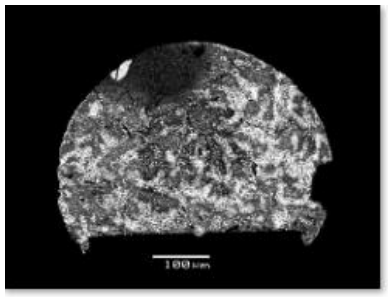

1

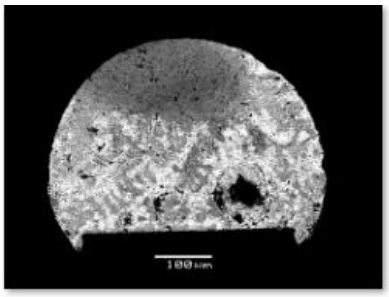

2

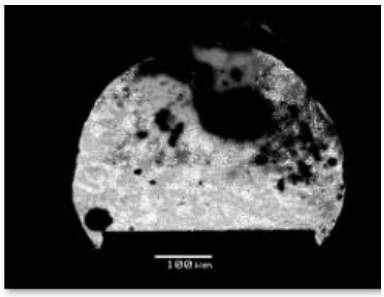

3

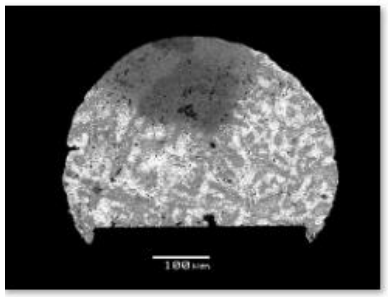

4

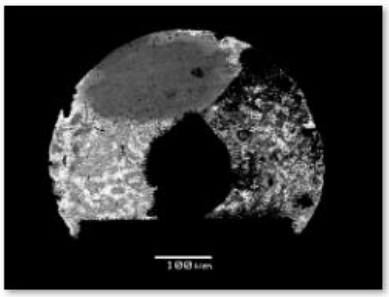

5

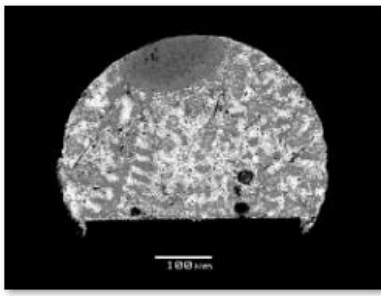

6

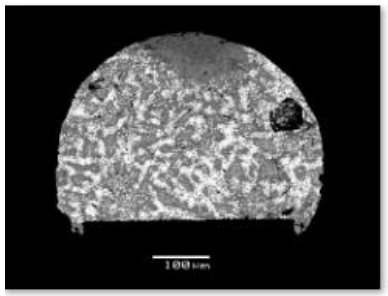

7

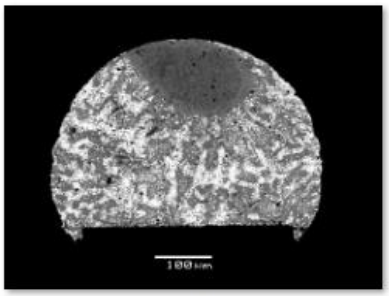

8

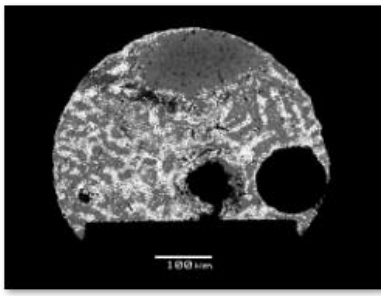

9

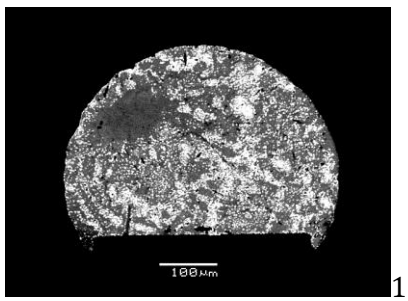

10

Mixing Images for SnBi58%

TAM:120_Peak Temp180C

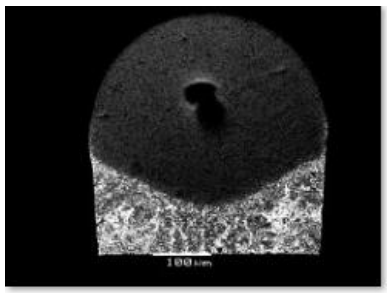

1

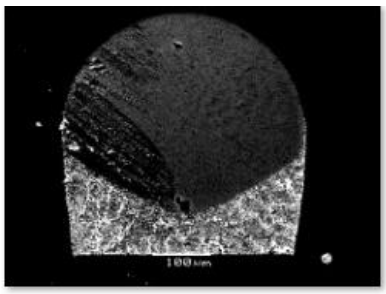

2

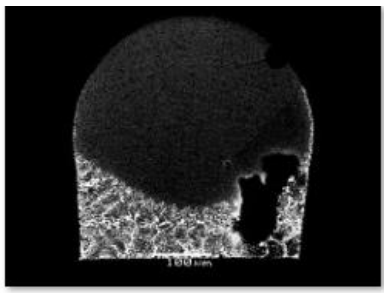

3

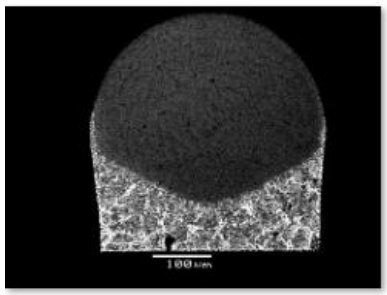

4

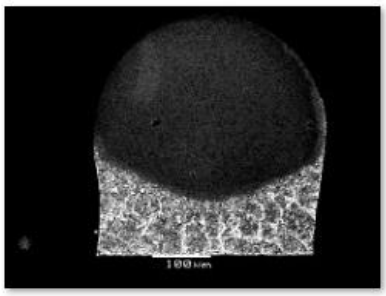

5

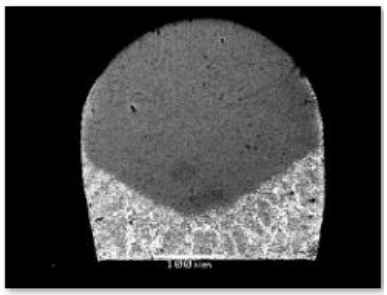

6

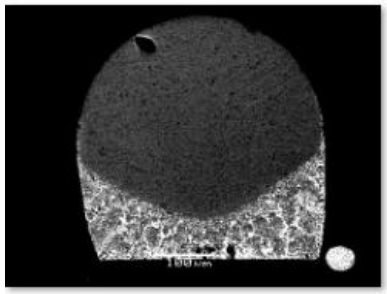

7

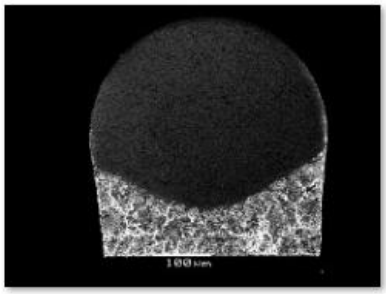

8

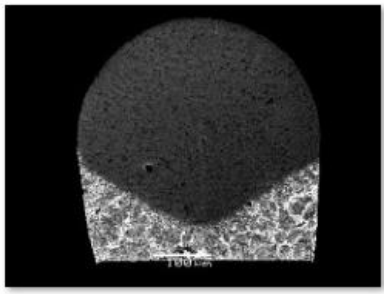

9

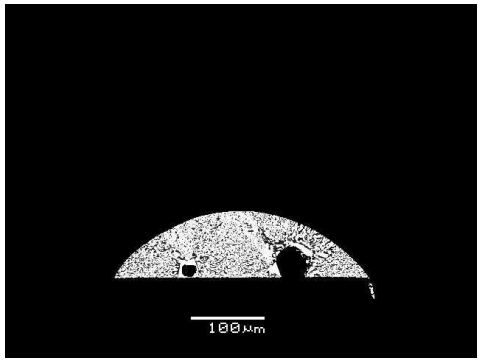

10

TAM:120_Peak Temp195C

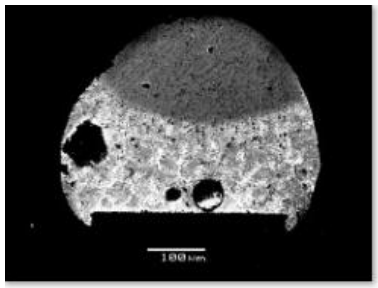

1

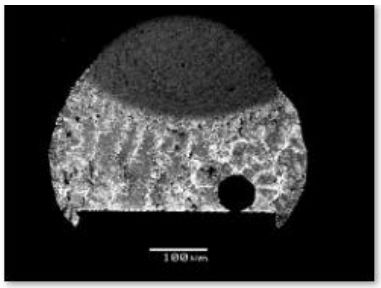

2

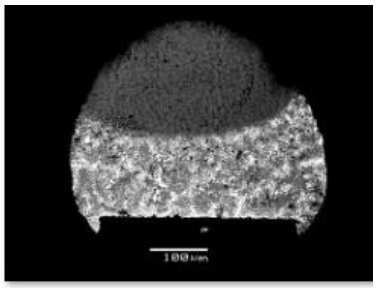

3

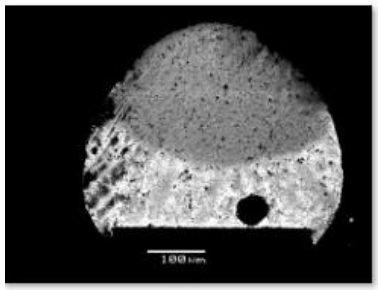

4

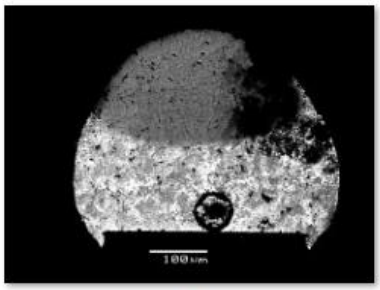

5

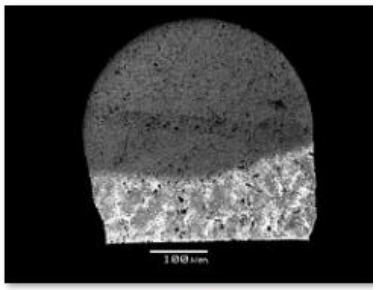

6

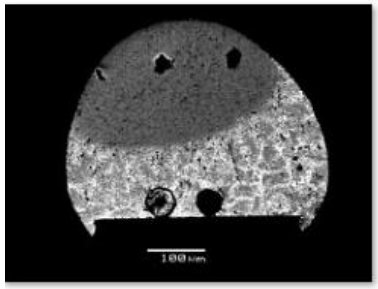

7

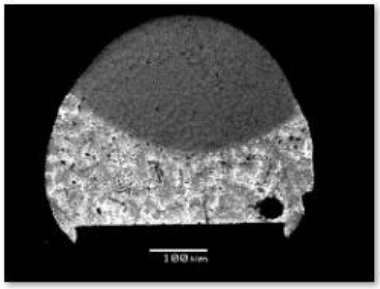

8

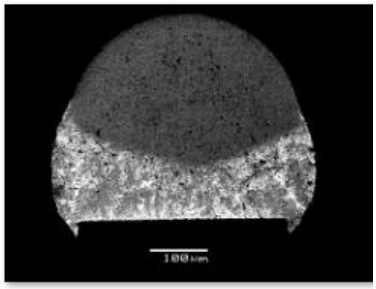

9

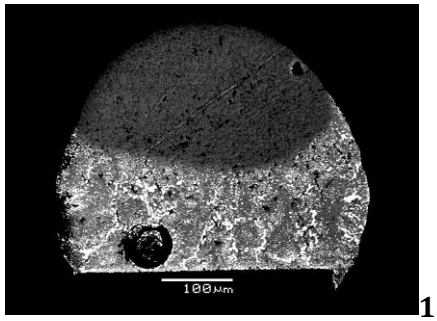

10

TAM:120_Peak Temp205C

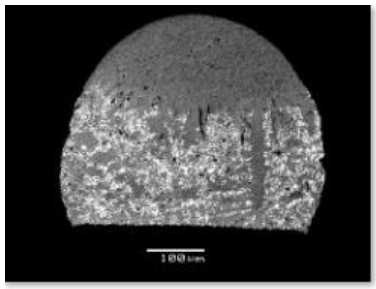

1

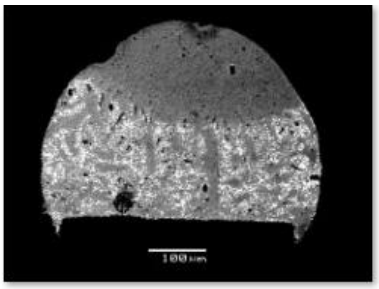

2

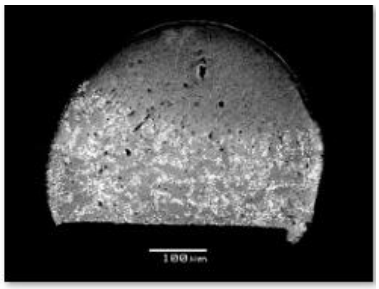

3

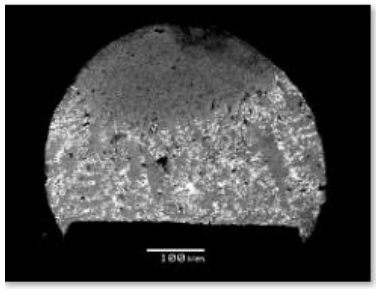

4

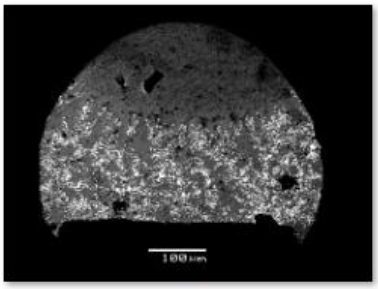

5

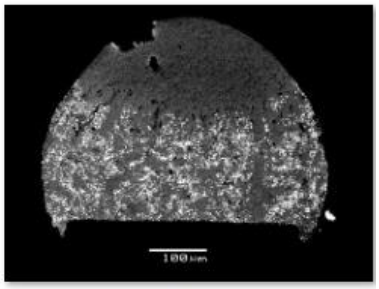

6

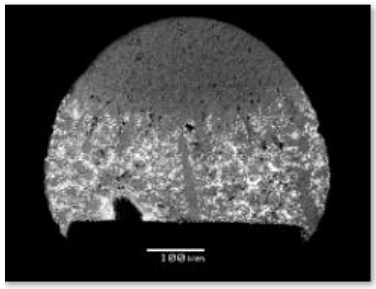

7

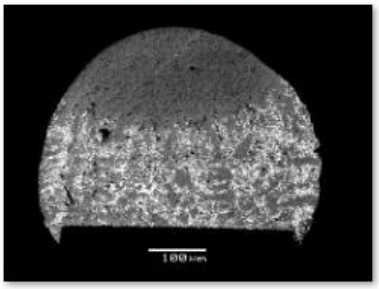

8

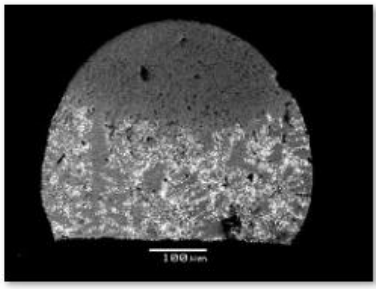

9

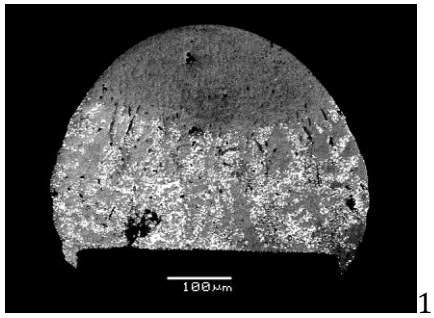

10

TAM:240_Peak Temp180C

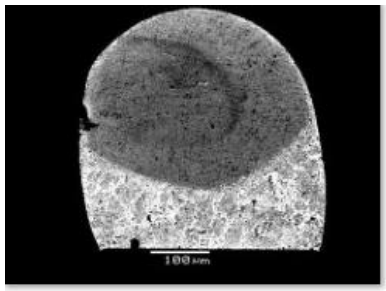

1

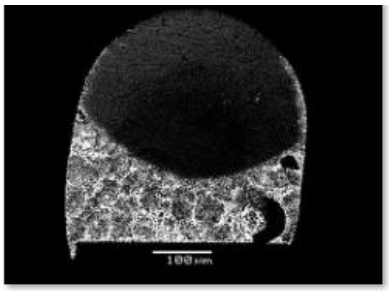

2

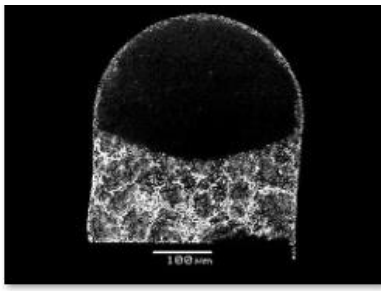

3

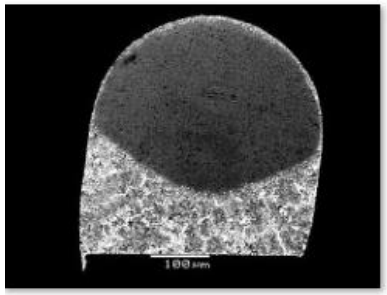

4

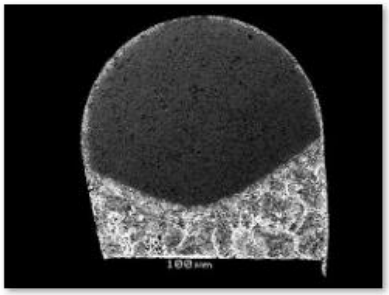

5

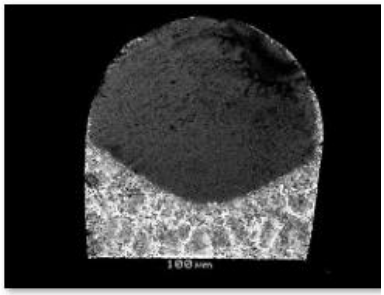

6

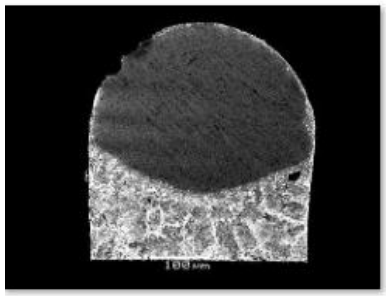

7

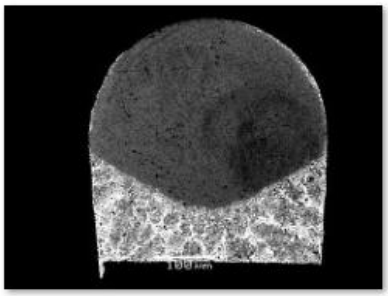

8

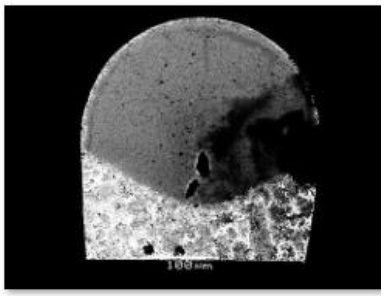

9

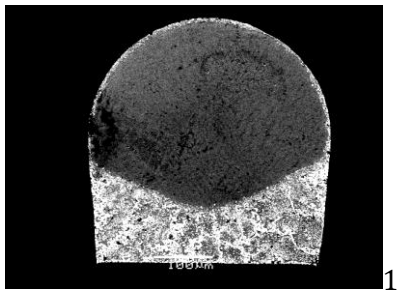

10

TAM:240_Peak Temp195C

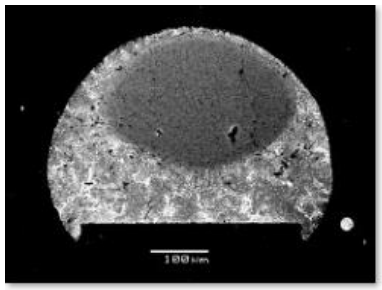

1

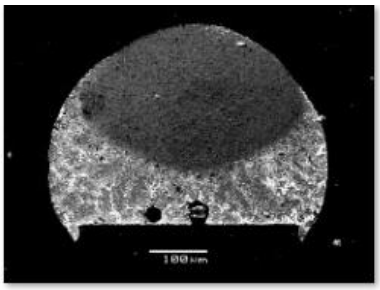

2

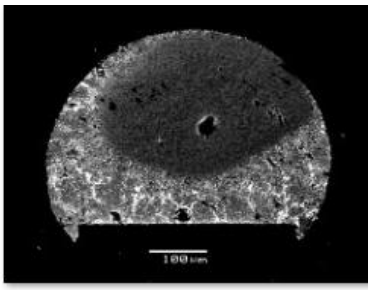

3

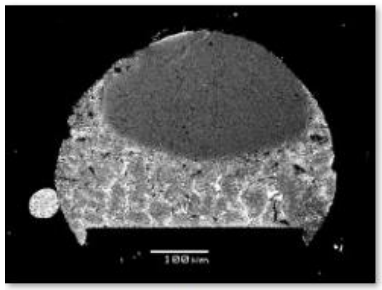

4

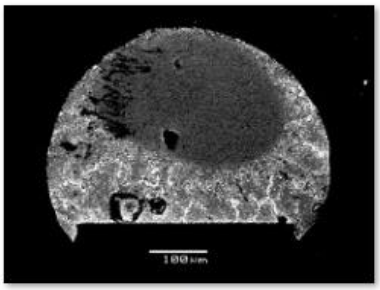

5

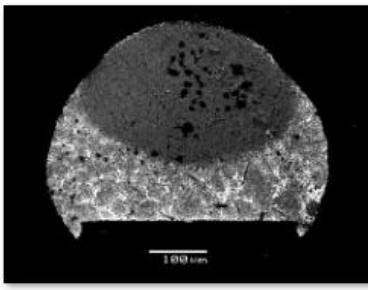

6

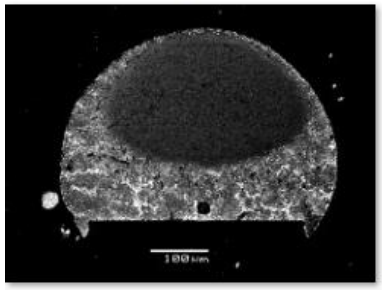

7

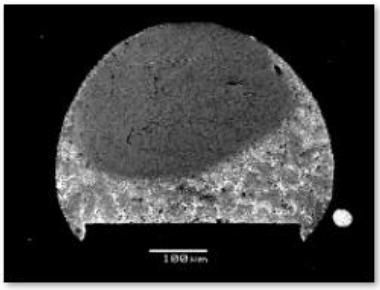

8

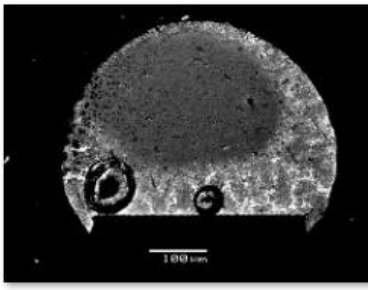

9

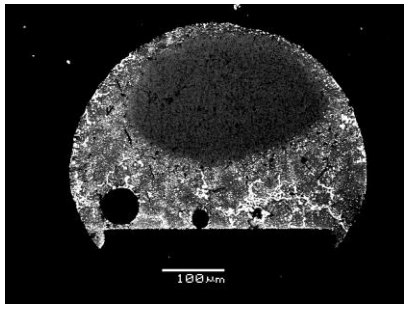

10

TAM:240_Peak Temp205C

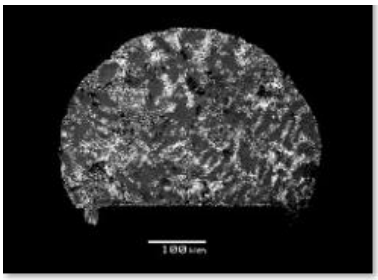

1

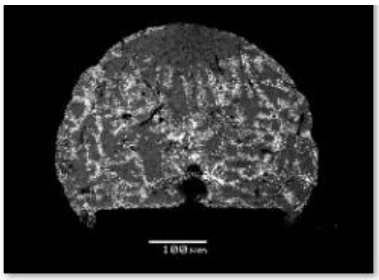

2

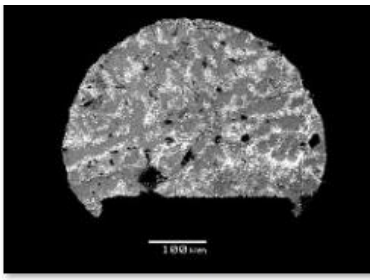

3

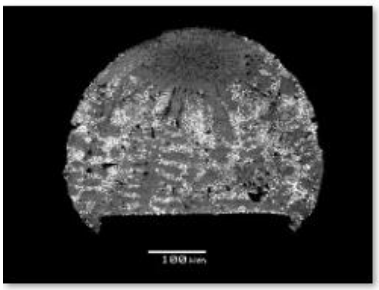

4

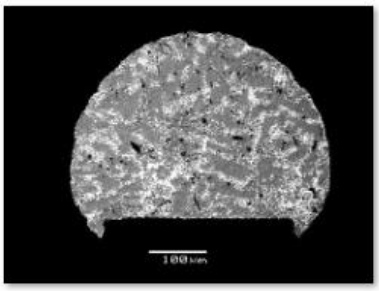

5

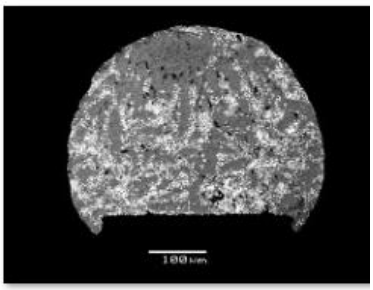

6

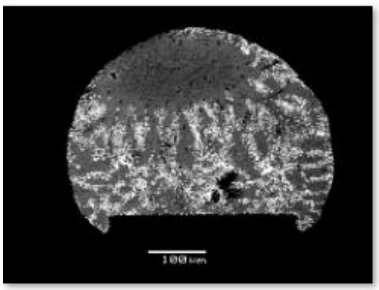

7

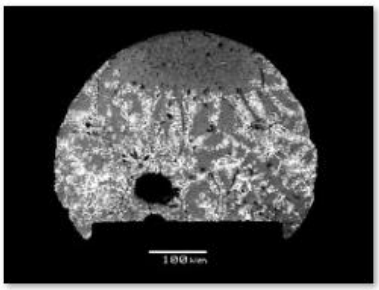

8

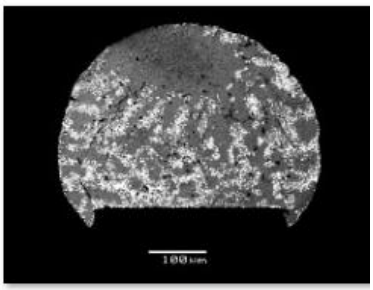

9

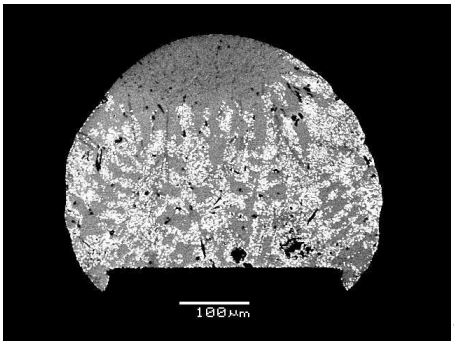

10

Mixing Images for SnBi57%

TAM:120_Peak Temp180C

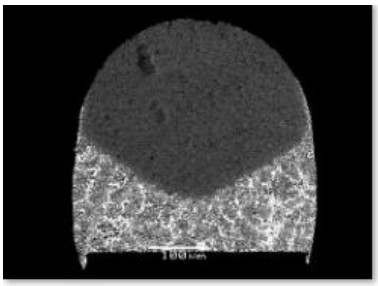

1

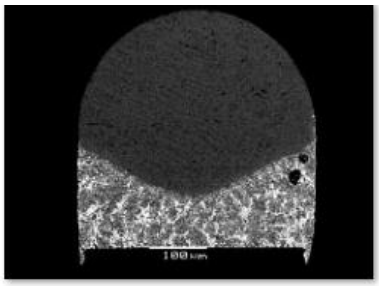

2

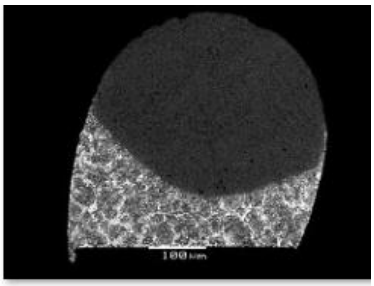

3

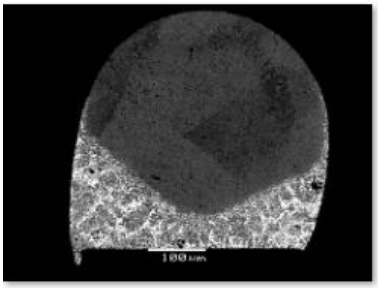

4

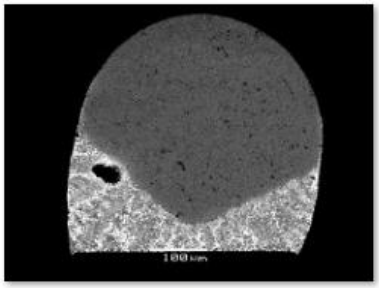

5

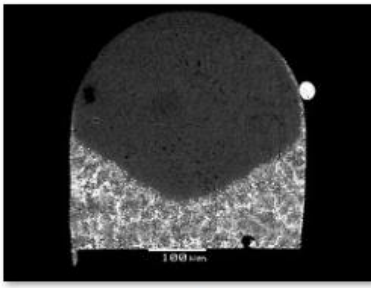

6

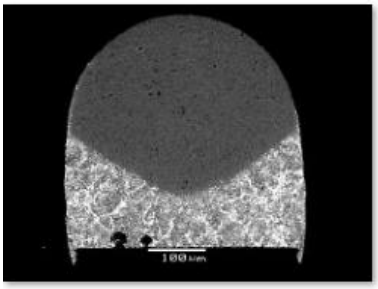

7

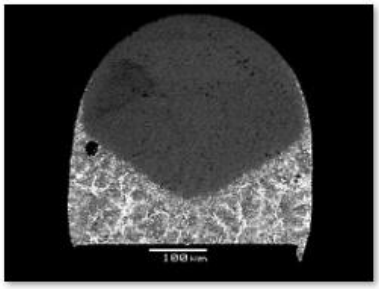

8

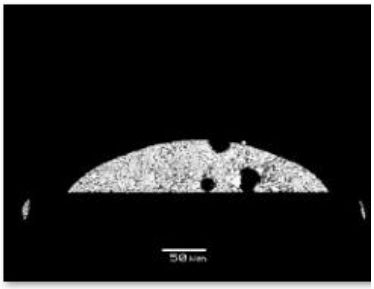

9

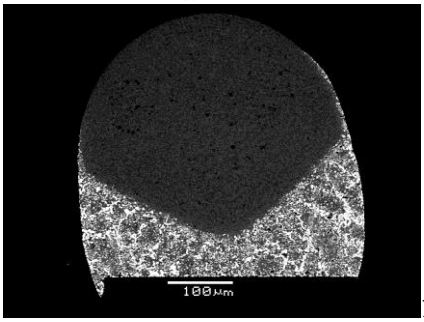

10

TAM:120_Peak Temp195C

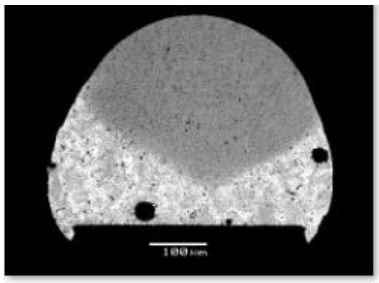

1

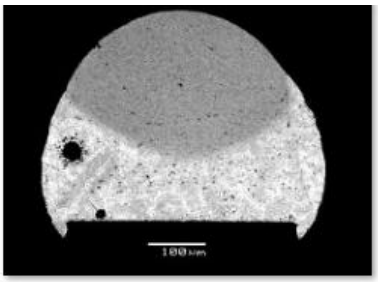

2

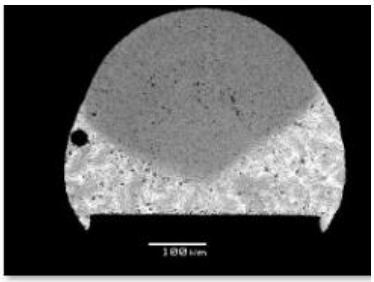

3

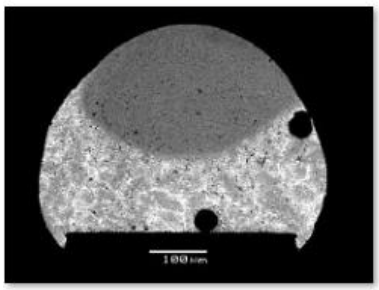

4

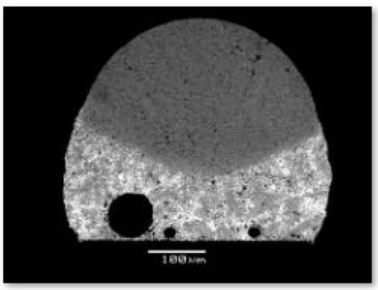

5

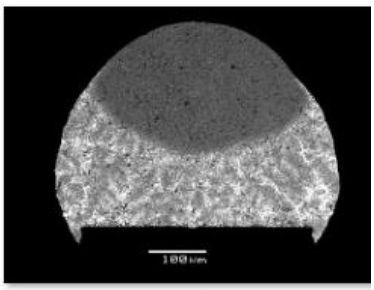

6

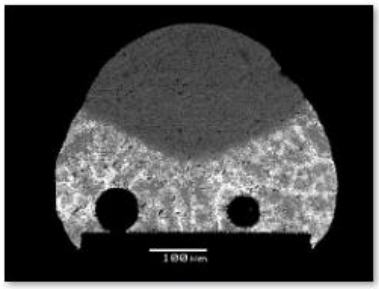

7

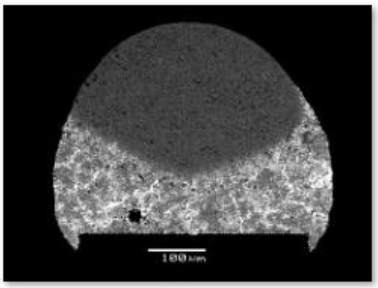

8

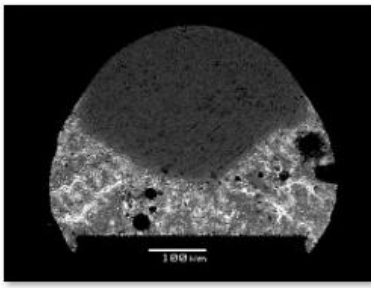

9

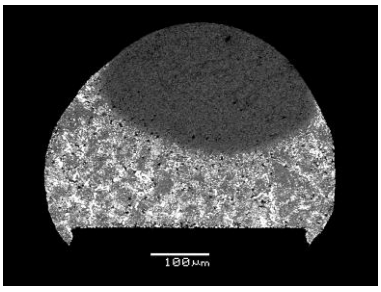

10

TAM:120_Peak Temp205C

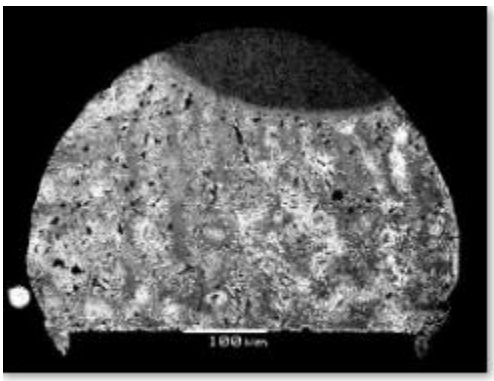

1a

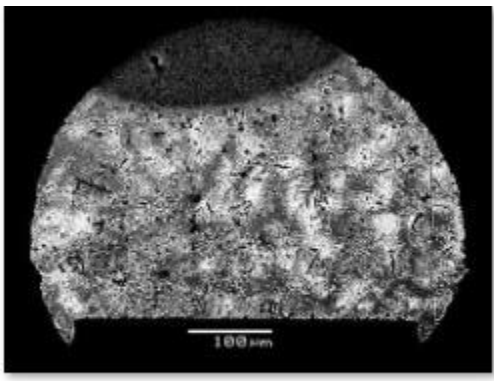

2a

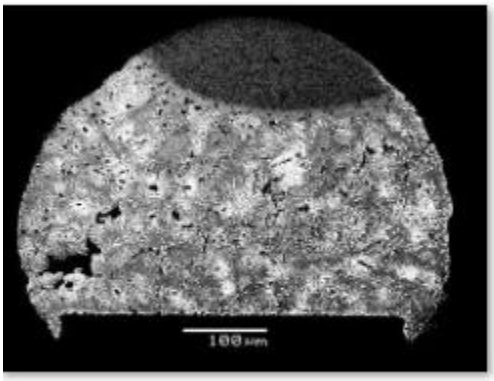

3a

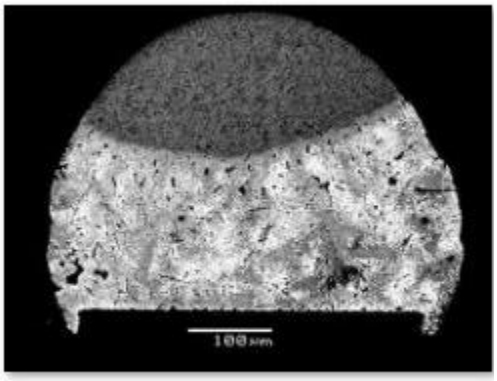

4a

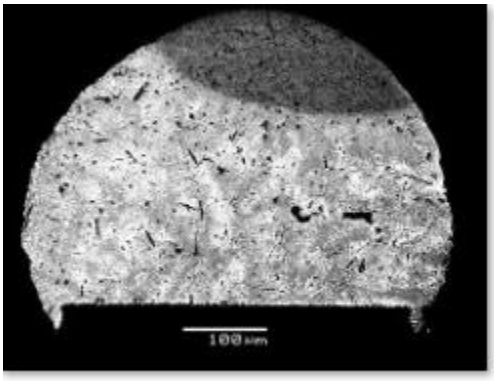

5a

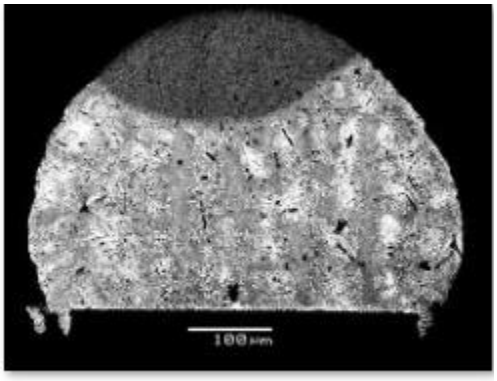

6a

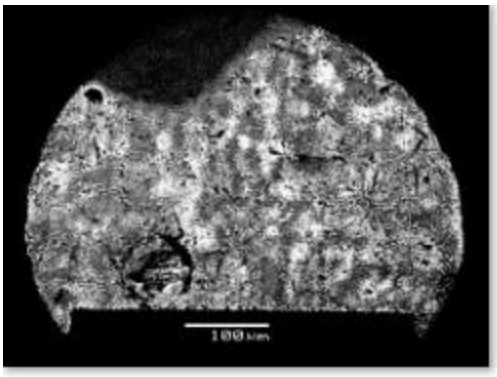

7a

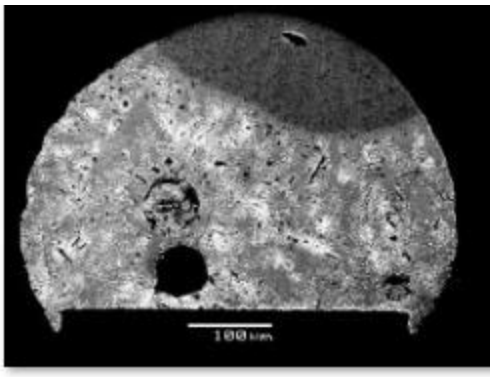

8a

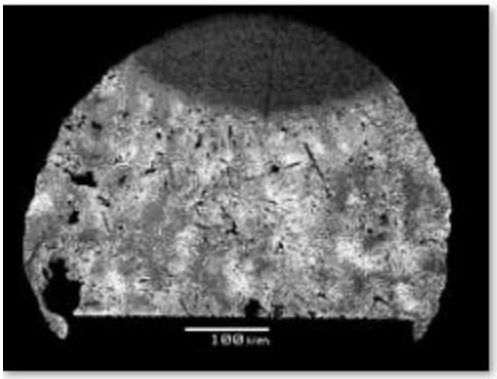

9a

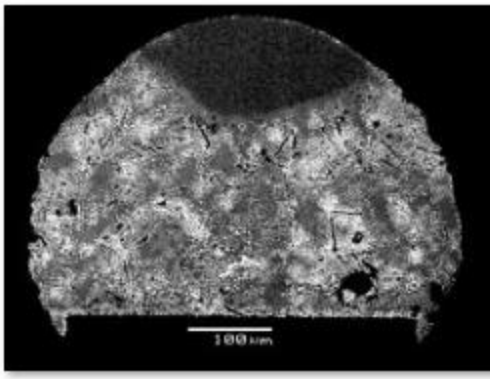

10a

TAM:240_PeakTemp180C

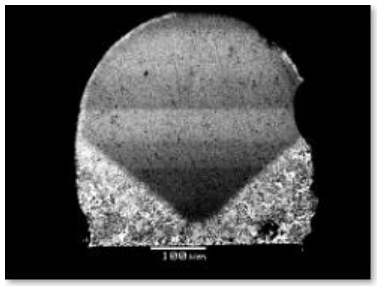

1a

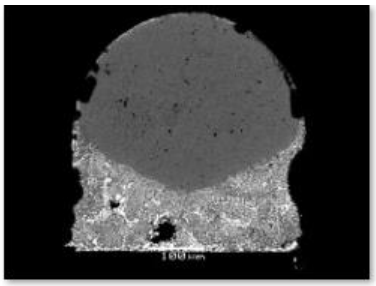

2

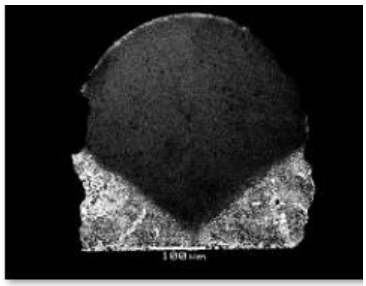

2a

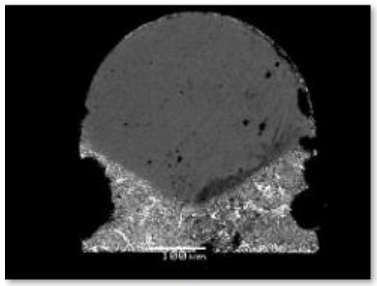

3

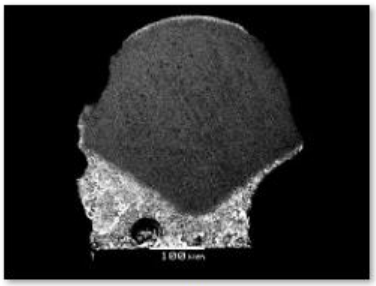

3a

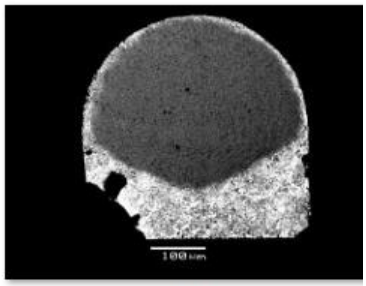

8a

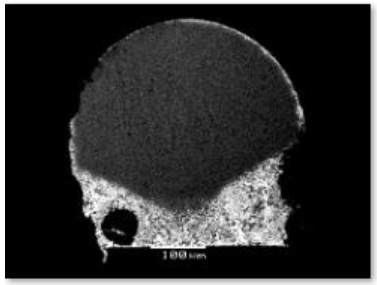

10a

TAM:240_PeakTemp195C

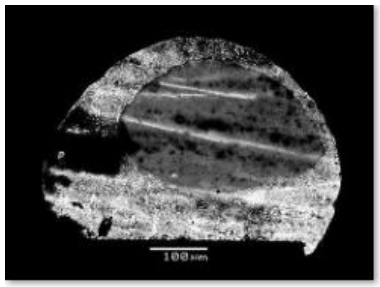

1a

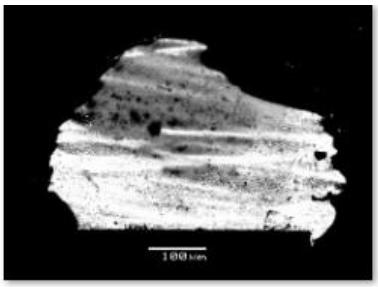

2

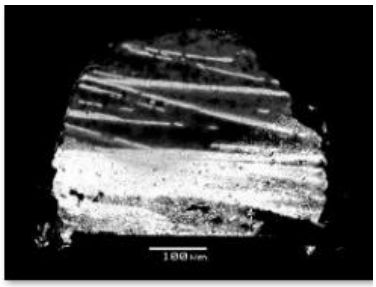

3

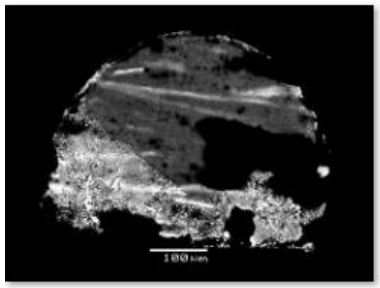

4

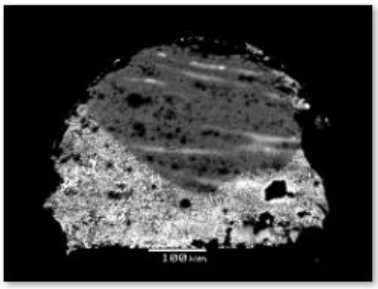

5

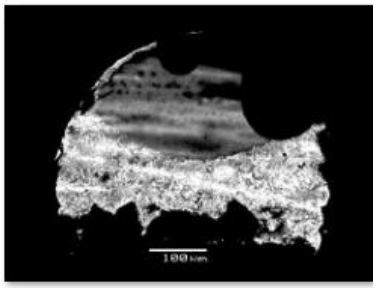

6

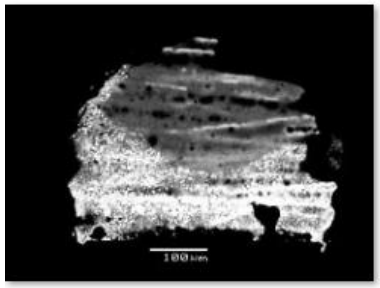

7

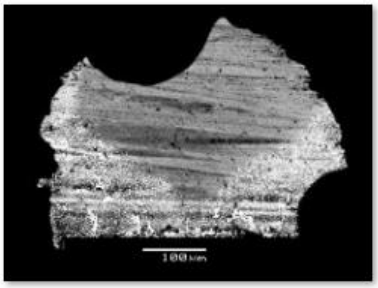

8

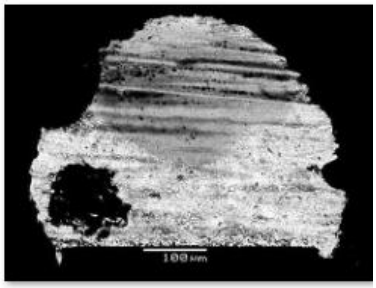

9

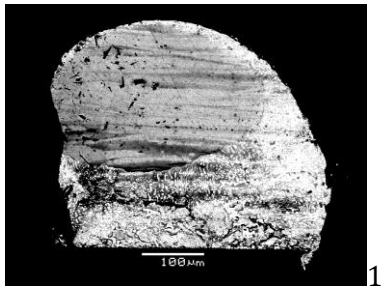

10

TAM:240_PeakTemp205C

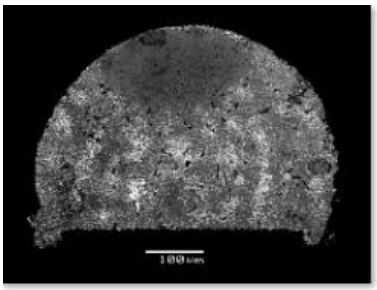

1

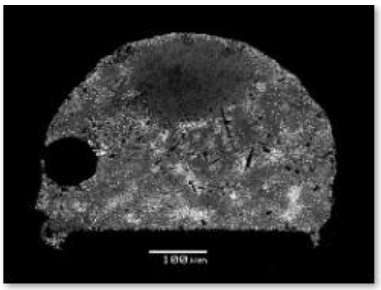

2

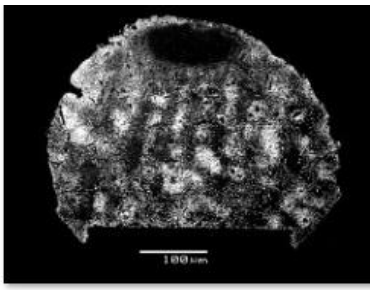

3a

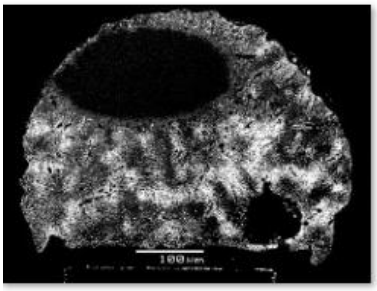

4a

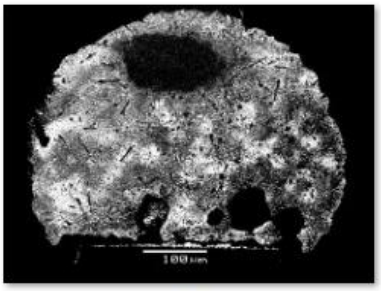

5a

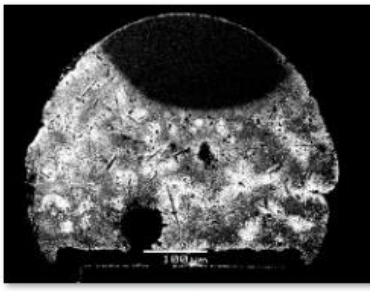

6a

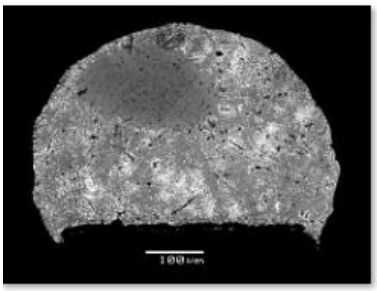

7

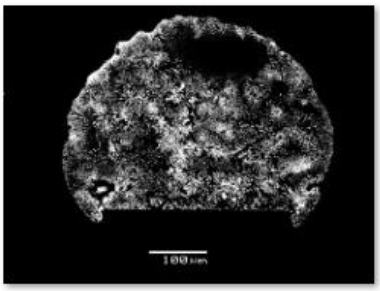

8a

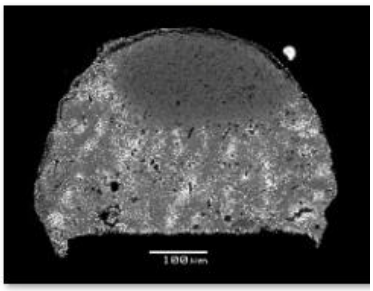

9

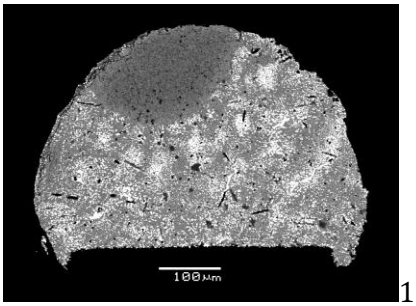

10

Reflow Profile details

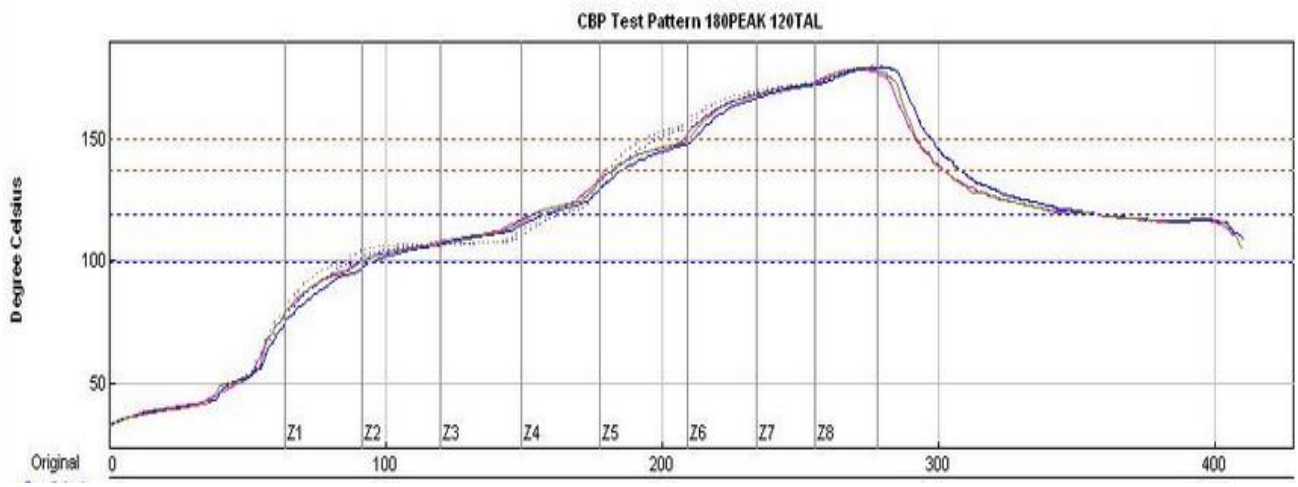

Belt speed 64 cm/min	Zone 1	Zone 2	Zone 3	Zone 4	Zone 5	Zone 6	Zone 7	Zone 8
	110	110	115	128	155	176	179	190

Table 28 Reflow Profile Tpeak=180˚C TAM=120sec

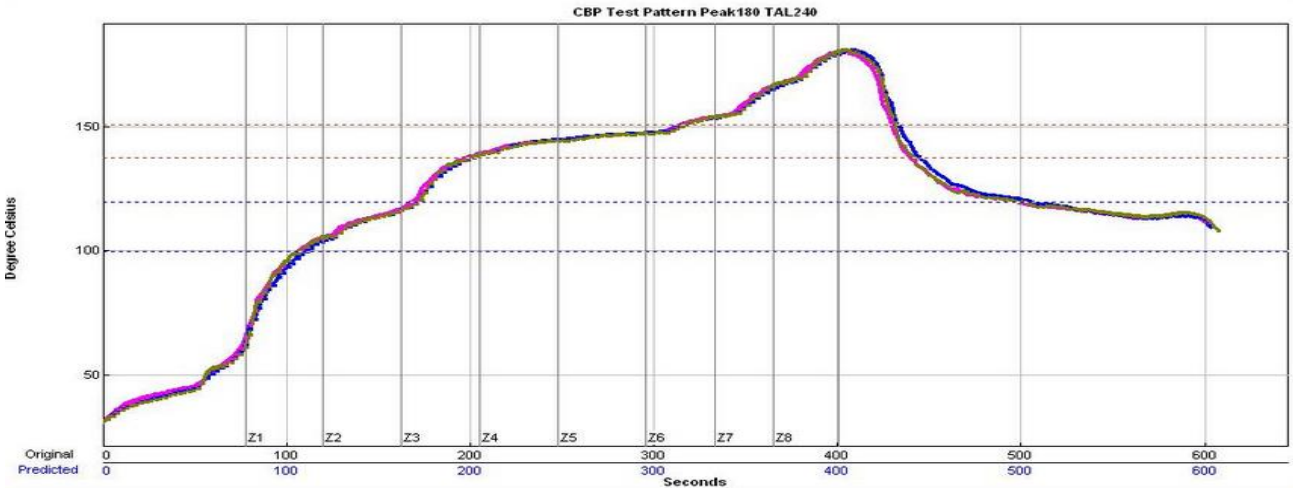

Belt speed 42.5 cm/min	Zone 1	Zone 2	Zone 3	Zone 4	Zone 5	Zone 6	Zone 7	Zone 8
	114	116	145	148	150	157	175	191

Table 29 Reflow Profile Tpeak= 180˚C TAM=240sec

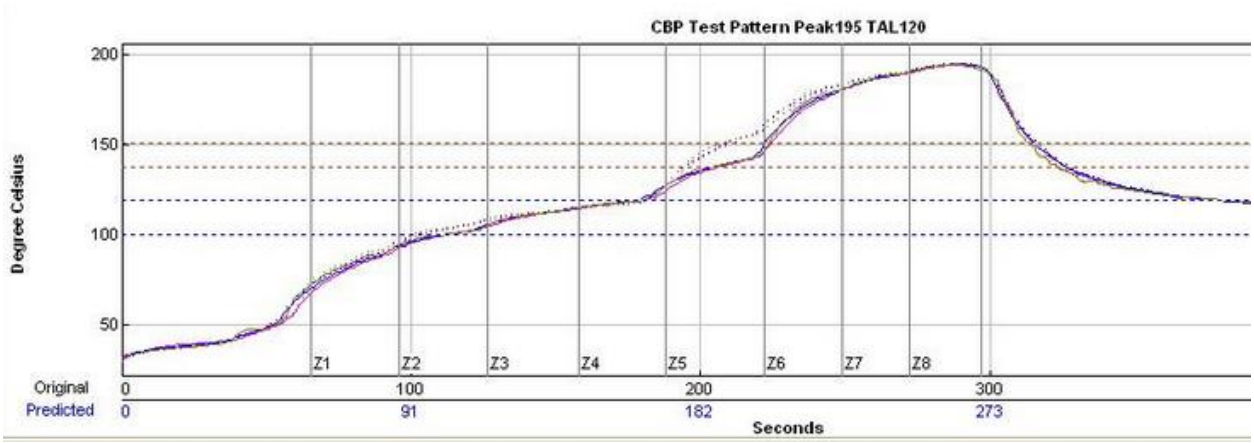

Belt speed 59.5 cm/min	**Zone 1**	**Zone 2**	**Zone 3**	**Zone 4**	**Zone 5**	**Zone 6**	**Zone 7**	**Zone 8**
	97	105	117	120	147	191	198	205

Table 30 Reflow Profile Tpeak= 195˚C TAM=120sec

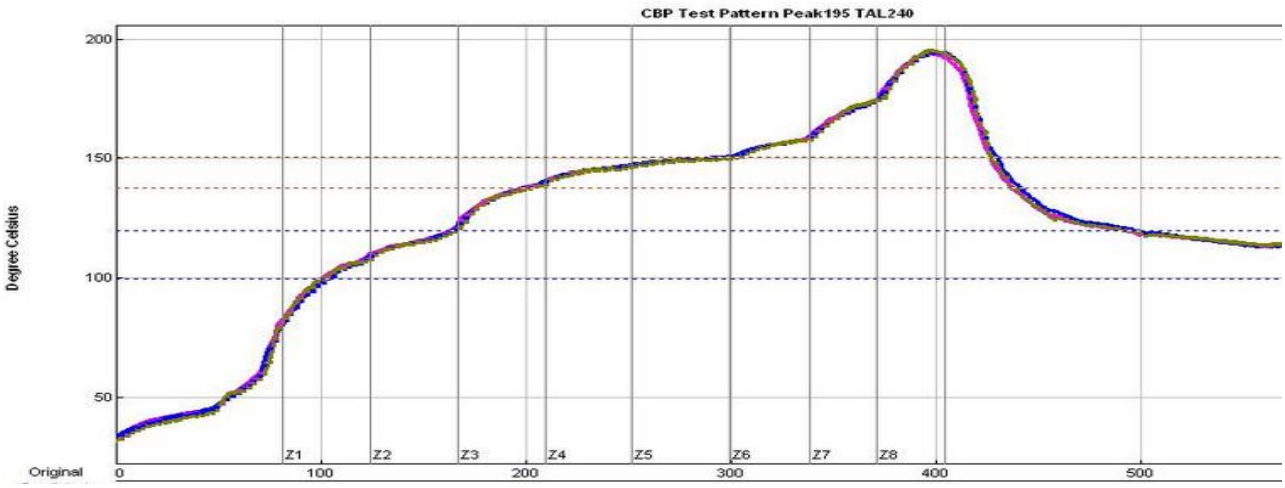

	Zone 1	**Zone 2**	**Zone 3**	**Zone 4**	**Zone 5**	**Zone 6**	**Zone 7**	**Zone 8**

Belt speed 42.5 cm/min	115	118	146	150	153	160	180	210

Table 31 Reflow Profile Tpeak=195˚C TAM=240sec

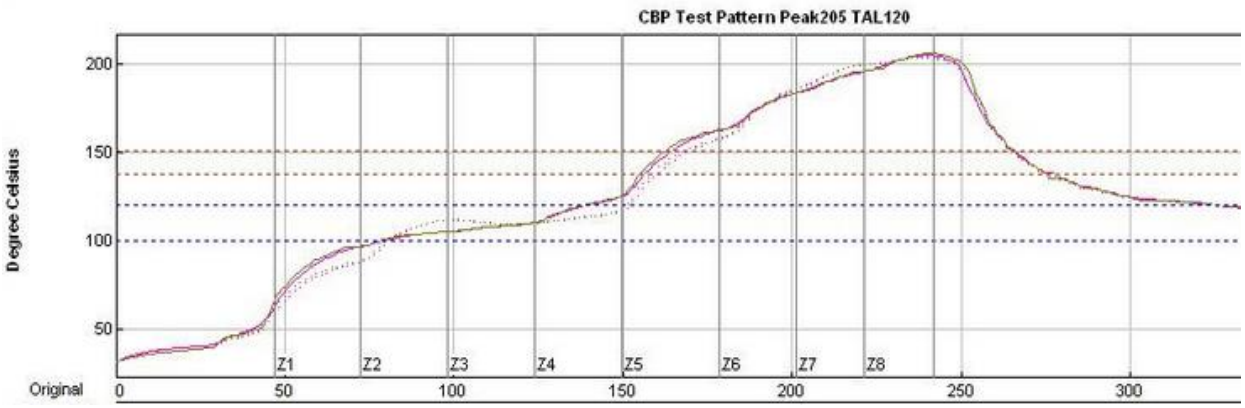

Belt speed 70.4 cm/min	**Zone 1**	**Zone 2**	**Zone 3**	**Zone 4**	**Zone 5**	**Zone 6**	**Zone 7**	**Zone 8**
	118	109	112	126	177	195	207	221

Table 32 Reflow Profile Tpeak= 205˚C TAM=120sec

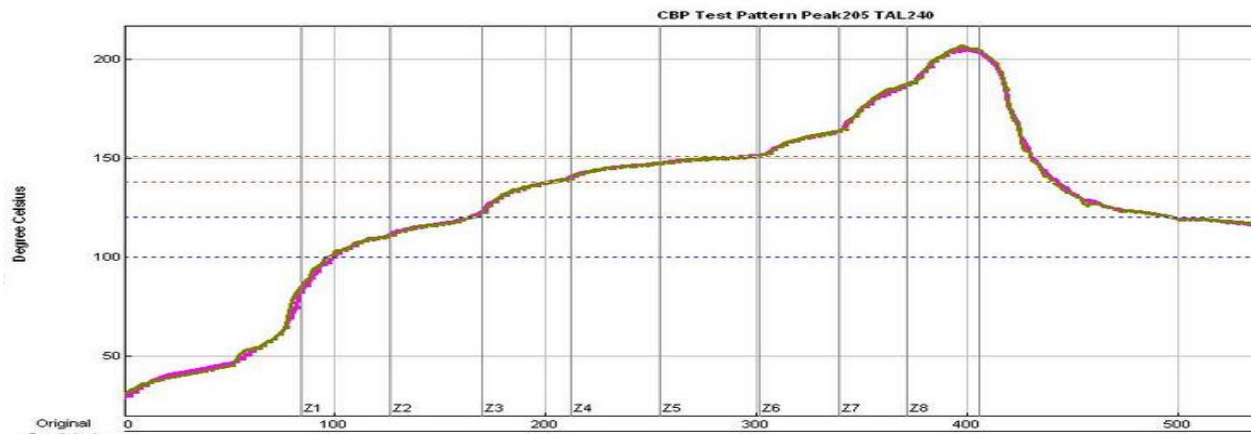

Belt speed 43.0 cm/min	Zone 1	Zone 2	Zone 3	Zone 4	Zone 5	Zone 6	Zone 7	Zone 8
	120	118	143	150	153	165	195	221

Table 33 Reflow Profile Tpeak=205˚C TAM=240sec

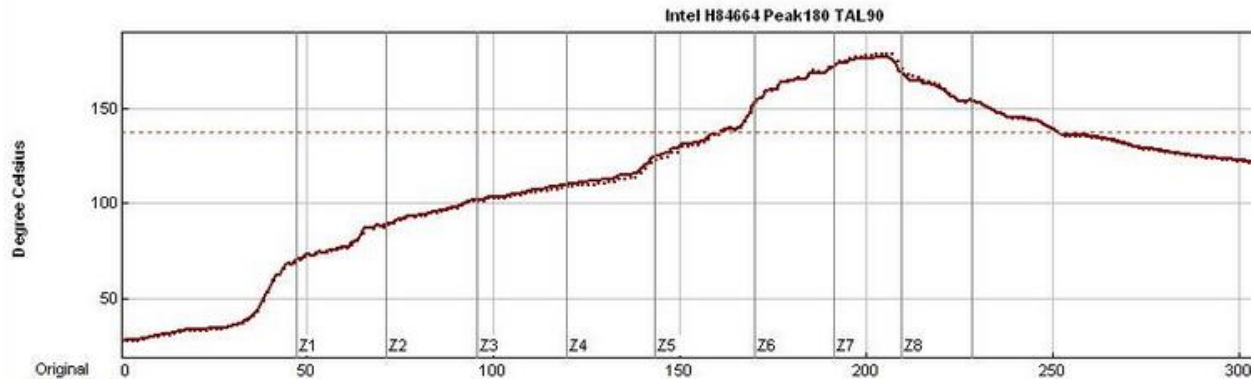

Belt speed 78.1 cm/min	Zone 1	Zone 2	Zone 3	Zone 4	Zone 5	Zone 6	Zone 7	Zone 8
	122	111	116	119	151	200	205	152

Table 34 Reflow Profile Tpeak=180˚C TAM=90sec

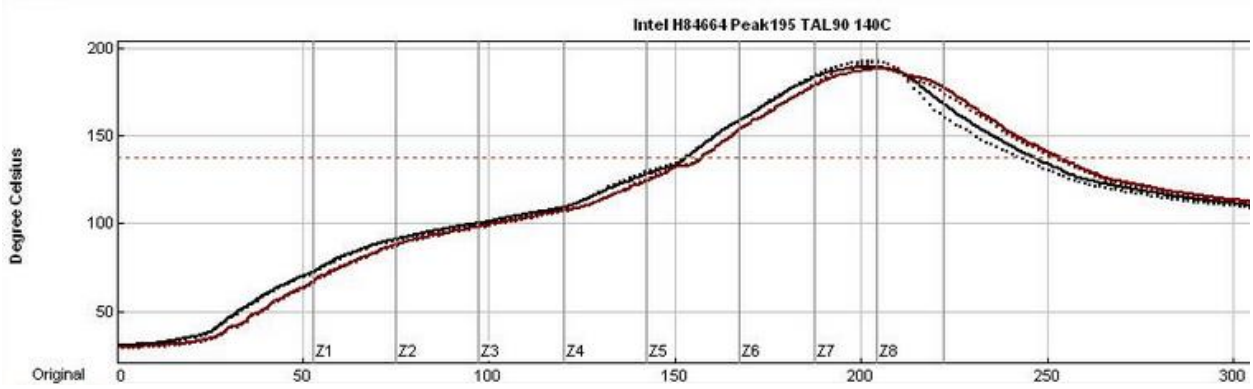

Belt speed 79.2 cm/min	Zone 1	Zone 2	Zone 3	Zone 4	Zone 5	Zone 6	Zone 7	Zone 8
	118	108	109	120	154	207	240	179

Table 35 Reflow Profile Tpeak=195˚C TAM=90sec

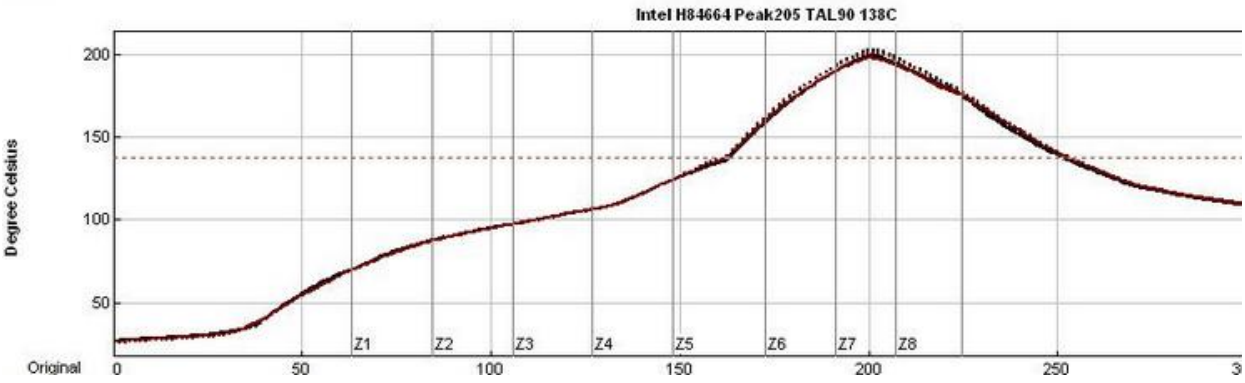

Belt speed 79.4 cm/min	Zone 1	Zone 2	Zone 3	Zone 4	Zone 5	Zone 6	Zone 7	Zone 8
	125	105	109	119	165	250	255	150

Table 36 Reflow Profile Tpeak=205˚C TAM=90sec

APPENDIX B

All Comparative T-Tests

Two-Sample T-Test and CI: Bi40+,Tpk:180C_TAM:120sec, ... TAM:120sec

Method

μ_1: mean of Bi40+,Tpk:180C_TAM:120sec
μ_2: mean of Bi57,Tpk:180C_TAM:120sec
Difference: $\mu_1 - \mu_2$

Equal variances are not assumed for this analysis.

Descriptive Statistics

Sample	N	Mean	StDev	SE Mean
Bi40+,Tpk:180C_TAM:120sec	10	0.3254	0.0200	0.0063
Bi57,Tpk:180C_TAM:120sec	9	0.4078	0.0361	0.012

Estimation for Difference

Difference	95% CI for Difference
-0.0824	(-0.1120, -0.0528)

Test

Null hypothesis H_0: $\mu_1 - \mu_2 = 0$
Alternative hypothesis H_1: $\mu_1 - \mu_2 \neq 0$

T-Value	DF	P-Value
-6.07	12	0.000

Two-Sample T-Test and CI: Bi40+,Tpk:180C_TAM:120sec, ... TAM:120sec

Method

μ_1: mean of Bi40+,Tpk:180C_TAM:120sec
μ_2: mean of Bi58,Tpk:180C_TAM:120sec
Difference: $\mu_1 - \mu_2$

Equal variances are not assumed for this analysis.

Descriptive Statistics

Sample	N	Mean	StDev	SE Mean
Bi40+,Tpk:180C_TAM:120sec	10	0.3254	0.0200	0.0063
Bi58,Tpk:180C_TAM:120sec	9	0.3349	0.0209	0.0070

Estimation for Difference

Difference	95% CI for Difference
-0.00952	(-0.02950, 0.01046)

Test

Null hypothesis H_0: $\mu_1 - \mu_2 = 0$
Alternative hypothesis H_1: $\mu_1 - \mu_2 \neq 0$

T-Value	DF	P-Value
-1.01	16	0.327

Two-Sample T-Test and CI: Bi57,Tpk:180C_TAM:120sec, ... _TAM:120sec

Method

μ_1: mean of Bi57,Tpk:180C_TAM:120sec
μ_2: mean of Bi58,Tpk:180C_TAM:120sec
Difference: $\mu_1 - \mu_2$

Equal variances are not assumed for this analysis.

Descriptive Statistics

Sample	N	Mean	StDev	SE Mean
Bi57,Tpk:180C_TAM:120sec	9	0.4078	0.0361	0.012
Bi58,Tpk:180C_TAM:120sec	9	0.3349	0.0209	0.0070

Estimation for Difference

Difference	95% CI for Difference
0.0729	(0.0426, 0.1032)

Test

Null hypothesis $H_0: \mu_1 - \mu_2 = 0$
Alternative hypothesis $H_1: \mu_1 - \mu_2 \neq 0$

T-Value	DF	P-Value
5.25	12	0.000

Two-Sample T-Test and CI: Bi40+,Tpk:180C_TAM:240sec, ... AM:240sec

Method

μ_1: mean of Bi40+,Tpk:180C_TAM:240sec
μ_2: mean of Bi57,Tpk:180C_TAM:240sec
Difference: $\mu_1 - \mu_2$

Equal variances are not assumed for this analysis.

Descriptive Statistics

Sample	N	Mean	StDev	SE Mean
Bi40+,Tpk:180C_TAM:240sec	10	0.4308	0.0257	0.0081
Bi57,Tpk:180C_TAM:240sec	6	0.3991	0.0432	0.018

Estimation for Difference

Difference	95% CI for Difference
0.0316	(-0.0143, 0.0776)

Test

Null hypothesis $H_0: \mu_1 - \mu_2 = 0$
Alternative hypothesis $H_1: \mu_1 - \mu_2 \neq 0$

T-Value	DF	P-Value
1.63	7	0.147

Two-Sample T-Test and CI: Bi40+,Tpk:180C_TAM:240sec, ... AM:240sec

Method

μ_1: mean of Bi40+,Tpk:180C_TAM:240sec
μ_2: mean of Bi58,Tpk:180C_TAM:240sec
Difference: $\mu_1 - \mu_2$

Equal variances are not assumed for this analysis.

Descriptive Statistics

Sample	N	Mean	StDev	SE Mean
Bi40+,Tpk:180C_TAM:240sec	10	0.4308	0.0257	0.0081
Bi58,Tpk:180C_TAM:240sec	10	0.4542	0.0461	0.015

Estimation for Difference

Difference	95% CI for Difference
-0.0234	(-0.0593, 0.0124)

Test

Null hypothesis $H_0: \mu_1 - \mu_2 = 0$
Alternative hypothesis $H_1: \mu_1 - \mu_2 \neq 0$

T-Value	DF	P-Value
-1.40	14	0.183

Two-Sample T-Test and CI: Bi57,Tpk:180C_TAM:240sec, ... _TAM:240sec

Method

μ_1: mean of Bi57,Tpk:180C_TAM:240sec
μ_2: mean of Bi58,Tpk:180C_TAM:240sec
Difference: $\mu_1 - \mu_2$

Equal variances are not assumed for this analysis.

Descriptive Statistics

Sample	N	Mean	StDev	SE Mean
Bi57,Tpk:180C_TAM:240sec	6	0.3991	0.0432	0.018
Bi58,Tpk:180C_TAM:240sec	10	0.4542	0.0461	0.015

Estimation for Difference

Difference	95% CI for Difference
-0.0551	(-0.1054, -0.0047)

Test

Null hypothesis $H_0: \mu_1 - \mu_2 = 0$
Alternative hypothesis $H_1: \mu_1 - \mu_2 \neq 0$

T-Value	DF	P-Value
-2.41	11	0.035

Two-Sample T-Test and CI: Bi40+,Tpk:195C_TAM:120sec, ... TAM:120sec

Method

μ_1: mean of Bi40+,Tpk:195C_TAM:120sec
μ_2: mean of Bi57,Tpk:195C_TAM:120sec
Difference: $\mu_1 - \mu_2$

Equal variances are not assumed for this analysis.

Descriptive Statistics

Sample	N	Mean	StDev	SE Mean
Bi40+,Tpk:195C_TAM:120sec	10	0.5828	0.0924	0.029
Bi57,Tpk:195C_TAM:120sec	10	0.5410	0.0557	0.018

Estimation for Difference

Difference	95% CI for Difference
0.0418	(-0.0314, 0.1150)

Test

Null hypothesis H_0: $\mu_1 - \mu_2 = 0$
Alternative hypothesis H_1: $\mu_1 - \mu_2 \neq 0$

T-Value	DF	P-Value
1.23	14	0.241

Two-Sample T-Test and CI: Bi40+,Tpk:195C_TAM:120sec, ... TAM:120sec

Method

μ_1: mean of Bi40+,Tpk:195C_TAM:120sec
μ_2: mean of Bi58,Tpk:195C_TAM:120sec
Difference: $\mu_1 - \mu_2$

Equal variances are not assumed for this analysis.

Descriptive Statistics

Sample	N	Mean	StDev	SE Mean
Bi40+,Tpk:195C_TAM:120sec	10	0.5828	0.0924	0.029
Bi58,Tpk:195C_TAM:120sec	10	0.5669	0.0973	0.031

Estimation for Difference

Difference	95% CI for Difference
0.0159	(-0.0737, 0.1054)

Test

Null hypothesis H_0: $\mu_1 - \mu_2 = 0$
Alternative hypothesis H_1: $\mu_1 - \mu_2 \neq 0$

T-Value	DF	P-Value
0.37	17	0.713

Two-Sample T-Test and CI: Bi57,Tpk:195C_TAM:120sec, ... _TAM:120sec

Method

μ_1: mean of Bi57,Tpk:195C_TAM:120sec
μ_2: mean of Bi58,Tpk:195C_TAM:120sec
Difference: $\mu_1 - \mu_2$

Equal variances are not assumed for this analysis.

Descriptive Statistics

Sample	N	Mean	StDev	SE Mean
Bi57,Tpk:195C_TAM:120sec	10	0.5410	0.0557	0.018
Bi58,Tpk:195C_TAM:120sec	10	0.5669	0.0973	0.031

Estimation for Difference

Difference	95% CI for Difference
-0.0260	(-0.1020, 0.0501)

Test

Null hypothesis H_0: $\mu_1 - \mu_2 = 0$
Alternative hypothesis H_1: $\mu_1 - \mu_2 \neq 0$

T-Value	DF	P-Value
-0.73	14	0.476

Two-Sample T-Test and CI: Bi40+,Tpk:195C_TAM:240sec, ... AM:240sec

Method

μ_1: mean of Bi40+,Tpk:195C_TAM:240sec
μ_2: mean of Bi57,Tpk:195C_TAM:240sec
Difference: $\mu_1 - \mu_2$

Equal variances are not assumed for this analysis.

Descriptive Statistics

Sample	N	Mean	StDev	SE Mean
Bi40+,Tpk:195C_TAM:240sec	10	0.5110	0.0714	0.023
Bi57,Tpk:195C_TAM:240sec	10	0.6050	0.0411	0.013

Estimation for Difference

Difference	95% CI for Difference
-0.0940	(-0.1499, -0.0381)

Test

Null hypothesis H_0: $\mu_1 - \mu_2 = 0$
Alternative hypothesis H_1: $\mu_1 - \mu_2 \neq 0$

T-Value	DF	P-Value
-3.61	14	0.003

Two-Sample T-Test and CI: Bi40+,Tpk:195C_TAM:240sec, ... AM:240sec

Method

μ_1: mean of Bi40+,Tpk:195C_TAM:240sec
μ_2: mean of Bi58,Tpk:195C_TAM:240sec
Difference: $\mu_1 - \mu_2$

Equal variances are not assumed for this analysis.

Descriptive Statistics

Sample	N	Mean	StDev	SE Mean
Bi40+,Tpk:195C_TAM:240sec	10	0.5110	0.0714	0.023
Bi58,Tpk:195C_TAM:240sec	10	0.6009	0.0542	0.017

Estimation for Difference

Difference	95% CI for Difference
-0.0899	(-0.1500, -0.0298)

Test

Null hypothesis $H_0: \mu_1 - \mu_2 = 0$
Alternative hypothesis $H_1: \mu_1 - \mu_2 \neq 0$

T-Value	DF	P-Value
-3.17	16	0.006

Two-Sample T-Test and CI: Bi58,Tpk:195C_TAM:240sec, ... _TAM:240sec

Method

μ_1: mean of Bi58,Tpk:195C_TAM:240sec
μ_2: mean of Bi57,Tpk:195C_TAM:240sec
Difference: $\mu_1 - \mu_2$

Equal variances are not assumed for this analysis.

Descriptive Statistics

Sample	N	Mean	StDev	SE Mean
Bi58,Tpk:195C_TAM:240sec	10	0.6009	0.0542	0.017
Bi57,Tpk:195C_TAM:240sec	10	0.6050	0.0411	0.013

Estimation for Difference

Difference	95% CI for Difference
-0.0041	(-0.0497, 0.0415)

Test

Null hypothesis $H_0: \mu_1 - \mu_2 = 0$
Alternative hypothesis $H_1: \mu_1 - \mu_2 \neq 0$

T-Value	DF	P-Value
-0.19	16	0.850

Two-Sample T-Test and CI: Bi40+,Tpk:205C_TAM:120sec, ... AM:120sec

Method

μ_1: mean of Bi40+,Tpk:205C_TAM:120sec
μ_2: mean of Bi57,Tpk:205C_TAM:120sec
Difference: $\mu_1 - \mu_2$

Equal variances are not assumed for this analysis.

Descriptive Statistics

Sample	N	Mean	StDev	SE Mean
Bi40+,Tpk:205C_TAM:120sec	10	0.814	0.129	0.041
Bi57,Tpk:205C_TAM:120sec	10	0.8673	0.0620	0.020

Estimation for Difference

Difference	95% CI for Difference
-0.0537	(-0.1523, 0.0450)

Test

Null hypothesis H_0: $\mu_1 - \mu_2 = 0$
Alternative hypothesis H_1: $\mu_1 - \mu_2 \neq 0$

T-Value	DF	P-Value
-1.18	12	0.259

Two-Sample T-Test and CI: Bi40+,Tpk:205C_TAM:120sec, ... AM:120sec

Method

μ_1: mean of Bi40+,Tpk:205C_TAM:120sec
μ_2: mean of Bi58,Tpk:205C_TAM:120sec
Difference: $\mu_1 - \mu_2$

Equal variances are not assumed for this analysis.

Descriptive Statistics

Sample	N	Mean	StDev	SE Mean
Bi40+,Tpk:205C_TAM:120sec	10	0.814	0.129	0.041
Bi58,Tpk:205C_TAM:120sec	10	0.7256	0.0220	0.0069

Estimation for Difference

Difference	95% CI for Difference
0.0881	(-0.0056, 0.1818)

Test

Null hypothesis H_0: $\mu_1 - \mu_2 = 0$
Alternative hypothesis H_1: $\mu_1 - \mu_2 \neq 0$

T-Value	DF	P-Value
2.13	9	0.062

Two-Sample T-Test and CI: Bi57,Tpk:205C_TAM:120sec, ... _TAM:120sec

Method

μ_1: mean of Bi57,Tpk:205C_TAM:120sec
μ_2: mean of Bi58,Tpk:205C_TAM:120sec
Difference: $\mu_1 - \mu_2$

Equal variances are not assumed for this analysis.

Descriptive Statistics

Sample	N	Mean	StDev	SE Mean
Bi57,Tpk:205C_TAM:120sec	10	0.8673	0.0620	0.020
Bi58,Tpk:205C_TAM:120sec	10	0.7256	0.0220	0.0069

Estimation for Difference

Difference	95% CI for Difference
0.1418	(0.0960, 0.1875)

Test

Null hypothesis H_0: $\mu_1 - \mu_2 = 0$
Alternative hypothesis H_1: $\mu_1 - \mu_2 \neq 0$

T-Value	DF	P-Value
6.82	11	0.000

Two-Sample T-Test and CI: Bi40+,Tpk:205C_TAM:240sec, ... AM:240sec

Method

μ_1: mean of Bi40+,Tpk:205C_TAM:240sec
μ_2: mean of Bi57,Tpk:205C_TAM:240sec
Difference: $\mu_1 - \mu_2$

Equal variances are not assumed for this analysis.

Descriptive Statistics

Sample	N	Mean	StDev	SE Mean
Bi40+,Tpk:205C_TAM:240sec	10	0.8883	0.0612	0.019
Bi57,Tpk:205C_TAM:240sec	10	0.9434	0.0625	0.020

Estimation for Difference

Difference	95% CI for Difference
-0.0551	(-0.1134, 0.0033)

Test

Null hypothesis H_0: $\mu_1 - \mu_2 = 0$
Alternative hypothesis H_1: $\mu_1 - \mu_2 \neq 0$

T-Value	DF	P-Value
-1.99	17	0.063

Two-Sample T-Test and CI: Bi40+,Tpk:205C_TAM:240sec, ... AM:240sec

Method

μ_1: mean of Bi40+,Tpk:205C_TAM:240sec
μ_2: mean of Bi58,Tpk:205C_TAM:240sec
Difference: $\mu_1 - \mu_2$

Equal variances are not assumed for this analysis.

Descriptive Statistics

Sample	N	Mean	StDev	SE Mean
Bi40+,Tpk:205C_TAM:240sec	10	0.8883	0.0612	0.019
Bi58,Tpk:205C_TAM:240sec	11	0.9266	0.0905	0.027

Estimation for Difference

Difference	95% CI for Difference
-0.0382	(-0.1088, 0.0324)

Test

Null hypothesis H_0: $\mu_1 - \mu_2 = 0$
Alternative hypothesis H_1: $\mu_1 - \mu_2 \neq 0$

T-Value	DF	P-Value
-1.14	17	0.269

Two-Sample T-Test and CI: Bi57,Tpk:205C_TAM:240sec, ... TAM:240sec

Method

μ_1: mean of Bi57,Tpk:205C_TAM:240sec
μ_2: mean of Bi58,Tpk:205C_TAM:240sec
Difference: $\mu_1 - \mu_2$

Equal variances are not assumed for this analysis.

Descriptive Statistics

Sample	N	Mean	StDev	SE Mean
Bi57,Tpk:205C_TAM:240sec	10	0.9434	0.0625	0.020
Bi58,Tpk:205C_TAM:240sec	11	0.9266	0.0905	0.027

Estimation for Difference

Difference	95% CI for Difference
0.0168	(-0.0542, 0.0879)

Test

Null hypothesis H_0: $\mu_1 - \mu_2 = 0$
Alternative hypothesis H_1: $\mu_1 - \mu_2 \neq 0$

T-Value	DF	P-Value
0.50	17	0.624

Two-Sample T-Test and CI: Bi40+,Tpk:180C_TAM:90sec, ... _TAM:90sec

Method

μ_1: mean of Bi40+,Tpk:180C_TAM:90sec
μ_2: mean of Bi57,Tpk:180C_TAM:90sec
Difference: $\mu_1 - \mu_2$

Equal variances are not assumed for this analysis.

Descriptive Statistics

Sample	N	Mean	StDev	SE Mean
Bi40+,Tpk:180C_TAM:90sec	73	0.4431	0.0457	0.0054
Bi57,Tpk:180C_TAM:90sec	67	0.4715	0.0457	0.0056

Estimation for Difference

Difference	95% CI for Difference
-0.02831	(-0.04360, -0.01301)

Test

Null hypothesis H_0: $\mu_1 - \mu_2 = 0$
Alternative hypothesis H_1: $\mu_1 - \mu_2 \neq 0$

T-Value	DF	P-Value
-3.66	136	0.000

Two-Sample T-Test and CI: Bi40+,Tpk:180C_TAM:90sec, ... _TAM:90sec

Method

μ_1: mean of Bi40+,Tpk:180C_TAM:90sec
μ_2: mean of Bi58,Tpk:180C_TAM:90sec
Difference: $\mu_1 - \mu_2$

Equal variances are not assumed for this analysis.

Descriptive Statistics

Sample	N	Mean	StDev	SE Mean
Bi40+,Tpk:180C_TAM:90sec	73	0.4431	0.0457	0.0054
Bi58,Tpk:180C_TAM:90sec	80	0.4705	0.0464	0.0052

Estimation for Difference

Difference	95% CI for Difference
-0.02732	(-0.04204, -0.01260)

Test

Null hypothesis H_0: $\mu_1 - \mu_2 = 0$
Alternative hypothesis H_1: $\mu_1 - \mu_2 \neq 0$

T-Value	DF	P-Value
-3.67	150	0.000

Two-Sample T-Test and CI: Bi57,Tpk:180C_TAM:90sec, ... 0C_TAM:90sec

Method

μ_1: mean of Bi57,Tpk:180C_TAM:90sec
μ_2: mean of Bi58,Tpk:180C_TAM:90sec
Difference: $\mu_1 - \mu_2$

Equal variances are not assumed for this analysis.

Descriptive Statistics

Sample	N	Mean	StDev	SE Mean
Bi57,Tpk:180C_TAM:90sec	67	0.4715	0.0457	0.0056
Bi58,Tpk:180C_TAM:90sec	80	0.4705	0.0464	0.0052

Estimation for Difference

Difference	95% CI for Difference
0.00098	(-0.01408, 0.01605)

Test

Null hypothesis H_0: $\mu_1 - \mu_2 = 0$
Alternative hypothesis H_1: $\mu_1 - \mu_2 \neq 0$

T-Value	DF	P-Value
0.13	141	0.897

Two-Sample T-Test and CI: Bi40+,Tpk:195C_TAM:90sec, ... _TAM:90sec

Method

μ_1: mean of Bi40+,Tpk:195C_TAM:90sec
μ_2: mean of Bi57,Tpk:195C_TAM:90sec
Difference: $\mu_1 - \mu_2$

Equal variances are not assumed for this analysis.

Descriptive Statistics

Sample	N	Mean	StDev	SE Mean
Bi40+,Tpk:195C_TAM:90sec	69	0.5787	0.0526	0.0063
Bi57,Tpk:195C_TAM:90sec	70	0.7710	0.0585	0.0070

Estimation for Difference

Difference	95% CI for Difference
-0.19230	(-0.21096, -0.17363)

Test

Null hypothesis H_0: $\mu_1 - \mu_2 = 0$
Alternative hypothesis H_1: $\mu_1 - \mu_2 \neq 0$

T-Value	DF	P-Value
-20.37	135	0.000

Two-Sample T-Test and CI: Bi40+,Tpk:195C_TAM:90sec, ... _TAM:90sec

Method

μ_1: mean of Bi40+,Tpk:195C_TAM:90sec
μ_2: mean of Bi58,Tpk:195C_TAM:90sec
Difference: $\mu_1 - \mu_2$

Equal variances are not assumed for this analysis.

Descriptive Statistics

Sample	N	Mean	StDev	SE Mean
Bi40+,Tpk:195C_TAM:90sec	69	0.5787	0.0526	0.0063
Bi58,Tpk:195C_TAM:90sec	56	0.6961	0.0596	0.0080

Estimation for Difference

Difference	95% CI for Difference
-0.1175	(-0.1376, -0.0973)

Test

Null hypothesis $H_0: \mu_1 - \mu_2 = 0$
Alternative hypothesis $H_1: \mu_1 - \mu_2 \neq 0$

T-Value	DF	P-Value
-11.54	110	0.000

Two-Sample T-Test and CI: Bi57,Tpk:195C_TAM:90sec, ... 5C_TAM:90sec

Method

μ_1: mean of Bi57,Tpk:195C_TAM:90sec
μ_2: mean of Bi58,Tpk:195C_TAM:90sec
Difference: $\mu_1 - \mu_2$

Equal variances are not assumed for this analysis.

Descriptive Statistics

Sample	N	Mean	StDev	SE Mean
Bi57,Tpk:195C_TAM:90sec	70	0.7710	0.0585	0.0070
Bi58,Tpk:195C_TAM:90sec	56	0.6961	0.0596	0.0080

Estimation for Difference

Difference	95% CI for Difference
0.0748	(0.0538, 0.0958)

Test

Null hypothesis $H_0: \mu_1 - \mu_2 = 0$
Alternative hypothesis $H_1: \mu_1 - \mu_2 \neq 0$

T-Value	DF	P-Value
7.06	117	0.000

Two-Sample T-Test and CI: Bi40+,Outer_Tpk180C, Bi58,Outer_Tpk180C

Method

μ_1: mean of Bi40+,Outer_Tpk180C
μ_2: mean of Bi58,Outer_Tpk180C
Difference: $\mu_1 - \mu_2$

Equal variances are not assumed for this analysis.

Descriptive Statistics

Sample	N	Mean	StDev	SE Mean
Bi40+,Outer_Tpk180C	39	0.4792	0.0244	0.0039
Bi58,Outer_Tpk180C	38	0.5005	0.0276	0.0045

Estimation for Difference

Difference	95% CI for Difference
-0.02127	(-0.03312, -0.00942)

Test

Null hypothesis H_0: $\mu_1 - \mu_2 = 0$
Alternative hypothesis H_1: $\mu_1 - \mu_2 \neq 0$

T-Value	DF	P-Value
-3.58	73	0.001

T-Tests for SnBi58

Two-Sample T-Test and CI: Outer_Tpk180C, Inner_Tpk180C

Method

μ_1: mean of Outer_Tpk180C
μ_2: mean of Inner_Tpk180C
Difference: $\mu_1 - \mu_2$

Equal variances are not assumed for this analysis.

Descriptive Statistics

Sample	N	Mean	StDev	SE Mean
Outer_Tpk180C	51	43.94	2.24	0.31
Inner_Tpk180C	29	52.49	1.90	0.35

Estimation for Difference

Difference	95% CI for Difference
-8.549	(-9.492, -7.606)

Test

Null hypothesis H_0: $\mu_1 - \mu_2 = 0$
Alternative hypothesis H_1: $\mu_1 - \mu_2 \neq 0$

T-Value	DF	P-Value
-18.10	66	0.000

Two-Sample T-Test and CI: Tpk:195C_TAM:85sec, Tpk:195C_TAM:120sec

Method

μ_1: mean of Tpk:195C_TAM:85sec
μ_2: mean of Tpk:195C_TAM:120sec
Difference: $\mu_1 - \mu_2$

Equal variances are not assumed for this analysis.

Descriptive Statistics

Sample	N	Mean	StDev	SE Mean
Tpk:195C_TAM:85sec	9	0.5310	0.0224	0.0075
Tpk:195C_TAM:120sec	10	0.5669	0.0973	0.031

Estimation for Difference

Difference	95% CI for Difference
-0.0360	(-0.1065, 0.0346)

Test

Null hypothesis H_0: $\mu_1 - \mu_2 = 0$
Alternative hypothesis H_1: $\mu_1 - \mu_2 \neq 0$

T-Value	DF	P-Value
-1.14	10	0.282

Two-Sample T-Test and CI: Tpk:195C_TAM:85sec, ... :195C_TAM:240sec

Method

μ_1: mean of Tpk:195C_TAM:85sec
μ_2: mean of Tpk:195C_TAM:240sec
Difference: $\mu_1 - \mu_2$

Equal variances are not assumed for this analysis.

Descriptive Statistics

Sample	N	Mean	StDev	SE Mean
Tpk:195C_TAM:85sec	9	0.5310	0.0224	0.0075
Tpk:195C_TAM:240sec	10	0.6009	0.0542	0.017

Estimation for Difference

Difference	95% CI for Difference
-0.0699	(-0.1106, -0.0292)

Test

Null hypothesis H_0: $\mu_1 - \mu_2 = 0$
Alternative hypothesis H_1: $\mu_1 - \mu_2 \neq 0$

T-Value	DF	P-Value
-3.74	12	0.003

Two-Sample T-Test and CI: Tpk:195C_TAM:120sec, ... :195C_TAM:240sec

Method

μ_1: mean of Tpk:195C_TAM:120sec
μ_2: mean of Tpk:195C_TAM:240sec
Difference: $\mu_1 - \mu_2$

Equal variances are not assumed for this analysis.

Descriptive Statistics

Sample	N	Mean	StDev	SE Mean
Tpk:195C_TAM:120sec	10	0.5669	0.0973	0.031
Tpk:195C_TAM:240sec	10	0.6009	0.0542	0.017

Estimation for Difference

Difference	95% CI for Difference
-0.0340	(-0.1095, 0.0416)

Test

Null hypothesis H_0: $\mu_1 - \mu_2 = 0$
Alternative hypothesis H_1: $\mu_1 - \mu_2 \neq 0$

T-Value	DF	P-Value
-0.96	14	0.351

Two-Sample T-Test and CI: Outer_Tpk195C, Inner_Tpk195C

Method

μ_1: mean of Outer_Tpk195C
μ_2: mean of Inner_Tpk195C
Difference: $\mu_1 - \mu_2$

Equal variances are not assumed for this analysis.

Descriptive Statistics

Sample	N	Mean	StDev	SE Mean
Outer_Tpk195C	39	73.00	2.44	0.39
Inner_Tpk195C	17	61.85	3.99	0.97

Estimation for Difference

Difference	95% CI for Difference
11.15	(8.98, 13.32)

Test

Null hypothesis H_0: $\mu_1 - \mu_2 = 0$
Alternative hypothesis H_1: $\mu_1 - \mu_2 \neq 0$

T-Value	DF	P-Value
10.68	21	0.000

Two-Sample T-Test and CI: Tpk:205C_TAM:85sec, ... :205C_TAM:120sec

Method

μ_1: mean of Tpk:205C_TAM:85sec
μ_2: mean of Tpk:205C_TAM:120sec
Difference: $\mu_1 - \mu_2$

Equal variances are not assumed for this analysis.

Descriptive Statistics

Sample	N	Mean	StDev	SE Mean
Tpk:205C_TAM:85sec	9	0.9668	0.0315	0.011
Tpk:205C_TAM:120sec	10	0.7256	0.0220	0.0069

Estimation for Difference

Difference	95% CI for Difference
0.2413	(0.2143, 0.2683)

Test

Null hypothesis H_0: $\mu_1 - \mu_2 = 0$
Alternative hypothesis H_1: $\mu_1 - \mu_2 \neq 0$

T-Value	DF	P-Value
19.15	14	0.000

Two-Sample T-Test and CI: Tpk:205C_TAM:85sec, ... :205C_TAM:240sec

Method

μ_1: mean of Tpk:205C_TAM:85sec
μ_2: mean of Tpk:205C_TAM:240sec
Difference: $\mu_1 - \mu_2$

Equal variances are not assumed for this analysis.

Descriptive Statistics

Sample	N	Mean	StDev	SE Mean
Tpk:205C_TAM:85sec	9	0.9668	0.0315	0.011
Tpk:205C_TAM:240sec	11	0.9266	0.0905	0.027

Estimation for Difference

Difference	95% CI for Difference
0.0403	(-0.0234, 0.1040)

Test

Null hypothesis H_0: $\mu_1 - \mu_2 = 0$
Alternative hypothesis H_1: $\mu_1 - \mu_2 \neq 0$

T-Value	DF	P-Value
1.38	12	0.194

Two-Sample T-Test and CI: Tpk:205C_TAM:120sec, ... 205C_TAM:240sec

Method

μ_1: mean of Tpk:205C_TAM:120sec
μ_2: mean of Tpk:205C_TAM:240sec
Difference: $\mu_1 - \mu_2$

Equal variances are not assumed for this analysis.

Descriptive Statistics

Sample	N	Mean	StDev	SE Mean
Tpk:205C_TAM:120sec	10	0.7256	0.0220	0.0069
Tpk:205C_TAM:240sec	11	0.9266	0.0905	0.027

Estimation for Difference

Difference	95% CI for Difference
-0.2010	(-0.2630, -0.1390)

Test

Null hypothesis H_0: $\mu_1 - \mu_2 = 0$
Alternative hypothesis H_1: $\mu_1 - \mu_2 \neq 0$

T-Value	DF	P-Value
-7.14	11	0.000

Two-Sample T-Test and CI: Tpk:180C_TAM:85sec, Tpk:180C_TAM:120sec

Method

μ_1: mean of Tpk:180C_TAM:85sec
μ_2: mean of Tpk:180C_TAM:120sec
Difference: $\mu_1 - \mu_2$

Equal variances are not assumed for this analysis.

Descriptive Statistics

Sample	N	Mean	StDev	SE Mean
Tpk:180C_TAM:85sec	9	0.3112	0.0539	0.018
Tpk:180C_TAM:120sec	9	0.3349	0.0209	0.0070

Estimation for Difference

Difference	95% CI for Difference
-0.0237	(-0.0667, 0.0193)

Test

Null hypothesis H_0: $\mu_1 - \mu_2 = 0$
Alternative hypothesis H_1: $\mu_1 - \mu_2 \neq 0$

T-Value	DF	P-Value
-1.23	10	0.247

Two-Sample T-Test and CI: Tpk:180C_TAM:85sec, ... :180C_TAM:240sec

Method

μ_1: mean of Tpk:180C_TAM:85sec
μ_2: mean of Tpk:180C_TAM:240sec
Difference: $\mu_1 - \mu_2$

Equal variances are not assumed for this analysis.

Descriptive Statistics

Sample	N	Mean	StDev	SE Mean
Tpk:180C_TAM:85sec	9	0.3112	0.0539	0.018
Tpk:180C_TAM:240sec	10	0.4542	0.0461	0.015

Estimation for Difference

Difference	95% CI for Difference
-0.1430	(-0.1924, -0.0937)

Test

Null hypothesis H_0: $\mu_1 - \mu_2 = 0$
Alternative hypothesis H_1: $\mu_1 - \mu_2 \neq 0$

T-Value	DF	P-Value
-6.18	15	0.000

Two-Sample T-Test and CI: Tpk:180C_TAM:85sec, Tpk:180C_TAM:90sec

Method

μ_1: mean of Tpk:180C_TAM:85sec
μ_2: mean of Tpk:180C_TAM:90sec
Difference: $\mu_1 - \mu_2$

Equal variances are not assumed for this analysis.

Descriptive Statistics

Sample	N	Mean	StDev	SE Mean
Tpk:180C_TAM:85sec	9	0.3112	0.0539	0.018
Tpk:180C_TAM:90sec	80	0.4705	0.0464	0.0052

Estimation for Difference

Difference	95% CI for Difference
-0.1593	(-0.2016, -0.1170)

Test

Null hypothesis H_0: $\mu_1 - \mu_2 = 0$
Alternative hypothesis H_1: $\mu_1 - \mu_2 \neq 0$

T-Value	DF	P-Value
-8.51	9	0.000

Two-Sample T-Test and CI: Tpk:180C_TAM:90sec, ... :180C_TAM:240sec

Method

μ_1: mean of Tpk:180C_TAM:90sec
μ_2: mean of Tpk:180C_TAM:240sec
Difference: $\mu_1 - \mu_2$

Equal variances are not assumed for this analysis.

Descriptive Statistics

Sample	N	Mean	StDev	SE Mean
Tpk:180C_TAM:90sec	80	0.4705	0.0464	0.0052
Tpk:180C_TAM:240sec	10	0.4542	0.0461	0.015

Estimation for Difference

Difference	95% CI for Difference
0.0163	(-0.0178, 0.0503)

Test

Null hypothesis H_0: $\mu_1 - \mu_2 = 0$
Alternative hypothesis H_1: $\mu_1 - \mu_2 \neq 0$

T-Value	DF	P-Value
1.05	11	0.316

Two-Sample T-Test and CI: Tpk:180C_TAM:90sec, Tpk:180C_TAM:120sec

Method

μ_1: mean of Tpk:180C_TAM:90sec
μ_2: mean of Tpk:180C_TAM:120sec
Difference: $\mu_1 - \mu_2$

Equal variances are not assumed for this analysis.

Descriptive Statistics

Sample	N	Mean	StDev	SE Mean
Tpk:180C_TAM:90sec	80	0.4705	0.0464	0.0052
Tpk:180C_TAM:120sec	9	0.3349	0.0209	0.0070

Estimation for Difference

Difference	95% CI for Difference
0.13559	(0.11732, 0.15386)

Test

Null hypothesis H_0: $\mu_1 - \mu_2 = 0$
Alternative hypothesis H_1: $\mu_1 - \mu_2 \neq 0$

T-Value	DF	P-Value
15.59	18	0.000

Two-Sample T-Test and CI: Tpk:180C_TAM:120sec, ... :180C_TAM:240sec

Method

μ_1: mean of Tpk:180C_TAM:120sec
μ_2: mean of Tpk:180C_TAM:240sec
Difference: $\mu_1 - \mu_2$

Equal variances are not assumed for this analysis.

Descriptive Statistics

Sample	N	Mean	StDev	SE Mean
Tpk:180C_TAM:120sec	9	0.3349	0.0209	0.0070
Tpk:180C_TAM:240sec	10	0.4542	0.0461	0.015

Estimation for Difference

Difference	95% CI for Difference
-0.1193	(-0.1546, -0.0841)

Test

Null hypothesis H_0: $\mu_1 - \mu_2 = 0$
Alternative hypothesis H_1: $\mu_1 - \mu_2 \neq 0$

T-Value	DF	P-Value
-7.38	12	0.000

T-Tests for SnBi40-58

Two-Sample T-Test and CI: Tpk:180C_TAM:85sec, Tpk:180C_TAM:90sec

Method

μ_1: mean of Tpk:180C_TAM:85sec
μ_2: mean of Tpk:180C_TAM:90sec
Difference: $\mu_1 - \mu_2$

Equal variances are not assumed for this analysis.

Descriptive Statistics

Sample	N	Mean	StDev	SE Mean
Tpk:180C_TAM:85sec	9	0.3112	0.0539	0.018
Tpk:180C_TAM:90sec	73	0.4431	0.0457	0.0054

Estimation for Difference

Difference	95% CI for Difference
-0.1320	(-0.1744, -0.0895)

Test

Null hypothesis H_0: $\mu_1 - \mu_2 = 0$
Alternative hypothesis H_1: $\mu_1 - \mu_2 \neq 0$

T-Value	DF	P-Value
-7.04	9	0.000

Two-Sample T-Test and CI: Tpk:180C_TAM:85sec, Tpk:180C_TAM:120sec

Method

μ_1: mean of Tpk:180C_TAM:85sec
μ_2: mean of Tpk:180C_TAM:120sec
Difference: $\mu_1 - \mu_2$

Equal variances are not assumed for this analysis.

Descriptive Statistics

Sample	N	Mean	StDev	SE Mean
Tpk:180C_TAM:85sec	9	0.3112	0.0539	0.018
Tpk:180C_TAM:120sec	10	0.3254	0.0200	0.0063

Estimation for Difference

Difference	95% CI for Difference
-0.0142	(-0.0573, 0.0289)

Test

Null hypothesis H_0: $\mu_1 - \mu_2 = 0$
Alternative hypothesis H_1: $\mu_1 - \mu_2 \neq 0$

T-Value	DF	P-Value
-0.74	9	0.476

Two-Sample T-Test and CI: Tpk:180C_TAM:85sec, ... :180C_TAM:240sec

Method

μ_1: mean of Tpk:180C_TAM:85sec
μ_2: mean of Tpk:180C_TAM:240sec
Difference: $\mu_1 - \mu_2$

Equal variances are not assumed for this analysis.

Descriptive Statistics

Sample	N	Mean	StDev	SE Mean
Tpk:180C_TAM:85sec	9	0.3112	0.0539	0.018
Tpk:180C_TAM:240sec	10	0.4308	0.0257	0.0081

Estimation for Difference

Difference	95% CI for Difference
-0.1196	(-0.1630, -0.0762)

Test

Null hypothesis H_0: $\mu_1 - \mu_2 = 0$
Alternative hypothesis H_1: $\mu_1 - \mu_2 \neq 0$

T-Value	DF	P-Value
-6.06	11	0.000

Two-Sample T-Test and CI: Tpk:195C_TAM:85sec, Tpk:195C_TAM:90sec

Method

μ_1: mean of Tpk:195C_TAM:85sec
μ_2: mean of Tpk:195C_TAM:90sec
Difference: $\mu_1 - \mu_2$

Equal variances are not assumed for this analysis.

Descriptive Statistics

Sample	N	Mean	StDev	SE Mean
Tpk:195C_TAM:85sec	10	0.4056	0.0264	0.0083
Tpk:195C_TAM:90sec	69	0.5787	0.0526	0.0063

Estimation for Difference

Difference	95% CI for Difference
-0.1731	(-0.1949, -0.1513)

Test

Null hypothesis $H_0: \mu_1 - \mu_2 = 0$
Alternative hypothesis $H_1: \mu_1 - \mu_2 \neq 0$

T-Value	DF	P-Value
-16.53	21	0.000

Two-Sample T-Test and CI: Tpk:195C_TAM:85sec, Tpk:195C_TAM:120sec

Method

μ_1: mean of Tpk:195C_TAM:85sec
μ_2: mean of Tpk:195C_TAM:120sec
Difference: $\mu_1 - \mu_2$

Equal variances are not assumed for this analysis.

Descriptive Statistics

Sample	N	Mean	StDev	SE Mean
Tpk:195C_TAM:85sec	10	0.4056	0.0264	0.0083
Tpk:195C_TAM:120sec	10	0.5828	0.0924	0.029

Estimation for Difference

Difference	95% CI for Difference
-0.1772	(-0.2449, -0.1095)

Test

Null hypothesis $H_0: \mu_1 - \mu_2 = 0$
Alternative hypothesis $H_1: \mu_1 - \mu_2 \neq 0$

T-Value	DF	P-Value
-5.83	10	0.000

Two-Sample T-Test and CI: Tpk:195C_TAM:85sec, ... :195C_TAM:240sec

Method

μ_1: mean of Tpk:195C_TAM:85sec
μ_2: mean of Tpk:195C_TAM:240sec
Difference: $\mu_1 - \mu_2$

Equal variances are not assumed for this analysis.

Descriptive Statistics

Sample	N	Mean	StDev	SE Mean
Tpk:195C_TAM:85sec	10	0.4056	0.0264	0.0083
Tpk:195C_TAM:240sec	10	0.5110	0.0714	0.023

Estimation for Difference

Difference	95% CI for Difference
-0.1054	(-0.1584, -0.0524)

Test

Null hypothesis H_0: $\mu_1 - \mu_2 = 0$
Alternative hypothesis H_1: $\mu_1 - \mu_2 \neq 0$

T-Value	DF	P-Value
-4.38	11	0.001

Two-Sample T-Test and CI: Tpk:195C_TAM:90sec, Tpk:195C_TAM:120sec

Method

μ_1: mean of Tpk:195C_TAM:90sec
μ_2: mean of Tpk:195C_TAM:120sec
Difference: $\mu_1 - \mu_2$

Equal variances are not assumed for this analysis.

Descriptive Statistics

Sample	N	Mean	StDev	SE Mean
Tpk:195C_TAM:90sec	69	0.5787	0.0526	0.0063
Tpk:195C_TAM:120sec	10	0.5828	0.0924	0.029

Estimation for Difference

Difference	95% CI for Difference
-0.0041	(-0.0718, 0.0635)

Test

Null hypothesis H_0: $\mu_1 - \mu_2 = 0$
Alternative hypothesis H_1: $\mu_1 - \mu_2 \neq 0$

T-Value	DF	P-Value
-0.14	9	0.894

Two-Sample T-Test and CI: Tpk:195C_TAM:90sec, ... :195C_TAM:240sec

Method

μ_1: mean of Tpk:195C_TAM:90sec
μ_2: mean of Tpk:195C_TAM:240sec
Difference: $\mu_1 - \mu_2$

Equal variances are not assumed for this analysis.

Descriptive Statistics

Sample	N	Mean	StDev	SE Mean
Tpk:195C_TAM:90sec	69	0.5787	0.0526	0.0063
Tpk:195C_TAM:240sec	10	0.5110	0.0714	0.023

Estimation for Difference

Difference	95% CI for Difference
0.0677	(0.0154, 0.1199)

Test

Null hypothesis $H_0: \mu_1 - \mu_2 = 0$
Alternative hypothesis $H_1: \mu_1 - \mu_2 \neq 0$

T-Value	DF	P-Value
2.88	10	0.016

Two-Sample T-Test and CI: Tpk:195C_TAM:120sec, ... :195C_TAM:240sec

Method

μ_1: mean of Tpk:195C_TAM:120sec
μ_2: mean of Tpk:195C_TAM:240sec
Difference: $\mu_1 - \mu_2$

Equal variances are not assumed for this analysis.

Descriptive Statistics

Sample	N	Mean	StDev	SE Mean
Tpk:195C_TAM:120sec	10	0.5828	0.0924	0.029
Tpk:195C_TAM:240sec	10	0.5110	0.0714	0.023

Estimation for Difference

Difference	95% CI for Difference
0.0718	(-0.0065, 0.1501)

Test

Null hypothesis $H_0: \mu_1 - \mu_2 = 0$
Alternative hypothesis $H_1: \mu_1 - \mu_2 \neq 0$

T-Value	DF	P-Value
1.94	16	0.070

Two-Sample T-Test and CI: Tpk:205C_TAM:85sec, ... :205C_TAM:120sec

Method

μ_1: mean of Tpk:205C_TAM:85sec
μ_2: mean of Tpk:205C_TAM:120sec
Difference: $\mu_1 - \mu_2$

Equal variances are not assumed for this analysis.

Descriptive Statistics

Sample	N	Mean	StDev	SE Mean
Tpk:205C_TAM:85sec	10	0.866	0.102	0.032
Tpk:205C_TAM:120sec	10	0.814	0.129	0.041

Estimation for Difference

Difference	95% CI for Difference
0.0523	(-0.0574, 0.1620)

Test

Null hypothesis H_0: $\mu_1 - \mu_2 = 0$
Alternative hypothesis H_1: $\mu_1 - \mu_2 \neq 0$

T-Value	DF	P-Value
1.01	17	0.329

Two-Sample T-Test and CI: Tpk:205C_TAM:85sec, ... :205C_TAM:240sec

Method

μ_1: mean of Tpk:205C_TAM:85sec
μ_2: mean of Tpk:205C_TAM:240sec
Difference: $\mu_1 - \mu_2$

Equal variances are not assumed for this analysis.

Descriptive Statistics

Sample	N	Mean	StDev	SE Mean
Tpk:205C_TAM:85sec	10	0.866	0.102	0.032
Tpk:205C_TAM:240sec	10	0.8883	0.0612	0.019

Estimation for Difference

Difference	95% CI for Difference
-0.0224	(-0.1030, 0.0582)

Test

Null hypothesis H_0: $\mu_1 - \mu_2 = 0$
Alternative hypothesis H_1: $\mu_1 - \mu_2 \neq 0$

T-Value	DF	P-Value
-0.60	14	0.561

Two-Sample T-Test and CI: Tpk:205C_TAM:120sec, ... 205C_TAM:240sec

Method

μ_1: mean of Tpk:205C_TAM:120sec
μ_2: mean of Tpk:205C_TAM:240sec
Difference: $\mu_1 - \mu_2$

Equal variances are not assumed for this analysis.

Descriptive Statistics

Sample	N	Mean	StDev	SE Mean
Tpk:205C_TAM:120sec	10	0.814	0.129	0.041
Tpk:205C_TAM:240sec	10	0.8883	0.0612	0.019

Estimation for Difference

Difference	95% CI for Difference
-0.0747	(-0.1731, 0.0238)

Test

Null hypothesis $H_0: \mu_1 - \mu_2 = 0$
Alternative hypothesis $H_1: \mu_1 - \mu_2 \neq 0$

T-Value	DF	P-Value
-1.65	12	0.124

Two-Sample T-Test and CI: Tpk:180C_TAM:90sec, Tpk:180C_TAM:120sec

Method

μ_1: mean of Tpk:180C_TAM:90sec
μ_2: mean of Tpk:180C_TAM:120sec
Difference: $\mu_1 - \mu_2$

Equal variances are not assumed for this analysis.

Descriptive Statistics

Sample	N	Mean	StDev	SE Mean
Tpk:180C_TAM:90sec	73	0.4431	0.0457	0.0054
Tpk:180C_TAM:120sec	10	0.3254	0.0200	0.0063

Estimation for Difference

Difference	95% CI for Difference
0.11779	(0.10068, 0.13490)

Test

Null hypothesis $H_0: \mu_1 - \mu_2 = 0$
Alternative hypothesis $H_1: \mu_1 - \mu_2 \neq 0$

T-Value	DF	P-Value
14.21	24	0.000

Two-Sample T-Test and CI: Tpk:180C_TAM:90sec, ... :180C_TAM:240sec

Method

μ_1: mean of Tpk:180C_TAM:90sec
μ_2: mean of Tpk:180C_TAM:240sec
Difference: $\mu_1 - \mu_2$

Equal variances are not assumed for this analysis.

Descriptive Statistics

Sample	N	Mean	StDev	SE Mean
Tpk:180C_TAM:90sec	73	0.4431	0.0457	0.0054
Tpk:180C_TAM:240sec	10	0.4308	0.0257	0.0081

Estimation for Difference

Difference	95% CI for Difference
0.01237	(-0.00810, 0.03284)

Test

Null hypothesis H_0: $\mu_1 - \mu_2 = 0$
Alternative hypothesis H_1: $\mu_1 - \mu_2 \neq 0$

T-Value	DF	P-Value
1.27	18	0.220

Two-Sample T-Test and CI: Tpk:180C_TAM:120sec, ... :180C_TAM:240sec

Method

μ_1: mean of Tpk:180C_TAM:120sec
μ_2: mean of Tpk:180C_TAM:240sec
Difference: $\mu_1 - \mu_2$

Equal variances are not assumed for this analysis.

Descriptive Statistics

Sample	N	Mean	StDev	SE Mean
Tpk:180C_TAM:120sec	10	0.3254	0.0200	0.0063
Tpk:180C_TAM:240sec	10	0.4308	0.0257	0.0081

Estimation for Difference

Difference	95% CI for Difference
-0.1054	(-0.1273, -0.0836)

Test

Null hypothesis H_0: $\mu_1 - \mu_2 = 0$
Alternative hypothesis H_1: $\mu_1 - \mu_2 \neq 0$

T-Value	DF	P-Value
-10.22	16	0.000

Two-Sample T-Test and CI: Bi40+,Outer_Tpk195C, ... 0+,Inner_Tpk195C

Method

μ_1: mean of Bi40+,Outer_Tpk195C
μ_2: mean of Bi40+,Inner_Tpk195C
Difference: $\mu_1 - \mu_2$

Equal variances are not assumed for this analysis.

Descriptive Statistics

Sample	N	Mean	StDev	SE Mean
Bi40+,Outer_Tpk195C	35	0.6125	0.0469	0.0079
Bi40+,Inner_Tpk195C	34	0.5438	0.0312	0.0054

Estimation for Difference

Difference	95% CI for Difference
0.06873	(0.04959, 0.08787)

Test

Null hypothesis H_0: $\mu_1 - \mu_2 = 0$
Alternative hypothesis H_1: $\mu_1 - \mu_2 \neq 0$

T-Value	DF	P-Value
7.19	59	0.000

Two-Sample T-Test and CI: Bi40+,Outer_Tpk180C, ... 0+,Inner_Tpk180C

Method

μ_1: mean of Bi40+,Outer_Tpk180C
μ_2: mean of Bi40+,Inner_Tpk180C
Difference: $\mu_1 - \mu_2$

Equal variances are not assumed for this analysis.

Descriptive Statistics

Sample	N	Mean	StDev	SE Mean
Bi40+,Outer_Tpk180C	39	0.4792	0.0244	0.0039
Bi40+,Inner_Tpk180C	34	0.4018	0.0240	0.0041

Estimation for Difference

Difference	95% CI for Difference
0.07741	(0.06609, 0.08874)

Test

Null hypothesis H_0: $\mu_1 - \mu_2 = 0$
Alternative hypothesis H_1: $\mu_1 - \mu_2 \neq 0$

T-Value	DF	P-Value
13.64	69	0.000

T-Tests for SnBi57

Two-Sample T-Test and CI: Tpk:180C_TAM:90sec, ... :180C_TAM:240sec

Method

μ_1: mean of Tpk:180C_TAM:90sec
μ_2: mean of Tpk:180C_TAM:240sec
Difference: $\mu_1 - \mu_2$

Equal variances are not assumed for this analysis.

Descriptive Statistics

Sample	N	Mean	StDev	SE Mean
Tpk:180C_TAM:90sec	67	0.4715	0.0457	0.0056
Tpk:180C_TAM:240sec	6	0.3991	0.0432	0.018

Estimation for Difference

Difference	95% CI for Difference
0.0723	(0.0271, 0.1176)

Test

Null hypothesis H_0: $\mu_1 - \mu_2 = 0$
Alternative hypothesis H_1: $\mu_1 - \mu_2 \neq 0$

T-Value	DF	P-Value
3.91	6	0.008

Two-Sample T-Test and CI: Tpk:180C_TAM:90sec, Tpk:180C_TAM:120sec

Method

μ_1: mean of Tpk:180C_TAM:90sec
μ_2: mean of Tpk:180C_TAM:120sec
Difference: $\mu_1 - \mu_2$

Equal variances are not assumed for this analysis.

Descriptive Statistics

Sample	N	Mean	StDev	SE Mean
Tpk:180C_TAM:90sec	67	0.4715	0.0457	0.0056
Tpk:180C_TAM:120sec	9	0.4078	0.0361	0.012

Estimation for Difference

Difference	95% CI for Difference
0.0637	(0.0345, 0.0928)

Test

Null hypothesis H_0: $\mu_1 - \mu_2 = 0$
Alternative hypothesis H_1: $\mu_1 - \mu_2 \neq 0$

T-Value	DF	P-Value
4.80	11	0.001

Two-Sample T-Test and CI: Tpk:180C_TAM:120sec, ... :180C_TAM:240sec

Method

μ_1: mean of Tpk:180C_TAM:120sec
μ_2: mean of Tpk:180C_TAM:240sec
Difference: $\mu_1 - \mu_2$

Equal variances are not assumed for this analysis.

Descriptive Statistics

Sample	N	Mean	StDev	SE Mean
Tpk:180C_TAM:120sec	9	0.4078	0.0361	0.012
Tpk:180C_TAM:240sec	6	0.3991	0.0432	0.018

Estimation for Difference

Difference	95% CI for Difference
0.0087	(-0.0396, 0.0569)

Test

Null hypothesis H_0: $\mu_1 - \mu_2 = 0$
Alternative hypothesis H_1: $\mu_1 - \mu_2 \neq 0$

T-Value	DF	P-Value
0.41	9	0.694

Two-Sample T-Test and CI: Tpk:195C_TAM:90sec, Tpk:195C_TAM:120sec

Method

μ_1: mean of Tpk:195C_TAM:90sec
μ_2: mean of Tpk:195C_TAM:120sec
Difference: $\mu_1 - \mu_2$

Equal variances are not assumed for this analysis.

Descriptive Statistics

Sample	N	Mean	StDev	SE Mean
Tpk:195C_TAM:90sec	70	0.7710	0.0585	0.0070
Tpk:195C_TAM:120sec	10	0.5410	0.0557	0.018

Estimation for Difference

Difference	95% CI for Difference
0.2300	(0.1887, 0.2713)

Test

Null hypothesis H_0: $\mu_1 - \mu_2 = 0$
Alternative hypothesis H_1: $\mu_1 - \mu_2 \neq 0$

T-Value	DF	P-Value
12.14	12	0.000

Two-Sample T-Test and CI: Tpk:195C_TAM:90sec, ... :195C_TAM:240sec

Method

μ_1: mean of Tpk:195C_TAM:90sec
μ_2: mean of Tpk:195C_TAM:240sec
Difference: $\mu_1 - \mu_2$

Equal variances are not assumed for this analysis.

Descriptive Statistics

Sample	N	Mean	StDev	SE Mean
Tpk:195C_TAM:90sec	70	0.7710	0.0585	0.0070
Tpk:195C_TAM:240sec	10	0.6050	0.0411	0.013

Estimation for Difference

Difference	95% CI for Difference
0.1659	(0.1343, 0.1976)

Test

Null hypothesis H_0: $\mu_1 - \mu_2 = 0$
Alternative hypothesis H_1: $\mu_1 - \mu_2 \neq 0$

T-Value	DF	P-Value
11.23	14	0.000

Two-Sample T-Test and CI: Tpk:195C_TAM:120sec, ... :195C_TAM:240sec

Method

μ_1: mean of Tpk:195C_TAM:120sec
μ_2: mean of Tpk:195C_TAM:240sec
Difference: $\mu_1 - \mu_2$

Equal variances are not assumed for this analysis.

Descriptive Statistics

Sample	N	Mean	StDev	SE Mean
Tpk:195C_TAM:120sec	10	0.5410	0.0557	0.018
Tpk:195C_TAM:240sec	10	0.6050	0.0411	0.013

Estimation for Difference

Difference	95% CI for Difference
-0.0641	(-0.1105, -0.0177)

Test

Null hypothesis H_0: $\mu_1 - \mu_2 = 0$
Alternative hypothesis H_1: $\mu_1 - \mu_2 \neq 0$

T-Value	DF	P-Value
-2.93	16	0.010

Two-Sample T-Test and CI: Tpk:205C_TAM:120sec, ... 205C_TAM:240sec

Method

μ_1: mean of Tpk:205C_TAM:120sec
μ_2: mean of Tpk:205C_TAM:240sec
Difference: $\mu_1 - \mu_2$

Equal variances are not assumed for this analysis.

Descriptive Statistics

Sample	N	Mean	StDev	SE Mean
Tpk:205C_TAM:120sec	10	0.8673	0.0620	0.020
Tpk:205C_TAM:240sec	10	0.9434	0.0625	0.020

Estimation for Difference

Difference	95% CI for Difference
-0.0761	(-0.1348, -0.0174)

Test

Null hypothesis H_0: $\mu_1 - \mu_2 = 0$
Alternative hypothesis H_1: $\mu_1 - \mu_2 \neq 0$

T-Value	DF	P-Value
-2.73	17	0.014

Two-Sample T-Test and CI: Outer_Tpk180C, Inner_Tpk180C

Method

μ_1: mean of Outer_Tpk180C
μ_2: mean of Inner_Tpk180C
Difference: $\mu_1 - \mu_2$

Equal variances are not assumed for this analysis.

Descriptive Statistics

Sample	N	Mean	StDev	SE Mean
Outer_Tpk180C	39	0.4792	0.0244	0.0039
Inner_Tpk180C	34	0.4018	0.0240	0.0041

Estimation for Difference

Difference	95% CI for Difference
0.07741	(0.06609, 0.08874)

Test

Null hypothesis H_0: $\mu_1 - \mu_2 = 0$
Alternative hypothesis H_1: $\mu_1 - \mu_2 \neq 0$

T-Value	DF	P-Value
13.64	69	0.000

Two-Sample T-Test and CI: Outer_Tpk195C, Inner_Tpk195C

Method

μ_1: mean of Outer_Tpk195C
μ_2: mean of Inner_Tpk195C
Difference: $\mu_1 - \mu_2$

Equal variances are not assumed for this analysis.

Descriptive Statistics

Sample	N	Mean	StDev	SE Mean
Outer_Tpk195C	35	0.6125	0.0469	0.0079
Inner_Tpk195C	34	0.5438	0.0312	0.0054

Estimation for Difference

Difference	95% CI for Difference
0.06873	(0.04959, 0.08787)

Test

Null hypothesis H_0: $\mu_1 - \mu_2 = 0$
Alternative hypothesis H_1: $\mu_1 - \mu_2 \neq 0$

T-Value	DF	P-Value
7.19	59	0.000

Descriptive Statistics for the BGA Study

Descriptive Statistics: Bi40+,Tpk:180C_TAM:90sec, ... k:180C_TAM:90sec

Statistics

Variable	N	N*	Mean	SE Mean	StDev	Minimum	Q1	Median
Bi40+,Tpk:180C_TAM:90sec	73	0	0.44315	0.00535	0.04572	0.34884	0.40302	0.44475
Bi57,Tpk:180C_TAM:90sec	67	0	0.47145	0.00558	0.04569	0.37672	0.43998	0.47629
Bi58,Tpk:180C_TAM:90sec	80	0	0.47047	0.00519	0.04638	0.39200	0.43087	0.45763

Variable	Q3	Maximum
Bi40+,Tpk:180C_TAM:90sec	0.47954	0.53402
Bi57,Tpk:180C_TAM:90sec	0.50562	0.54460
Bi58,Tpk:180C_TAM:90sec	0.51563	0.56301

Descriptive Statistics: Bi40+,Tpk:195C_TAM:90sec, ... k:195C_TAM:90sec

Statistics

Variable	N	N*	Mean	SE Mean	StDev	Minimum	Q1	Median
Bi40+,Tpk:195C_TAM:90sec	69	0	0.57868	0.00634	0.05263	0.48811	0.53551	0.58228
Bi57,Tpk:195C_TAM:90sec	70	0	0.77098	0.00700	0.05853	0.65187	0.71526	0.78484
Bi58,Tpk:195C_TAM:90sec	56	0	0.69614	0.00796	0.05960	0.53855	0.64924	0.71613

Variable	Q3	Maximum
Bi40+,Tpk:195C_TAM:90sec	0.62640	0.69018
Bi57,Tpk:195C_TAM:90sec	0.82092	0.87356
Bi58,Tpk:195C_TAM:90sec	0.74507	0.76214